

Dear Dr. Slimane Bekki,

We are most grateful to you and the reviewers for the helpful comments on the original version of our manuscript. We have taken all the comments into account and submit a revised version of our paper here. Please find attached the comments of the referees and our replies (available also on-line) together with the revised manuscript with highlighted modifications.

Please note:

- We modified the reference “Yin et al. (manuscript in preparation, 2019)” into “Yin et al. (manuscript in preparation, **2020**)” throughout the revised manuscript.
- We added a text in the “Acknowledgements” to express our gratitude to anonymous reviewers.
- We added nine papers to the References according to the comments by referee #1 and #2; however they are not highlighted because of some technical issues with “`latexdiff`.” These modifications are all described in the following replies.

Thank you very much again for your guiding the editorial process of our manuscript. We are looking forward to hearing from you.

Yours sincerely,

Hiroshi Yamashita (on behalf of all co-authors)

We are grateful to the referee #1 for the very helpful and encouraging comments on the original version of our manuscript. We took all comments into account and rewrote the manuscript accordingly. Here are our replies:

- **General comment:** This paper documents the AirTraf version 2 submodel of the EMAC chemistry-climate model, developed to enable simulation of global air traffic in a climate model in order to investigate optimized routing strategies for the aviation sector. A set of one day simulations are run, showing that the model gives plausible output and the results are discussed in the context of previous literature. While the topic of abatement strategies for reducing aviation's climate impact is both important and current, and this modeling framework is a useful tool in this regard, the paper is not of a sufficient quality for publication in its current form. In general, the main messages can be polished and highlighted better. The introduction is long and unstructured, and it's difficult to extract the essence of what's new in this work (and why it's important). This does not really get much clearer in the methods where most of AirTraf 2 seems to follow AirTraf1 and is mostly described in Yamashita et al. 2016. While the discussion section is quite good, the results is only one page out of a 14-page paper, which is not quite convincing. The paper also needs substantial additional work to improve the writing and language. There are number strange formulations, short sentences and imprecise use of terminology that make the paper difficult to follow at times. Some examples are given below, but a general language check/copyediting is recommended.

Reply: We thank the referee #1 for the useful comments. We have addressed all the comments and structured our reply according to the reviewer's general comments into

- Highlight improvements
- Shortening and improved structure of the introduction
- Methods: clarifying the improvements of AirTraf 2.0 over AirTraf 1.0
- Extension of the results section
- Language improvements
- Modification of short sentences
- Explanation of terminologies
- Formula improvements
- Modification of references.

We believe that this revision represents a polishing of the whole paper.

#### a) Highlight improvements:

To highlight the main messages of this paper, we rewrote the abstract and the conclusions. We also modified the introduction to improve the structure, and to show what's new in this work and why AirTraf 2.0 is important. Details are described in the "b) Shortening and improved structure of the introduction" below.

#### [Abstract]

**Aviation contributes to climate change and the** Climate impact of aviation is expected to increase further. **Adaptions of Aircraft routings in order to reduce the climate impact** are an important **climate change mitigation** measure for climate impact reductions. To find an effective aircraft routing strategy for reducing the impact, the first version of the submodel AirTraf has been developed; this submodel can simulate global air traffic in the ECHAM/MESSy Atmospheric Chemistry (EMAC) model. The air traffic simulator AirTraf, as a submodel of the ECHAM/MESSy Atmospheric Chemistry (EMAC) model, enables the evaluation of such measures. For the first version of the submodel AirTraf, we concentrated on the general set-up of the model, including departure and arrival, performance and emissions, and technical aspects such as the parallelization of the aircraft trajectory calculation with only a limited set of optimization possibilities (time and distance). This paper describes the updated submodel AirTraf 2.0. Seven new aircraft routing options are introduced, including contrail avoidance, minimum economic costs, and minimum climate impact. Here, in the second version of AirTraf, we focus on enlarging the objective functions by seven new options to enable assessing operational improvements in many more aspects including economic costs, contrail occurrence and climate impact. We verify that the AirTraf set-up, e.g. in terms of number and choice of design variables for the genetic algorithm, allows finding solutions even with highly structured fields such as contrail occurrence. This is shown by example

simulations of the new routing options are presented by using, including around 100 north-Atlantic flights of an Airbus A330 aircraft for a typical winter day. The results clearly show that **AirTraf 2.0 can find the different families of optimum flight trajectories (three-dimensional) varies according to the for specific routing options; those trajectories minimize the corresponding objective functions successfully. The comparison of the results for various routing options reveals characteristics of the routing with respect to air traffic performances.** The minimum cost option obtains a trade-off solution lies between the minimum time and the minimum fuel solutions options. Thus, aircraft operating costs are minimized by taking the best compromise between flight time and fuel use. The aircraft routings for contrail avoidance and minimum climate impact reduce the potential climate impact, which is estimated by using algorithmic Climate Change Functions, whereas these two routings increase the flight aircraft operating costs. A trade-off between the aircraft operating costs and the climate impact is confirmed. The simulation results are compared with literature data and the consistency of the submodel AirTraf 2.0 is verified.

#### [Conclusions]

We revised the conclusions to highlight the outcomes in a better way, e.g., on page 14 lines 25-32, “AirTraf 2.0 simulates the one-day air traffic successfully for the newly developed routing option concerning different optimization objectives, e.g., contrail avoidance, cash operating cost, and climate impact (represented by average temperature response over 20 years), and finds the different families of optimum flight trajectories, which minimize the corresponding objective functions. The characteristics of these routing options were analyzed on the basis of the nine performance measures. include that Aaircraft was flown as the minimum economic cost with both, the SOC and the COC options. These options are comparably effective for economic cost indices. The AirTraf 2.0 differentiates the minimum time, the minimum fuel, and the minimum COC solutions options; that is, the COC option obtains a trade-off solution lies between the minimum time and the minimum fuel solutions options, and thus minimizes COC by taking the best compromise between the flight time and the fuel use into account. The NO<sub>x</sub> option minimizes NO<sub>x</sub> emission; this option differs from the fuel and the COC options. The contrail and the climate options decrease the climate impact (indicated by ATR20<sub>total</sub>), which causes extra operating costs. A trade-off between the cost and the climate impact certainly exists.”

#### b) Shortening and improved structure of the introduction:

To shorten the introduction and to improve its structure, we modified the text and structured the introduction into

- Background: the climate impact of aviation
- Introduction of a climate-optimized routing
- Previous studies: benefits of the climate-optimized routing
- Ultimate aims and introduction of the AirTraf model
- Objective of this study
- Significant aspects of AirTraf 2.0
- Contents of the paper.

The concrete modifications are as follows:

- We deleted some redundant sentences from the introduction (please see the replies to the referee comments (4), (8) and (15)).
- We deleted one paragraph from the introduction (please see the reply to the referee comment (18)).
- We rewrote the text: on page 4 line 3, “Here, we focus on mention the importance of the variety of the routing options.”

In addition, we modified the text to make clear what's new in this work and why AirTraf 2.0 is important, and to emphasize its advantage, compared to other models as follows:

- We added the text to the introduction (please see the reply to the referee comment (28)).
- We rewrote the text: on page 3 lines 27-29, “This paper presents a technical description of the new version of the submodel AirTraf 2.0 (version 2.0). The simple aircraft routing options of great circle (minimum flight distance) and flight time (minimum time) were developed in the previous version of AirTraf 1.0 (Yamashita et al., 2016). Here In AirTraf 2.0, seven new aircraft routing options have been introduced....”
- We added the word “2.0” to emphasize the new development in AirTraf 2.0: on page 4 line 3, “Various

routing options have been made available in AirTraf 2.0, because....”

**c) Methods: clarifying the improvements of AirTraf 2.0 over AirTraf 1.0:**

As the referee noted, AirTraf 2.0 builds on the previous version of AirTraf 1.0. AirTraf is a comprehensive model to enable air traffic simulations on-line in the chemistry-climate model EMAC. In AirTraf 1.0 (Yamashita et al., 2016), we developed the basic modules, including the main structure of trajectory calculations and the optimizer module for flight trajectory optimization. We had also introduced two simple routing options (the great circle and the time-optimal options) to verify, whether the whole system and the optimization module work correctly.

For our ultimate aims described on page 3 line 19, we have expanded the model framework substantially to include seven new routing options with respect to different optimization objectives. We highlight the key changes (i.e. what is new in AirTraf 2.0) in Fig. 1 (on page 22 in the caption, “updates from AirTraf 1.0 are highlighted by red texts and arrows”) and in Tables 1 and 2 (on pages 25-26 in the caption, “The column ‘New in V2.0’ denotes parameters/properties newly introduced in AirTraf 2.0”). We believe that they are useful for readers to recognize the new changes. To show the new changes more clearly, we added the text as follows:

- On page 5 line 2, “The present version is based on the model components of AirTraf 1.0, **and** thus, this section outlines them (**updates from AirTraf 1.0 are highlighted in Fig. 1**).”
- On page 5 line 7, “Table 1 lists the relevant data of an A330-301 aircraft and constant parameters used in AirTraf 2.0 (**the new parameters are listed in Table 1**).”
- On page 5 line 28, “The first step finds an optimum flight trajectory for a selected routing option by using the aircraft routing module (Fig. 1, light green), **in which the seven new routing options are introduced in AirTraf 2.0.**”
- On page 6 line 2, “In AirTraf 2.0, 15 new properties are calculated, **as highlighted in Table 2.**”
- On page 6 line 5, “... at the departure time of the flight. **The methodologies of the fuel-emissions calculation module developed in AirTraf 1.0 are expanded in AirTraf 2.0.** Details of the fuel-emissions-cost-climate calculation module (Fig. 1, light orange) and its reliability have been reported....”
- On page 6 line 13, “... are gathered along the flight segments (Table 2); **the global fields of PCC<sub>dist</sub> and ATR20s are newly calculated by AirTraf 2.0.**”
- On page 7 line 15, “**In AirTraf 2.0, seven new objective functions were developed....**”

**d) Extension of the results section:**

We analyzed simulation results in more detail and additionally rewrote the text for Sect. 3.2 and 3.3. Please see the reply to the referee comment (24).

**e) Language improvements:**

To improve the writing and language, we rechecked and modified the text, redundant words and sentences, articles, and consistency of wording in the manuscript. The referee comments (1), (2) and (4) also pointed out this issue, and thus we replied to them in the corresponding sections. We list here other modifications:

- On page 3 line 6, “**In general, The benefits of flying climate-optimized trajectories the climate-optimized routing were investigated....**”
- On page 3 line 8, “... pulse AGTP values for three **different** time horizons....”
- On page 3 line 10, “... for the medium-term climate goal, i.e., **the time horizon** of 50 years....”
- On page 3 line 34, “... are referred to simply as, e.g. the “fuel option”).”
- On page 10 line 14, “... whereas these trajectories **of the westbound flights** are shifted northward **for the westbound flights.**”
- On page 10 line 26, “... decrease the respective objects (target measures) **to which should** be minimized. ...”
- On page 10 line 29, “... Table 4 lists a summary of **typical nine** performance measures of....”
- On page 11 line 26, “... which offers additional aircraft routing options for defining overall target functions for **aircraft the flight** trajectory optimization.”
- On page 11 line 29, “The quantitative values of the changes in **the** performance measures vary....”
- On page 24 in the caption of Fig. 3, “... climate impact indicated by ATR20total **for one day during the**

day (from December 1, 2015 00:00:00 to December 2, 2015 00:00:00 UTC)."

**f) Modification of short sentences:**

We rewrote the three short sentences as follows:

- On page 4 line 5, "The time option is useful for delay recovery. **Because** Delays cause costs to airlines, **Thus**, pilots are often forced to temporarily use the time option during a flight to maintain flight schedules. ...."
- On page 4 line 11, "AirTraf enables analyzing those subjects." We modified the sentence in reply to the referee comment (28).
- On page 5 line 3, "Thus, this section outlines them." We modified the sentence in reply to the "Methods: clarifying the improvements of AirTraf 2.0 over AirTraf 1.0" described above.

**g) Explanation of terminologies:**

Some terminologies related to the genetic algorithm optimization are used in the present manuscript. We added the explanations to the words and rewrote the text:

- On page 6 line 29, "... and creates an initial "population,"; which ~~consists of~~ **represents** a random set of solutions. ~~(population approach; the~~ population size is set by  $n_p$  and **ARMOGA starts its search with the solutions**). An evaluation function  $f$  (**called an objective function**) is defined, depending on a selected routing option...."
- On page 7 line 4, "... the stochastic universal sampling selection (Baker, 1985) was used for the selection operator **to pick two solutions (parent solutions) from the population**; the Blend crossover operator (BLX-alpha; Eshelman, 1993) was applied to the ~~population~~ **parent solutions** to create new solutions (child solutions) ~~by picking two solutions (parent solutions) from the population~~; the revised polynomial mutation operator (Deb and Agrawal, 1999) was used to add a disturbance to the child solutions. When ~~the evolution~~ **those processes** ~~is~~ **are** iterated for a number of generations (**the term "generation" represents one iteration of ARMOGA**; this is set by  $n_g$ )...."
- We changed the word "RI" into "RF" (please see the reply to the referee comment (6)).

**h) Formula improvements:**

We added the definitions (equations) of the five ATR20s to the revised manuscript. Please see the reply to the referee comment (21). In addition, we added explanations on Eq. (A5), which is the algorithmic Climate Change Functions of contrails (aCCF<sub>contrail</sub>) to the Appendix. Please see the reply to the referee comment (22).

**i) Modification of references:**

We modified the wrong references as follows:

- On page 3 line 31, "...Yin et al., 2018ab...."
- On page 8 line 9, "Yin et al. (2018a) and Yin et al. (manuscript in preparation, 2019)...."
- On page 9 line 17, "...Yin et al., 2018ab...."
- On page 15 line 13, "... published by Van Manen (2017), **Yin et al. (2018b)**, and Van Manen and Grewe (2019); the aCCF of contrails is described by ~~Yin et al. (2018a)~~ and Yin et al. (manuscript in preparation, 2019)."

• **Selected specific comments:**

- (1) Title: suggest removing "Various". Makes it seem vague.

Reply: Thank you very much. We removed the word "Various" from the title, and rewrote the title as "**Newly developed** aircraft routing options for air traffic simulation in the chemistry-climate model EMAC 2.53: AirTraf 2.0".

• (2) Abstract: Line 1: Add "the" before "climate impact of aviation...."

Reply: We added the word "the" to the revised manuscript: on page 1 line 1 in Abstract, "... **the** climate impact of aviation...."

- (3) Abstract: Line 6-9: unclear, I don't really understand what the important result here is.

Reply: We rewrote the text to highlight the messages: on page 1 lines 6-9, “The results clearly show that **AirTraf 2.0 can find the different families of optimum flight trajectories (three-dimensional) varies according to the for specific routing options; those trajectories minimize the corresponding objective functions successfully.** The comparison of the results for various routing options reveals characteristics of the routing with respect to air traffic performances. The minimum cost option obtains a trade-off solution lies between the minimum time and the minimum fuel solutions options. Thus, aircraft operating costs are minimized by taking the best compromise between flight time and fuel use.”

- (4) Pg1: Line 16: The sentence starting with “the aviation sector is not” is redundant as you've just said that aviation contributes only 5% total climate impact.

Reply: Thank you very much. We removed the sentence: on page 1 line 16, “~~The aviation is not the largest contributor to climate impact at the moment (e.g., the road transport contributes 11 % to the anthropogenic climate impact; Skeie et al., 2009)~~. However, the aviation's contribution....” Related to this, we added the word “only” to the revised manuscript: on page 1 line 15, “Nowadays the global aviation contributes **only** about 5 % to the anthropogenic climate impact....”

- (5) Pg1: Line 23: a more up-to-date reference would be the Brasseur et al. 2016 paper in BAMS.

Reply: Thank you very much. We referred to the paper in the revised manuscript: on page 1 line 23, “... (Wuebbles et al., 2007; Lee et al., 2009; **Brasseur et al., 2016**)”. This paper is listed in the present References.

- (6) Pg2: Line 1: I don't understand the rationale behind introducing the terminology radiative impact (RI) instead of keeping well-established radiative forcing (RF). This is confusing and adds nothing to the paper. Please explain or change.

Reply: Thank you very much. We believe that the term “radiative impact” is the more general term, and the two sentences, starting from page 1 line 23 “These effects change ... a radiative impact (RI). The RI potentially ... through temperature changes” describe the general mechanism of climate change. Thus, the term “radiative impact” would be appropriate. On the other hand, Lee et al. (2009) and other literature use the term “RF” to report those figures (in  $\text{mW/m}^2$ ). By following the referee comment, the best modification would be to remove the abbreviation “RI” in the two sentences, and to use the word “radiative forcing (RF)” in other sentences. Finally, we rewrote the text: from page 1 line 23 to page 2 line 4, “... cause a radiative impact (RI). The RI radiative impact potentially drives the climate system into a new state of equilibrium through temperature changes. Lee et al. (2009) stated that the  $\text{CO}_2$  emission has the main impact and that the estimated RI radiative forcing (RF) of aviation  $\text{CO}_2$  in 2005 was  $28.0 \text{ mWm}^{-2}$  ( $15.2\text{--}40.8 \text{ mWm}^{-2}$ , 90 % likelihood range). The non- $\text{CO}_2$  emissions and the induced clouds also have a large effect on RI's RFs; for example, the estimated RI's RFs in 2005....”

- (7) Pg2: Line 5: there are number of more recent studies showing higher contrail-cirrus forcing, reflecting more recent emission inventories. One example is the 2016 paper by Bock and Burkhardt in JGR-A. Such work should be reflected.

Reply: Thank you very much. We referred to the three recent papers here and rewrote the sentence: on page 2 line 4, “... the estimated RI's RFs in 2005 for total  $\text{NO}_x$  and for persistent linear contrails were  $12.6 \text{ mWm}^{-2}$  ( $3.8\text{--}15.7 \text{ mWm}^{-2}$ , 90 % likelihood range) and  $11.8 \text{ mWm}^{-2}$  ( $5.4\text{--}25.6 \text{ mWm}^{-2}$ , 90 % likelihood range), respectively (Lee et al., 2009). **In particular, the radiative impact of contrails remains uncertain and recent studies report higher RF.** Burkhardt and Kärcher (2011) estimated the contrail cirrus RF of  $37.5 \text{ mWm}^{-2}$  for the year 2002; Schumann et al. (2015) reported the RF of  $63 \text{ mWm}^{-2}$  for the year 2006; and

**Bock and Burkhardt estimated the RF of 56 mWm<sup>-2</sup> for the year 2006.”**

Related to this, we added the three papers to the References:

- On page 17 line 8, “**Bock, L., and Burkhardt, L.: Reassessing properties and radiative forcing of contrail cirrus using a climate model, Journal of Geophysical Research: Atmospheres, 121, 16, 9717–9736, <https://doi.org/10.1002/2016JD025112>, 2016.**”
- On page 17 line 13, “**Burkhardt, U., and Kärcher, B.: Global radiative forcing from contrail cirrus, Nature Clim Change, 1, 54–58, <https://doi.org/10.1038/nclimate1068>, 2011.**”
- On page 20 line 34, “**Schumann, U., Penner, J. E., Chen, Y., Zhou, C., and Graf, K.: Dehydration effects from contrails in a coupled contrail–climate model, Atmos. Chem. Phys., 15, 11179–11199, <https://doi.org/10.5194/acp-15-11179-2015>, 2015.**”

- (8) Pg2: Line 6: “Here the difference between time scales (...): suggest removing, no point in telling the reader what you will tell them next.

Reply: We removed the sentence and rewrote the text “As for time scales of their impacts” in context: on page 2 line 6, “~~Here, the difference between time scales of their impacts is noted. As for time scales of their impacts....~~”

- (9) Pg2 Line 6: “The emitted CO<sub>2</sub> (...): this is not precise; the emitted CO<sub>2</sub> does not have century-long timescale, the perturbation does.

Reply: We rewrote the sentence: on page 2 line 6, “~~The emitted CO<sub>2</sub> has a long residence time (a century) and becomes uniformly mixed in the whole atmosphere, the emitted CO<sub>2</sub> becomes uniformly mixed in the whole atmosphere and its perturbation remains for millennia.~~” This modification is related to our reply to the minor comment (2) of the referee #2.

- (10) Pg2: Line 7: “the impact is proportional to (...): this may be true for emission, and perhaps even for RF, but when approximating fuel with temperature impact or other climate change seems doubtful.

Reply: As the referee pointed out, the sentence is not precise. Actually, this sentence does not give any necessary information. Thus, we removed the sentence: on page 2 line 7, “~~... , i.e., its impact is proportional to fuel use.~~”

- (11) Pg2: Line 10: the recent work by Lund et al. 2017 ESD include all components and show how this translates into temperature impacts. Could be a useful references.

Reply: Thank you very much. We referred to the paper in the revised manuscript: on page 2 line 10, “... Mannstein et al., 2005; Gauss et al., 2006; Grawe and Stenke, 2008; Frömming et al., 2012; Brasseur et al., 2016; **Lund et al., 2017**.”

Related to this, we added this paper to the References: on page 19 line 26, “**Lund, M. T., Aamaas, B., Berntsen, T., Bock, L., Burkhardt, U., Fuglestvedt, J. S., and Shine, K. P.: Emission metrics for quantifying regional climate impacts of aviation, Earth Syst. Dynam., 8, 547–563, <https://doi.org/10.5194/esd-8-547-2017>, 2017.**”

- (12) Pg2: Line 17: Why is climate-optimized routing limited to the present-day fleet?

Reply: The climate-optimized routing is **not** limited to the present-day fleet. What we want to say here is that the climate-optimized routing is **immediately** applicable to the fleet, which airlines currently operate. Although technological measures (e.g. efficient engines, new aircraft) can significantly reduce the aviation climate impact, it takes a long time for airlines to introduce such new technological measures. To make clear the meaning of the sentence, we rewrote the text: on page 2 line 17, “The climate-optimized routing is

**immediately** applicable to present airline fleets, whereas other, more technical measures require several years before implementation.”

- (13) Pg2: Line 22: because of the long residence time of CO<sub>2</sub>, its impact is the same regardless of location of emission. Please be more precise.

Reply: Thank you very much. We rewrote the sentence more precisely: on page 2 line 21, “... Frömming et al. (2013) and Grewe et al. (2014b) developed Climate Cost Functions (CCFs) for the climate-optimized routing. ~~The CCFs can identify climate sensitive regions with respect to aviation's CO<sub>2</sub> and non-CO<sub>2</sub> effects (H<sub>2</sub>O, ozone, methane, primary mode ozone, and contrails) and estimate corresponding climate impacts. Here, ozone changes arizen from changes of methane are called primary mode ozone (Dahlmann et al., 2016). They calculated global-average RFs resulting from local unit emissions (CO<sub>2</sub>, NO<sub>x</sub>, H<sub>2</sub>O and contrails) over the north-Atlantic for typical weather patterns by using the ECHAM5/MESSy Atmospheric Chemistry model EMAC (Jöckel et al 2010, 2016). Those RFs were used to calculate the global and temporal average near-surface temperature response over 20 years, which describe the climate impacts (i.e. future temperature changes) caused by those emissions on a per unit basis. The resulting data set is called the Climate Cost Functions (CCFs). The CCFs describe the climate impact which is induced by aviation's CO<sub>2</sub> and non-CO<sub>2</sub> effects (H<sub>2</sub>O, ozone, methane, ozone originating from methane changes, and contrails including the spread into contrail-cirrus); and the CCFs of those effects except CO<sub>2</sub> are a function of geographic location, altitude and time. Because of the long residence time of CO<sub>2</sub>, its impact is the same regardless of location, altitude and time of emission. The obtained CCFs can be used as a measure of the climate impact of aviation and form the basis for the climate-optimized routing.”~~

Related to this, we rewrote the following text, because the modified sentences described above refer to the word “EMAC” for the first time in the revised manuscript: on page 3 line 22, “... developed as one of the submodels of the ECHAM/MESSy Atmospheric Chemistry (EMAC) model EMAC....”

- (14) Pg2: Line 22: Please add a more detailed definition of CCS as the reader needs this later on.

Reply: Thank you very much. We added the details of the Climate Cost Functions (CCFs) to the revised manuscript. Please see the reply to the comment (13).

- (15) Pg2: Line 24: Another strange sentence to suddenly introduce here instead of adding above when listing aviation non-CO<sub>2</sub> effects.

Reply: We deleted this sentence: on page 2 line 24, “~~Here, ozone changes arizen from changes of methane are called primary mode ozone (Dahlmann et al., 2016)~~”. In addition, we added this description to the list of non-CO<sub>2</sub> effects: on page 2 line 23, “... and non-CO<sub>2</sub> effects (H<sub>2</sub>O, ozone, methane, **ozone originating from methane changes**, and contrails....” Please see the reply to the comment (13).

- (16) Pg2: Line 29: what about trade-offs between e.g., contrail avoidance and increased fuel use?

Reply: As the referee pointed out, the trade-off between contrail avoidance and increased fuel use is also an important subject. Actually, this is the reason why we develop many routing options in AirTraf 2.0; one can analyze the trade-off by using AirTraf 2.0. This point is described in the paragraph (on page 4 lines 3-13). On the other hand, the paragraph (on page 2 lines 20-33) focuses on the “climate-optimized routing,” and thus we did not mention trade-offs between other routing strategies there.

To emphasize the importance of analyzing other trade-offs, we rewrote the text: on page 4 line 9, “Moreover, conflicting scenarios (trade-offs) between different routing strategies have been studied; for example, **avoiding contrail formation generally increases fuel use and CO<sub>2</sub> emissions**. Irvine et al. (2014) assessed a **the trade-off between climate impact of contrails contrail avoidance and extra increased CO<sub>2</sub> emission (~ extra increased fuel use)** for a single flight.”

- (17) Pg3: Line 2: Presumably this is global-mean temperature response? Please specify.

Reply: The referee is right. This represents the global-mean temperature response. Unfortunately, this part is deleted by following the referee comment (18). Please see the reply to the comment (18) below.

- (18) Pg3: Line 5: what about the other way around, does a cost-optimized route increase climate impact?

Reply: In this paragraph (on page 2 line 34 - on page 3 line 5), Lührs et al. (2016) clearly show a trade-off between climate impact and economic cost. Thus, as the referee pointed out, one can say that the cost-optimized route increases climate impact with a decrease in cost, compared to the climate-optimized route.

On the other hand, we deleted this paragraph to shorten the introduction by following the referee's general comment. This paragraph introduces the study of Lührs et al. (2016) which clearly shows the trade-off between climate impact and economic costs; however, the previous paragraph (on page 2 lines 20-33) has already introduced two studies to show the same trade-off on the basis of the same climate metrics CCFs. Thus, this paragraph would be redundant. On page 2 line 34, “~~Lührs et al. (2016) performed a flight trajectory optimization for nine sample trans-Atlantic routes for a specific weather pattern in winter by the Trajectory Optimization Module (TOM). The trajectories were optimized for economic cost (expressed by the cash operating cost (COC; Liebeck et al., 1995; see Sect. 2.5.6), which is commonly used as a criterion for airline economies) and for climate impact (measured as average temperature response estimated by integrating the CCFs). The results showed that the climate-optimal route differed from the cost-optimal route. The climate-optimum trajectory (3D-optimized trajectory in lateral and vertical) decreased the climate impact by about 45 % over that of the economical route, whereas it increased COC by 2 %. Thus, the climate impact drastically decreased with a small increase of economic cost.”~~

Related to this, we moved the reference “Lührs et al. (2016)” from the current position (on page 2 line 34) to another position: on page 2 line 21, “... 2013; Søvde et al., 2014; **Lührs et al., 2016**....” In addition, we rewrote the text, because the deleted paragraph refers to the word “COC” for the first time in the present manuscript: on page 3 line 29, “... simple operating cost (SOC), **cash operating cost** (COC), and climate impact....”

- (19) Pg3: Line 6: do you mean using different emission metrics, of which AGTP is one? And which other metrics do you find in the literature? Here you only describe one approach. (from here on I do not list language issues, but note that there are a number of them also in the next pages...)

Reply: Yes. We believe that it is important to show that the benefit of the climate-optimized routing is confirmed on the basis of different climate assessment metrics (AGTP is one of them). On page 3 line 6, Ng et al. (2014) clarified the benefit by using the three AGTP values for the short (25 years), medium (50 years) and long-term (100 years) climate goals. As we only described the results for the medium-term climate goal in the present manuscript, we added the text below to the revised manuscript.

As the referee pointed out, there are other climate metrics. For example, Grewe et al. (2014a) compared the trade-off between economic costs and climate impact from one-day trans-Atlantic air traffic simulations with respect to three climate metrics. The results indicated that all metrics show a similar trade-off between economic costs and climate impact. We believe that this information would be useful for readers, and thus we added this information to the revised manuscript.

Finally, we rewrote the text: on page 3 line 14, “... between climate impact and economic cost.; **this trade-off was also found for the short-term (25 years) and long-term (100 years) climate goals. Grewe et al. (2014a) compared the trade-off between economic costs and climate impact from the one-day trans-Atlantic air traffic simulations described above with respect to three climate metrics: the average temperature response with future increasing emissions (F-ATR20) and the absolute global warming**

**potential with pulse emissions at a 20 year time horizon (P-AGWP20) for short-term climate impacts, and P-AGWP100 (time horizon of 100 years) for long-term climate impacts. The trade-offs obtained with the three metrics were very similar.”**

Concerning language issues, we rechecked the manuscript and added some modifications to the revised manuscript. We list them in the reply to the referee’s general comment.

- (20) Pg8: Section 2.5.4: The treatment of contrail-cirrus is quite essential for routing strategies and I would like to see some more details of how this is done and what the limitations are (e.g., natural cloud suppression, life cycle etc.) here, not just a reference to earlier work.

Reply: Thank you very much. We rewrote the paragraph to describe more details of how this routing option is made and its limitations: on page 8 line 9, “Yin et al. (2018a) and Yin et al. (manuscript in preparation, 2019) developed the routing option ~~for contrail avoidance to avoid contrail formations by using the submodel CONTRAIL (version 1.0; Frömming et al., 2014)~~, which calculates the potential persistent contrail cirrus coverage Potcov (Ponater et al., 2002; Burkhardt et al., 2008; Burkhardt and Kärcher, 2009; Grewe et al. 2014b) within an EMAC grid box. This option avoids regions where persistent contrail formation is expected. The Potcov represents the fraction of the grid box, which can be maximally covered by contrails under the simulated atmospheric condition. The threshold for contrail formation is determined from a parameterization scheme based on the thermodynamic theory of contrails, i.e., the Schmidt-Appleman theory (Schmidt, 1941; Appleman, 1953; Schumann, 1996). In the CONTRAIL submodel, Potcov indicates the difference between the maximum possible coverage of both, contrails and cirrus, and the coverage of natural cirrus alone; values of Potcov along the waypoints are taken from the nearest grid box (Table 2). With that, we define a contrail distance (PCC<sub>dist</sub>) in km(contrail) as Potcov multiplied by the flight distance in km. The corresponding routing option minimizes the total contrail distance of a flight and thus the objective function represents a total contrail distance km(contrail) of a flight is formulated as:....”

In addition, we rewrote the text: on page 8 lines 14-19 in the same paragraph, “PCC<sub>dist,i</sub> is calculated by using the potential contrail coverage Potcov (Ponater et al., 2002; Burkhardt et al., 2008; Burkhardt and Kärcher, 2009; details of Potcov have been reported by Frömming et al., 2014). The Potcov represents fractional areas in which contrails can maximally occur under a given atmospheric condition. The Potcov is calculated by the submodel CONTRAIL (version 1.0; Frömming et al., 2014), using a parameterization scheme based on the thermodynamic theory of contrails, i.e., the Schmidt-Appleman theory (Schmidt, 1941; Appleman, 1953; Schumann, 1996) Note that the objective function is formulated in the simple form to consider only the contrail distance. Thus, further physical processes such as contrail spreading, changes in contrail coverage area, contrail lifetime, and the contrail radiative forcing are not included.”

- (21) Pg9: Line 20: ATR20 needs a definition. Is it calculated based on input of RF? What is assumed for contrail-cirrus properties?

Reply: Thank you very much. We replied the three referee comments, respectively.

[“ATR20 needs a definition.”]

Table 2 (on page 26) included the definitions (equations) of the five ATR20s; however, as the referee noted, those definitions are important information for readers to understand the climate impact routing option. Thus, we moved those equations from Table 2 to Sect. 2.5.7 and rewrote the text as follows:

- On page 26 in Table 2 (the second group divided by rows), “ $ATR20_{O_3,r} = aCCF_{O_3,r} \times NO_{x,r} \times 10^{-3}$  See Eq. (8);  $ATR20_{CH_4,r} = aCCF_{CH_4,r} \times NO_{x,r} \times 10^{-3}$  See Eq. (9);  $ATR20_{H_2O,r} = aCCF_{H_2O,r} \times FUEL_i$  See Eq. (10);  $ATR20_{CO_2,r} = aCCF_{CO_2} \times FUEL_i$  See Eq. (11);  $ATR20_{\text{contrail},r} = aCCF_{\text{contrail},r} \times PCC_{\text{dist},i}$  See Eq. (12); See Eq. (8) See Eq. (13).”
- On page 9 line 20, “... ATR20s of ozone, methane, water vapour, CO<sub>2</sub>, and contrails are estimated on a per

unit basis by (the definition of the aCCFs are given in the Appendix and examples are shown in Fig. S1 in the Supplementary material).

$$\text{ATR20}_{\text{O}_3,i} = \text{aCCF}_{\text{O}_3,i} \text{NO}_{x,i} \times 10^{-3} \quad (8)$$

$$\text{ATR20}_{\text{CH}_4,i} = \text{aCCF}_{\text{CH}_4,i} \text{NO}_{x,i} \times 10^{-3} \quad (9)$$

$$\text{ATR20}_{\text{H}_2\text{O},i} = \text{aCCF}_{\text{H}_2\text{O},i} \text{FUEL}_i \quad (10)$$

$$\text{ATR20}_{\text{CO}_2,i} = \text{aCCF}_{\text{CO}_2} \text{FUEL}_i \quad (11)$$

$$\text{ATR20}_{\text{contrail},i} = \text{aCCF}_{\text{contrail},i} \text{PCC}_{\text{dist},i} \quad (12)$$

where the respective aCCF values of ozone, methane, water vapour, CO<sub>2</sub>, and contrails are given as flight properties at the  $i^{\text{th}}$  waypoint. These five ATR20s are....”

- On page 9 line 24, “ATR20<sub>total,i</sub> = ..., (8)(13).”
- On page 9 line 25, “ $f = \dots, (9)(14)$ .”

[“Is it calculated based on input of RF?”]

In AirTraf 2.0, ATR20s are calculated for the climate-optimized routing by using the algorithmic Climate Change Functions (aCCFs) of ozone, methane, water vapour, CO<sub>2</sub>, and contrails (shown in the Appendix), for which RF is not used as an input parameter. However, the aCCFs are approximation functions based on regression analyses for the CCFs data set (this point is described on page 9 line 18). As we reply to the referee comment (13), the CCFs data set was obtained from detailed EMAC model simulations including RF calculations (for contrails, the calculated RF data set was obtained in a different way; details are described in the “What is assumed for contrail-cirrus properties?” below); the CCFs data set describes the climate impact which is induced by ozone (plus ozone originating from methane changes), methane, H<sub>2</sub>O, CO<sub>2</sub>, and contrails. Thus, the aCCFs approximately express the climate impact (ATR20) by taking radiative impacts into account.

[“What is assumed for contrail-cirrus properties?”]

The ATR20 of contrails is calculated by using the approximation function of aCCF<sub>contrail</sub> in AirTraf 2.0; the aCCF<sub>contrail</sub> was created from contrail RF calculations based on the ERA-Interim reanalysis data and contrail trajectory data. To reply to this referee comment, let us explain the derivation of aCCF<sub>contrail</sub> briefly. First, the contrail RF data set was calculated following these steps:

- (a) Lagrangian trajectories (air parcels) were computed by using the ERA-Interim reanalysis data (the methodology is described by Irvine et al., 2014); the trajectories were initialized over the north Atlantic (1 degree horizontal spacing) at three vertical levels (300, 250 and 200 hPa) in winters of 1994, 1995 and 2003. The contrail lifetime was calculated by analyzing each of the trajectories to see how long the conditions persisted for: relative humidity with respect to ice above 98 % and a temperature below 235 K.
- (b) Contrail properties were calculated along the trajectories by following Schumann et al. (2017), where an effective radius for contrail cirrus ice particle was set to 23 microns described by Schumann et al. (2011). The contrail optical depth was calculated by a simple formula for the extinction coefficient (Unterstrasser and Gierens, 2010), where the initial contrail depth was set to 200 m (Grewe et al., 2014).
- (c) The long-wave and short-wave RFs were calculated from the trajectory data by using the parametric equations described by Schumann et al. (2012). The area covered by each contrail was assumed constant along the trajectory. By taking values from Grewe et al. (2014), we used a contrail width of 200 m, and a contrail length of the square root of the grid box area (1 degree by 1 degree grid). The net RF was calculated for each contrail and was converted to a global-mean value by following Grewe et al. (2014). The contrail RF data set was obtained, in which the lifetime of contrails ranges from 3 to 48 hours.

The aCCF<sub>contrail</sub> was derived based on regression analyses for the RF data set. The methodology was based on that used by van Manen and Grewe (2019) to derive the other aCCFs for ozone, methane and water vapour. For the regression analyses, a constraint on deriving aCCF<sub>contrail</sub> was that only meteorological information available at the time of flight can be used. In addition, we restricted the calculation to conventional meteorological data, so that aCCF<sub>contrail</sub> was simple to implement. This means, for example, no information on

the contrail lifetime could be used, because this is not something which can be estimated a priori from meteorological data. Since a lifetime was required to be input to the net RF calculations, we chose a contrail lifetime of six hours for all contrails, because 92 % of contrails have a lifetime up to six hours in the data set. Night-time and day-time contrails were analyzed separately. The night-time contrails referred to contrails with their entire (six hours) lifetime occurring at night; the day-time contrails referred to contrails which existed only during daylight hours and those which had part of their lifetime during the day. The obtained aCCF<sub>contrail</sub> (Eq. (A5) on page 15 in the Appendix) was converted from RF to ATR20 by multiplying a factor of 0.114 (provided by Katrin Dahlmann, DLR).

The derived aCCF<sub>contrail</sub> has been assessed by plotting the original net RF with the RF calculated by using aCCF<sub>contrail</sub>. In addition, the performance of aCCF<sub>contrail</sub> has been assessed against the rest of the contrails with lifetimes of 3 to 48 hours in the data set. The Spearman's rank correlation coefficient and the ability to correctly predict the sign of the forcing were examined. For day-time contrails with lifetimes of 6 hours, for example, the coefficient was  $R = 0.86$ , and the ability (in percentage) was 88 %; for those with lifetimes of 12 hours,  $R = 0.83$  and 78 % were obtained. These results provide the confidence in the use of aCCF<sub>contrail</sub> in the aircraft routing decision.

Here, we would like to make clear that the literature, which is given on page 9 lines 17-18, describes how to develop aCCFs from the CCFs data set, and their limitations in detail. The aCCFs are calculated online in EMAC by another submodel named ACCF in MESSy (version 2.54), and thus the AirTraf submodel uses the ACCF submodel for the climate routing option. In addition, the detailed description of the CCFs data set was added to the revised manuscript by following the referee comment (13).

Finally, we rewrote the text to show the relation between the CCFs data and the aCCFs more clearly: on page 9 line 18, “The aCCFs are approximation functions based on regression analyses for the simulated CCFs data set, which was obtained from detailed EMAC model simulations including radiative impacts (see Sect. 1); the CCFs data set for contrails was exceptionally obtained from contrail RF calculations based on the European Centre for Medium-Range Weather Forecasts (ECMWF) Re-Analysis Interim (ERA-Interim) data (Dee et al. 2011) and contrail trajectory data (Yin et al. (manuscript in preparation, 2019); the definition of the aCCFs are is provided in the Appendix and examples are shown in Fig. S1 in the Supplementary material). †The aCCFs represent....”

Related to this, we added this paper to the References:

– On page 17 line 32, “Dee, D. P., Uppala, S. M., Simmons, A. J., Berrisford, P., Poli, P., Kobayashi, S., Andrae, U., Balmaseda, M. A., Balsamo, G., Bauer, P., Bechtold, P., Beljaars, A. C. M., van de Berg, L., Bidlot, J., Bormann, N., Delsol, C., Dragani, R., Fuentes, M., Geer, A. J., Haimberger, L., Healy, S. B., Hersbach, H., Hólm, E. V., Isaksen, L., Kállberg, P., Köhler, M., Matricardi, M., McNally, A. P., Monge-Sanz, B. M., Morcrette, J.-J., Park, B-K., Peubey, C., de Rosnay, P., Tavolato, C., Thepaut, J-N., Vitart, F.: The ERA-Interim reanalysis: configuration and performance of the data assimilation system., Q. J. R. Meteorol. Soc., 137, 553–597, <https://doi.org/10.1002/qj.828>, 2011.”

#### References:

Grewe, V., Frömming, C., Matthes, S., Brinkop, S., Ponater, M., Dietmüller, S., Jöckel, P., Garny, H., Tsati, E., Dahlmann, K., et al.: Aircraft routing with minimal climate impact: the REACT4C climate cost function modelling approach (V1.0), Geoscientific Model Development, 7, 175–201, <https://doi.org/10.5194/gmd-7-175-2014>, 2014.

Irvine, E. A., Hoskins, B. J., Shine, K. P.: A Lagrangian analysis of ice-supersaturated air over the North Atlantic, J. Geophys. Res., 119, 1, 90–100, <https://doi.org/10.1002/2013JD020251>, 2014.

Schumann, U., Baumann, R., Baumgardner, D., Bedka, S. T., Duda, D. P., Freudenthaler, V., Gayet, J.-F., Heymsfield, A. J., Minnis, P., Quante, M., Raschke, E., Schlager, H., Vázquez-Navarro, M., Voigt, C., and Wang, Z.: Properties of individual contrails: a compilation of observations and some comparisons, Atmos.

Chem. Phys., 17, 403–438, <https://doi.org/10.5194/acp-17-403-2017>, 2017.

Schumann, U., Mayer, B., Graf, K., and Mannstein, H.: A Parametric Radiative Forcing Model for Contrail Cirrus, *Journal of Applied Meteorology and Climatology*, 51, 6, <https://doi.org/10.1175/JAMC-D-11-0242.1>, 1391–1406, 2012.

Schumann, U., Mayer, B., Gierens, K., Unterstrasser, S., Jessberger, P., Petzold, A., Voigt, C., and Gayet, J-F.: Effective Radius of Ice Particles in Cirrus and Contrails, *Journal of the Atmospheric Sciences*, 68, 2, 300–321, <https://doi.org/10.1175/2010JAS3562.1>, 2011.

Unterstrasser, S. and Gierens, K.: Numerical simulations of contrail-to-cirrus transition – Part 1: An extensive parametric study, *Atmos. Chem. Phys.*, 10, 2017–2036, <https://doi.org/10.5194/acp-10-2017-2010>, 2010.

Van Manen, J. and Grewe, V.: Algorithmic climate change functions for the use in eco-efficient flight planning, *Transportation Research Part D: Transport and Environment*, 67, 388–405, <https://doi.org/10.1016/j.trd.2018.12.016>, 2019.

- (22) Pg9: Line 26: But ATR20 is an average over 20 years? How can values be negative when the overall contrail-cirrus effect is a warming? Perhaps related to the above comment...

Reply: Yes. ATR20 represents an average over 20 years. In AirTraf 2.0, the ATR20 of contrails is calculated by using the approximation function of  $aCCF_{contrail}$ . The  $aCCF_{contrail}$  consists of two formulas for the day-time and night-time contrails, as shown in Eq. (A5) on page 15 in the Appendix. The  $aCCF_{contrail}$  for the day-time contrails can take positive and negative values, depending on the outgoing long-wave radiation (OLR) (the threshold is  $-193.18 \text{ Wm}^{-2}$ ), whereas the  $aCCF_{contrail}$  for the night-time contrails takes positive values.

In the revised manuscript, we rewrote the text to make clear the points described above:

- On page 9 line 26, “...  $ATR20_{contrail,i}$  can take positive and negative values, because of **the  $aCCF_{contrail}$  consists of two formulas for the day-time and night-time contrail effects (see Eqs. (12) and (A5) in the Appendix).**”
- On page 16 line 6 in the Appendix, “... calculated by AirClim. **The  $aCCF_{contrail}$  for the night-time contrails takes positive values; if the temperature is less than 201 K,  $aCCF_{contrail}$  for the night-time contrails is set to zero.** The  $aCCF_{contrail}$  for the day-time contrails can take positive and negative values, depending on the OLR (the threshold is  $-193.18 \text{ Wm}^{-2}$ ).” The rewriting highlighted by blue texts comes from our reply to the major comment (2) (starting with “Firstly, Eq. (A5) assumes”) of the referee #2.

This referee comment is related to the referee comment (21). We describe how  $ATR20_{contrail}$  is calculated in the AirTraf submodel, and how  $aCCF_{contrail}$  was created in the reply to the referee comment (21).

- (23) Pg10: Line 3: how sensitive are results and conclusions to the running of only one day? E.g., dependence on meteorological conditions that day?

Reply: We acknowledge that the simulation results depend on the atmospheric conditions of the target day. If we perform an AirTraf simulation with the same flight plan for another day, we obtain different optimized trajectories and performance measures. Thus, we clarified this point: on page 11 line 22, “Note that this performance is a narrow result obtained using AirTraf 2.0 under the specific conditions (e.g., the simulations were carried out with the 103 north-Atlantic flights on December 1, 2015...”); and on page 11 line 29, “The quantitative values of the changes in performance measures vary, depending on different methodologies, atmospheric conditions...”

We believe that it is an important point to examine whether the findings described in the Conclusions (e.g. the trade-off between the cost and the climate impact) are common under any atmospheric conditions. Actually, this is our next study. Recently, Yamashita et al. (2020) examined this for representative weather types over

the North Atlantic by using EMAC with AirTraf 2.0.

To emphasize the importance of the point, we added the text: on page 15 line 5, “The integration of AirTraf into EMAC allows one to optimize **flight trajectories** and to study flight trajectories **aircraft routings** under historical, present-day and future conditions of the climate system. **We acknowledge that the simulation results depend on the atmospheric conditions of the target day. Thus, it is important to examine whether the findings, e.g., the trade-off between the cost and the climate impact, are common under any atmospheric conditions.** Recently, Yamashita et al. (2020) examined this for **representative weather types over the North Atlantic by using EMAC with AirTraf 2.0.** Furthermore, the integrated aircraft routing options could be extended to conflicting scenarios. Recently, Yin et al. (2018a)....”

Related to this, we added the literature “Yamashita et al. (2020)” to the References: on page 21 line 25, “**Yamashita, H., Yin, F., Grewe, V., Jöckel, P., Matthes, S., Kern, B., Dahlmann, K., and Frömming, C.: Comparison of various aircraft routing strategies using the air traffic simulation model AirTraf 2.0, 3rd ECATS Conference, Gothenburg, Sweden, 1–4, 2020.**”

- (24) Pg10: Line 11: showing direct results is not a verification of simulations output.

Reply: Thank you very much. As the referee pointed out, the sentence starting with “To verify” is inappropriate. Section 3 focuses on a demonstration of AirTraf 2.0, and we intend to show the simulation output as an example in Sect. 3.2. On the other hand, Sect. 4 verifies the consistency of the simulation results with literature data. For the appropriate wording, we changed the word “verify” into the “demonstrate”: on page 10 line 11, “To **verify demonstrate** the simulation output...”; on page 14 line 24, “To **verify demonstrate** the submodel AirTraf 2.0, example simulations were carried out....”

This referee comment is related to the referee’s general comment: “While the discussion section is quite good, the result is only one page out of a 14-page paper, which is not quite convincing.” To provide convincing explanations for the simulation output, we analyzed the simulation results in more detail, added the two new figures “**Figure 3**” and “**Figure 5**”, and additionally wrote the text as follows:

[Section 3.2]

– On page 10 line 18, “... flight altitudes ( $\sim$ FL410, 12.5 km);, **Figure 3 shows the mean fuel consumption (in kg(fuel)/min<sup>-1</sup>) vs. mean flight altitude (in km) for individual flights for the three routing options.** Because fuel consumption decreases **due to as a result of aerodynamic drag reduction at high altitudes** (Fichter et al., 2005; Schumann et al., 2011; Yamashita et al., 2016), **the COC optimum trajectories select the high flight altitudes, as shown in Fig. 3. We acknowledge that limitations of BADA 3 affect the selection of the flight altitudes (the same applies to the fuel, the NO<sub>x</sub>, the H<sub>2</sub>O and the SOC options; see Fig. S3 in the Supplementary material).** According to Nuic et al. (2010), BADA 3 has a tendency to underestimate aircraft fuel consumption at high altitudes and Mach numbers, as the compressibility effect and wave drag are not modeled. These effects will cause differences in the selection of the flight altitudes.” This rewriting comes from our reply to the major comment (3) of the referee #2.

As we add the new figure, we changed the original figure number: on page 10 line 21, “Figure 34 shows ...”; on page 10 line 25, “... it is apparent from Fig. 34 ...”; and on page 24 in the caption, “Figure 34.”

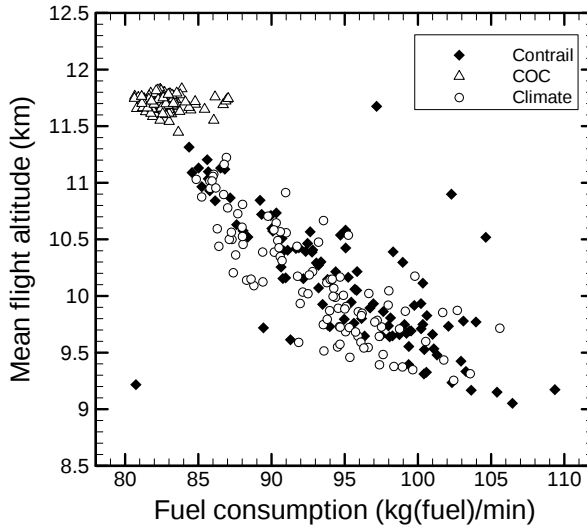


**Figure 3. Mean fuel consumption vs. mean flight altitude for 103 individual flights obtained by the contrail formation, the COC and the climate impact routing options.**

– On page 10 line 22, “We see from Figs. 4b, 4e and 4h that the contrail option certainly decreases the contrail distance formation, which is mostly located over northwest Europe and over the east coast of the U.S.;–Comparison of Figs. 4a, 4d and 4g shows that the COC option shows produces a narrower fuel distribution than that of the contrail and climate options; and In addition, Figs. 4c, 4f and 4i show that the climate option shows decreases the positive values of  $ATR20_{total}$  (warming effects) over northwest Europe and over the east coast of the U.S., and produces regionally negative values (cooling effects) near Iceland and over eastern Canada, which result in the net climate impact reduction (the local negative values, i.e. cooling effects, are mainly caused by contrails).”

[Section 3.3]

– On page 11 line 4, “**The individual routing options are now discussed in turn.** We see from Table 4 that the great circle option has the minimum flight distance **of  $660.3 \times 10^3$  km**, whereas this option increases **the** other measures. The time option shows the minimum flight time **of 739.4 h** with a **large** penalty on fuel use,  $NO_x$  emission....”

– On page 11 line 6, “... (further discussion in Sect. 4). **The fuel option shows the minimum fuel use of 3758.5 ton.** **Of the nine routing options,** ~~the~~ the fuel (and also the  $H_2O$ ), the  $NO_x$ , the SOC, and the COC options obtain similar values on all the measures (see also Supplement Fig. S4); ~~Of the nine routing options,~~ these options show decreased fuel use,  $NO_x$  and  $H_2O$  emissions....”

– On page 11 line 9, “... is considered significant for airline operations and thus is discussed **in more detail** in Sect. 4. The contrail option shows the minimum contrail distance **of  $26.3 \times 10^3$  km** and decreases the **second-lowest  $ATR20_{total}$  of  $3.45 \times 10^{-7}$  K**, whereas the other measures considerably increase **considerably**. This option allows aircraft to widely detour the potential contrail regions (because no constraint function is used in Eqs. (1) and (5); **see below for more discussion**). Thus, **the flight distance**, the flight time and the fuel use **drastically increase drastically**, which results in the increase of  $NO_x$  and  $H_2O$  emissions, SOC, and COC. **In particular,** ~~the~~ the contrail option shows the highest SOC and COC **of 5.99 Mil.USD** of the nine routing options.”

– On page 11 line 15, “The two options show similar values for all the measures and have the same minimum SOC **of 3.96 Mil.USD** and COC **of 5.35 Mil.USD**. This is because the objective function of the two options is

a function of flight time and fuel. In fact, the obtained optimum trajectories for the SOC and the COC those options are approximately the same (see Figs. 2c, 2d and Supplement Figs. S3k and S3l). This is because the objective function of the two options is a function of flight time and fuel, as defined in Eqs. (6) and (7). An interesting aspect of their performance measures is that both options do not correspond to the minimum flight time and fuel use (see further discussion in Sect. 4)."

– On page 11 line 18, "The climate option achieves the minimum  $ATR20_{total}$  of  $1.96 \times 10^{-7}$  K and decreases shows the second-shortest contrail distance of  $92.6 \times 10^3$  km, whereas this option increases all the other measures increase, particularly SOC and COC increase sharply this option shows the second-highest COC of 5.87 Mil.USD. The present results indicate that the contrail and the climate options considerably reduce the climate impact indicated by  $ATR20_{total}$ ; however, these options increase COC."

– On page 11 line 24, "Figure 5 shows the contrail distance (in  $\times 10^3$  km) vs.  $ATR20_{contrail}$  (in  $\times 10^{-7}$  K) for individual flights for the contrail, the COC, and the climate options. We see that the contrail option decreases the contrail distance drastically and shows the positive values of  $ATR20_{contrail}$  for almost all the flights. On the other hand, the climate option has the longer contrail distances than those of the contrail option (although the climate option achieves the second-shortest total contrail distance, as shown in Table 4) and shows the negative values of  $ATR20_{contrail}$  for many flights. These results imply that the contrail option minimizes the overall contrail distance at all times, whereas the climate option actively forms cooling contrails during the day and avoids the formation of warming contrails during the day and night." This rewriting comes from our reply to the major comment (4) of the referee #2.

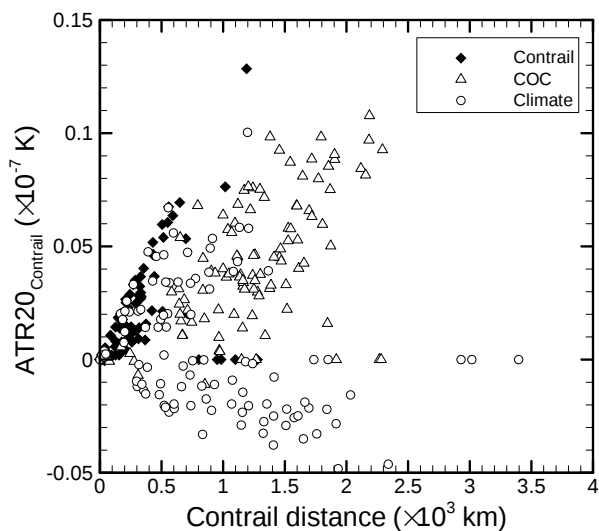


**Figure 5. Contrail distance vs.  $ATR20_{contrail}$  for 103 individual flights obtained by the contrail formation, the COC and the climate impact routing options.**

- (25) Pg10: Line 21: over what time frame is the km coverage estimated? Integrated over the 1-day simulations?

Reply: Yes. We integrated the contrail distance [km] of the total 103 flights over the target day. To clarify this point, we rewrote the text: on page 10 line 21, "Figure 3 shows the global fields of fuel use, contrail distance, and climate impact indicated by  $ATR20_{total}$  for the three options are shown in Fig. 3, where distributions represent sum of all the flights during the day."

- (26) Pg11: Line 2-3: this is a very strange argument for correctness.

Reply: We rewrote the text: on page 11 line 2, "These results confirm the correctness of the new routing

**options that the new routing options work correctly in AirTraf 2.0**, since we solve a single-objective minimization problem defined by Eq. (1)....”

- (27) Pg14: Line 10-11: how well does the treatment of contrails work for longer time integrations (in particular decades as mentioned earlier)? Is the potcov based on present day conditions?

Reply: This is an important point, and this referee comment is related to the referee comments (20), (21) and (22). The climate routing option uses  $aCCF_{contrail}$ . The  $aCCF_{contrail}$  estimates the anticipated climate impact of contrails  $ATR20_{contrail}$ , which is caused by local contrail formation during the present day, on the basis of the present day conditions including potcov; the calculated impact of contrails is integrated over time. As we reply to the referee comments (20), (21) and (22),  $aCCF_{contrail}$  (as shown in Eq. (A5) on page 15 in the Appendix) represents the climate impact of contrails, taking into account physical processes of contrails over a longer time period (e.g. contrail lifetime, contrail radiative forcing, etc.). This is because  $aCCF_{contrail}$  has been developed from the CCFs data sets obtained from contrail RF calculations based on the ERA-Interim reanalysis data and contrail trajectory data over a longer time period, in which such physical processes of contrails were included.

We believe that the replies to the referee comments (20), (21) and (22) describe this point in detail; those descriptions were added to the revised manuscript (please see the replies to the referee comments (20), (21) and (22)).

- (28) Pg14: Line 5-10: this type of information would be useful in the introduction.

Reply: Thank you very much. We moved the information from the current position (on page 14 lines 5-10) to the introduction, and then we rewrote the text as follows:

– On page 14 lines 4-11, “As discussed above, the many previous studies ~~verify corroborate~~ the consistency of the AirTraf simulations. Before concluding the discussion, two superior aspects of the AirTraf submodel are ~~emphasized, compared to the simulation models used in the previous studies. First, AirTraf enables an intercomparison for various aircraft routing options all at once, because all the options are integrated. Normally, one or two specific routing options are available for a flight trajectory optimization in other models. Second, AirTraf performs air traffic simulations not under ISA conditions, not under a fixed atmospheric condition for a specific day, but under comprehensive atmospheric conditions which are calculated by the chemistry-climate model EMAC. AirTraf can simulate air traffic for long-term period in EMAC, which enables one to examine effects of aircraft routing strategies on climate impact on a long time scale.”~~

– On page 4 line 11, “... for a single flight. AirTraf 2.0 enables analyzing those subjects all at once, because **all the options are integrated. Normally, one or two specific routing options are available for a flight trajectory optimization in other models. Another aspect to be emphasized compared to other models is that AirTraf performs air traffic simulations not under International Standard Atmospheric (ISA) conditions, not under a fixed atmospheric condition for a specific day, but under comprehensive atmospheric conditions which are calculated by EMAC; that is, AirTraf can simulate air traffic for long-term periods in EMAC, which enables one to examine effects of aircraft routing strategies on climate impact on a long time scale.** Last but not least, the aCCFs are new proxies....”

Related to this, we rewrote the following text, because the modified sentences described above refer to the word “ISA” for the first time in the revised manuscript: on page 12 line 8, “... respectively, under **International Standard Atmospheric (ISA) conditions. A typical single-aisle aircraft....”**

We are grateful to the referee #2 for the very helpful and encouraging comments on the original version of our manuscript. We took all comments into account and rewrote the manuscript accordingly. Here are our replies:

- This paper proposes an updated sub-model in the ECHAM Atmospheric Chemistry model for flight trajectory optimisation and is within the scope of the journal (GMD). The algorithm now enables the flight trajectory to be optimised based on various scenarios, which can assist relevant stakeholders and policymakers to evaluate the tradeoff between economic costs and the overall climate impact. Such a tool is expected to become increasingly important as the focus shifts to minimising aviation's overall environmental impact, including both CO<sub>2</sub> and non-CO<sub>2</sub> emissions.

While the work is well structured and written, there are several major aspects in the model that were not adequately addressed and must be significantly improved. Therefore, I believe that major revisions are necessary before this paper is accepted for publication.

Reply: We thank the referee #2 for these positive comments. We have addressed all the major and minor comments as follows.

- **Major Comments:**

1) [Page 6, Line 12] What is the rationale for selecting a 20-year time horizon for the average temperature response (ATR20)? Given that a proportion of CO<sub>2</sub> can remain in the atmosphere for over a millennium [Ref.1], the ATR20 can lead to a large underestimation in the CO<sub>2</sub> climate impacts. To overcome this, it is suggested that the authors perform a sensitivity analysis on the reported results by considering the use of different ATR time horizons (i.e. 100 years and 1000 years).

Reply: As the referee pointed out, a choice of the climate metric is an important issue. Grewe and Dahlmann (2015) pointed out that the different climate metrics, although targeting somehow climate change, provide "different physical quantities measuring climate change and hence they provide answers to different questions." From this viewpoint, we selected the climate metric of ATR20 on the basis of the five steps proposed by Grewe and Dahlmann (2015). First, we posed the detailed question: "what potential reduction in climate impact could be achieved by steadily applying a climate optimizing aircraft routing strategy in the next few decades?" From this objective, we considered a business-as-usual future air traffic scenario for one-day trans-Atlantic flights as a reference, and compared that to a scenario where we daily flew trans-Atlantic routings with a low climate impact. To answer the question, finally we selected an appropriate climate metric: the global and temporal average near-surface temperature response over 20 years after introducing the climate-optimized routing strategy. This metric enables the different climate relevant emissions to be placed on a common scale and thus be directly compared.

We have performed a sensitivity analysis on the climate metrics in previous research (Grewe et al., 2014). We optimized one-day trans-Atlantic air traffic with respect to three climate metrics: the average temperature response with future increasing emissions (F-ATR20) and the absolute global warming potential with pulse emissions at a 20 year time horizon (P-AGWP20) for short-term climate impacts, and P-AGWP100 (time horizon of 100 years) for long-term climate impacts. The results indicated that the Pareto fronts (optimal relation between climate change and costs) are similar for the three metrics (shown in Fig. 3 of Grewe et al., 2014). For each metric, the relative importance of individual species (CO<sub>2</sub>, contrails, ozone, methane, and total NO<sub>x</sub> (O<sub>3</sub> + CH<sub>4</sub> + PMO)) for a reduction of the climate impact was also investigated, and all metrics showed a similar pattern (shown in Fig. 4 of Grewe et al., 2014). These results were very robust in terms of dependence from the chosen metric and in terms of the role of individual components. We noticed that if we had adopted the more frequently used pulse-based metrics (e.g. Fuglestvedt et al., 2010), we would have found a much stronger sensitivity of the short-lived effects, e.g., contrails; the more contrast between the short-lived effects, such as contrails, and the long-lived emissions, such as CO<sub>2</sub>, would also be expected. However, these would not have been the best suited to quantifying the sustained impact of a permanent change in routing strategy on near-term climate change. That is, such metrics are not suitable to answer the aforementioned question.

On the basis of the rationale for selecting ATR20 described above, we applied the metric to the calculated RF, which was obtained from the detailed EMAC model simulations (for contrails, the RF data set was obtained in a different way; details are described in the reply to the referee major comment (2) starting with “Secondly, some contrails” below), and then obtained a relation between locally and temporarily specified emissions and the global-average impact on climate in terms of future temperature changes (ATR20). We call these 4-D response patterns as “climate-change functions (CCFs).” Algorithmic Climate Change Functions (aCCFs) are approximation functions based on regression analyses for the CCFs data set. Thus, aCCFs approximately express the climate impact indicated by ATR20. The aCCFs have already been published as the ACCF submodel in MESSy (version 2.54), and thus the AirTraf submodel uses the ACCF submodel for the climate-optimized routing. We would like to note that the literature, which is given on page 9 lines 17-18, describes how to develop aCCFs from the CCFs data set and why ATR20 was selected (e.g. Section 2.3 of van Manen and Grewe, 2019).

#### References:

Fuglestvedt, J. S., Shine, K. P., Berntsen, T., Cook, J., Lee, D. S., Stenke, A., Skeie, R. B., Velders, G. J. M., and Waitz, I. A.: Transport impacts on atmosphere and climate: metrics, *Atmospheric Environment*, 44, 4648–4677, <https://doi.org/10.1016/j.atmosenv.2009.04.044>, 2010.

Grewe, V., and Dahlmann, K.: How ambiguous are climate metrics? And are we prepared to assess and compare the climate impact of new air traffic technologies?, *Atmospheric Environment*, 106, 373–374, <https://doi.org/10.1016/j.atmosenv.2015.02.039>, 2015.

Grewe, V., Champougny, T., Matthes, S., Frömming, C., Brinkop, S., Søvde, O. A., Irvine, E. A., and Halscheidt, L.: Reduction of the air traffic’s contribution to climate change: A REACT4C case study, *Atmospheric Environment*, 94, 616–625, <https://doi.org/10.1016/j.atmosenv.2014.05.059>, 2014.

Van Manen, J. and Grewe, V.: Algorithmic climate change functions for the use in eco-efficient flight planning, *Transportation Research Part D: Transport and Environment*, 67, 388–405, <https://doi.org/10.1016/j.trd.2018.12.016>, 2019.

- 2) [Page 8, Section 2.5.4 and Appendix A] While the methodology selected to model the contrail climate impact was commonly used in previous studies, its limitations should be acknowledged and discussed in the paper. An optimization algorithm based on the contrail length might be overly simplistic because it does not account for differences in the contrail radiative forcing, lifetime and coverage area:

Reply: Thank you very much. We acknowledge that this routing option is the simple option for contrail avoidance and has limitations. Thus, we modified Section 2.5.4 to describe more details of what this routing option minimizes, and to clarify its limitations: on page 8 line 9, “... developed the routing option for contrail avoidance to avoid contrail formations by using the submodel CONTRAIL (version 1.0; Frömming et al., 2014), which calculates the potential persistent contrail cirrus coverage Potcov (Ponater et al., 2002; Burkhardt et al., 2008; Burkhardt and Kärcher, 2009; Grewe et al. 2014b) within an EMAC grid box. This option avoids regions where persistent contrail formation is expected. The Potcov represents the fraction of the grid box, which can be maximally covered by contrails under the simulated atmospheric condition. The threshold for contrail formation is determined from a parameterization scheme based on the thermodynamic theory of contrails, i.e., the Schmidt-Appleman theory (Schmidt, 1941; Appleman, 1953; Schumann, 1996). In the CONTRAIL submodel, Potcov indicates the difference between the maximum possible coverage of both, contrails and cirrus, and the coverage of natural cirrus alone; values of Potcov along the waypoints are taken from the nearest grid box (Table 2). With that, we define a contrail distance (PCC<sub>dist</sub>) in km(contrail) as Potcov multiplied by the flight distance in km. The corresponding routing option minimizes the total contrail distance of a flight and thus the objective function represents a total contrail distance km(contrail) of a flight is formulated as:....”

In addition, we added the text to the same Section 2.5.4: on page 8 line 19, “Note that the objective function

**is formulated in the simple form to consider only the contrail distance. Thus, further physical processes such as contrail spreading, changes in contrail coverage area, contrail lifetime, and the contrail radiative forcing are not included.”**

We believe that this contrail routing option (using  $PCC_{dist}$ ) is one of the important routing options to study characteristics of aircraft routing strategies regarding contrails. AirTraf 2.0 includes the climate routing option, in which contrail effects are included in a different way (using  $ATR20_{contrail}$ ). These two options work differently on contrail avoidance in flight trajectory optimizations; this interesting aspect is additionally discussed (please see the reply to the referee major comment (4)).

This modification is related to our reply to the comment (20) of referee #1.

- Firstly, Eq. (A5) assumes that contrails always cool during the day because it has a negative  $aCCF_{contrail}$  and  $ATR20_{contrail}$ . However, this is not true as many other studies have shown that contrails can either warm or cool during the day, depending on meteorology (such as ambient cirrus), radiation, and the solar zenith angle.

Reply: The  $aCCF_{contrail}$  for the day-time contrails, which is defined in Eq. (A5) on page 15 in the Appendix, can take positive and negative values, depending on the outgoing long-wave radiation (OLR) (the threshold is  $-193.18 \text{ Wm}^{-2}$ ).

Through the derivation process of  $aCCF_{contrail}$ , we have investigated the relationships between net RF for the day-time contrails and the relevant meteorological variables. The results showed the highest correlation with OLR ( $R = 0.86$ ), whereas the introduction of a second parameter, such as temperature and solar zenith angle, did not improve the correlation. Related to this, we are preparing another manuscript for Geoscientific Model Development, which is the model description paper on the submodel ACCF and describes the derivation of  $aCCF_{contrail}$  in detail; we refer to it as “Yin et al. (manuscript in preparation, 2019),” e.g. on page 9 line 18, and on page 15 line 14.

To make clear the point which the referee noted, we added the text: on page 16 line 6 in the Appendix, “... calculated by AirClim. **The  $aCCF_{contrail}$  for the night-time contrails takes positive values; if the temperature is less than 201 K,  $aCCF_{contrail}$  for the night-time contrails is set to zero. The  $aCCF_{contrail}$  for the day-time contrails can take positive and negative values, depending on the OLR (the threshold is  $-193.18 \text{ Wm}^{-2}$ ).**”

This modification is related to our reply to the comment (22) of referee #1.

- Secondly, some contrails formed during the day could also have lifetimes of up to 19 hours [Ref.2] and persist through the night, subsequently turning to a warming contrail, but the methodology does not appear to have considered the contrail lifetime. In Eq. (A5), it is also unclear on the conditions/time boundaries which constitutes as day-time and night-time.

Reply: Thank you very much. To reply to this referee comment and to the next referee comment, let us explain the derivation of  $aCCF_{contrail}$  briefly. First, the contrail RF data set was calculated following these steps:

- (a) Lagrangian trajectories (air parcels) were computed by using the ERA-Interim reanalysis data (the methodology is described by Irvine et al., 2014); the trajectories were initialized over the north Atlantic (1 degree horizontal spacing) at three vertical levels (300, 250 and 200 hPa) in winters of 1994, 1995 and 2003. The contrail lifetime was calculated by analyzing each of the trajectories to see how long the conditions persisted for: relative humidity with respect to ice above 98 % and a temperature below 235 K.
- (b) Contrail properties were calculated along the trajectories by following Schumann et al. (2017), where an effective radius for contrail cirrus ice particle was set to 23 microns described by Schumann et al. (2011). The contrail optical depth was calculated by a simple formula for the extinction coefficient (Unterstrasser

and Gierens, 2010), where the initial contrail depth was set to 200 m (Grewe et al., 2014).

(c) The long-wave and short-wave RFs were calculated from the trajectory data by using the parametric equations described by Schumann et al. (2012). The area covered by each contrail was assumed constant along the trajectory. By taking values from Grewe et al. (2014), we used a contrail width of 200 m, and a contrail length of the square root of the grid box area (1 degree by 1 degree grid). The net RF was calculated for each contrail and was converted to a global-mean value by following Grewe et al. (2014). The contrail RF data set was obtained, in which the lifetime of contrails ranges from 3 to 48 hours.

The  $aCCF_{contrail}$  was derived based on regression analyses for the RF data set. The methodology was based on that used by van Manen and Grewe (2019) to derive the other  $aCCFs$  for ozone, methane and water vapour. For the regression analyses, a constraint on deriving  $aCCF_{contrail}$  was that only meteorological information available at the time of flight can be used. In addition, we restricted the calculation to conventional meteorological data, so that  $aCCF_{contrail}$  was simple to implement. This means, for example, no information on the contrail lifetime could be used, because this is not something which can be estimated a priori from meteorological data. Since a lifetime was required to be input to the net RF calculations, we chose a contrail lifetime of six hours for all contrails, because 92 % of contrails have a lifetime up to six hours in the data set. Night-time and day-time contrails were analyzed separately. The night-time contrails referred to contrails with their entire (six hours) lifetime occurring at night; the day-time contrails referred to contrails which existed only during daylight hours and those which had part of their lifetime during the day. The obtained  $aCCF_{contrail}$  (Eq. (A5) on page 15 in the Appendix) was converted from RF to ATR20 by multiplying a factor of 0.114 (provided by Katrin Dahlmann, DLR).

The derived  $aCCF_{contrail}$  has been assessed by plotting the original net RF with the RF calculated by using  $aCCF_{contrail}$ . In addition, the performance of  $aCCF_{contrail}$  has been assessed against the rest of the contrails with lifetimes of 3 to 48 hours in the data set. The Spearman's rank correlation coefficient and the ability to correctly predict the sign of the forcing were examined. For day-time contrails with lifetimes of 6 hours, for example, the coefficient was  $R = 0.86$ , and the ability (in percentage) was 88 %; for those with lifetimes of 12 hours,  $R = 0.83$  and 78 % were obtained. These results provide the confidence in the use of  $aCCF_{contrail}$  (Eq. (A5)) in the aircraft routing decision.

As for the conditions/time boundaries, the procedure of calculating  $aCCF_{contrail}$  is as follows: for locations where contrails could form ( $potcov > 0$ ), the local time and solar zenith angle are calculated. If the contrail forms in darkness, the time of sunrise is then calculated. If the time between the local time and sunrise is greater than six hours, the night-time  $aCCF_{contrail}$  is applied. If the contrail forms in daylight, or in darkness but with less than six hours before sunrise, the day-time  $aCCF_{contrail}$  is applied. These calculations are implemented online in EMAC by another submodel named ACCF. The derivation of  $aCCF_{contrail}$  described above and details of the submodel ACCF will be described in the forthcoming paper of Yin et al. (manuscript in preparation, 2019), which is referred in the present manuscript, e.g. on page 9 line 18, and on page 15 line 14.

We believe that the conditions/time boundaries are useful information for readers. Thus, we added the text: on page 16 line 6 in the Appendix, “**As for the time boundaries of day and night, the local time and solar zenith angle are calculated for locations where contrails could form ( $potcov > 0$ ). For locations in darkness, the time of sunrise is then calculated. If the time between the local time and sunrise is greater than six hours, the  $aCCF_{contrail}$  for the night-time contrails is applied. If the contrail forms in daylight, or in darkness but with less than six hours before sunrise, the  $aCCF_{contrail}$  for the day-time contrails is applied. These calculations are performed online in EMAC by the submodel ACCF.**”

#### References:

Grewe, V., Frömming, C., Matthes, S., Brinkop, S., Ponater, M., Dietmüller, S., Jöckel, P., Garny, H., Tsati, E., Dahlmann, K., et al.: Aircraft routing with minimal climate impact: the REACT4C climate cost function modelling approach (V1.0), Geoscientific Model Development, 7, 175–201, <https://doi.org/10.5194/gmd-7-175-2014>, 2014.

Irvine, E. A., Hoskins, B. J., Shine, K. P.: A Lagrangian analysis of ice-supersaturated air over the North Atlantic, *J. Geophys. Res.*, 119, 1, 90–100, <https://doi.org/10.1002/2013JD020251>, 2014.

Schumann, U., Baumann, R., Baumgardner, D., Bedka, S. T., Duda, D. P., Freudenthaler, V., Gayet, J.-F., Heymsfield, A. J., Minnis, P., Quante, M., Raschke, E., Schlager, H., Vázquez-Navarro, M., Voigt, C., and Wang, Z.: Properties of individual contrails: a compilation of observations and some comparisons, *Atmos. Chem. Phys.*, 17, 403–438, <https://doi.org/10.5194/acp-17-403-2017>, 2017.

Schumann, U., Mayer, B., Graf, K., and Mannstein, H.: A Parametric Radiative Forcing Model for Contrail Cirrus, *Journal of Applied Meteorology and Climatology*, 51, 6, <https://doi.org/10.1175/JAMC-D-11-0242.1>, 1391–1406, 2012.

Schumann, U., Mayer, B., Gierens, K., Unterstrasser, S., Jessberger, P., Petzold, A., Voigt, C., and Gayet, J.-F.: Effective Radius of Ice Particles in Cirrus and Contrails, *Journal of the Atmospheric Sciences*, 68, 2, 300–321, <https://doi.org/10.1175/2010JAS3562.1>, 2011.

Unterstrasser, S. and Gierens, K.: Numerical simulations of contrail-to-cirrus transition – Part 1: An extensive parametric study, *Atmos. Chem. Phys.*, 10, 2017–2036, <https://doi.org/10.5194/acp-10-2017-2010>, 2010.

Van Manen, J. and Grewe, V.: Algorithmic climate change functions for the use in eco-efficient flight planning, *Transportation Research Part D: Transport and Environment*, 67, 388–405, <https://doi.org/10.1016/j.trd.2018.12.016>, 2019.

- Thirdly, the  $ATR20_{\text{contrail}}$  could also be influenced by contrail spreading and its coverage area. However, Eq. (A5) and “ $ATR20_{\text{contrail}} = aCCF_{\text{contrail}} \times PCC_{\text{dist}}$ ” does not account for the change in contrail coverage area. Further clarification on these aspects are required.

Reply: To calculate the contrail RF data set, which was used to derive  $aCCF_{\text{contrail}}$ , the area covered by each contrail was assumed constant along the contrail trajectory. By taking values from Grewe et al. (2014), we used a contrail width of 200 m, and a contrail length of the square root of the grid box area (1 degree by 1 degree grid). We believe that the replies to the referee major comment (2) (starting with “While the methodology”) and to the referee major comment mentioned above (starting with “Secondly, some contrails”) answer this referee comment. More details will be described in forthcoming paper of Yin et al. (manuscript in preparation, 2019), which is the model description paper on the submodel ACCF.

#### Reference:

Grewe, V., Frömming, C., Matthes, S., Brinkop, S., Ponater, M., Dietmüller, S., Jöckel, P., Garny, H., Tsati, E., Dahlmann, K., et al.: Aircraft routing with minimal climate impact: the REACT4C climate cost function modelling approach (V1.0), *Geoscientific Model Development*, 7, 175–201, <https://doi.org/10.5194/gmd-7-175-2014>, 2014.

- 3) [Page 10, Lines 17 to 19] The results and Figure 2 show that flight trajectories based on the cash operating cost (COC) optimization and minimum fuel consumption always selects a higher cruising altitude. However, this is very likely due to limitations of BADA 3. According to Nuic et al. [Ref.3], BADA 3 has a tendency to underestimate aircraft fuel consumption at higher altitudes and Mach numbers as the compressibility effect and wave drag are not modelled. While I understand that a more accurate version of BADA (BADA 4) is available, obtaining access to it can be challenging. Despite this, the authors should include more discussion on the effects of BADA 3 on their results, as well as acknowledge the limitations of BADA 3.

Reply: Thank you very much. We added the new figure “Figure 3” and rewrote the text to discuss the effects of BADA 3 and its limitations: on page 10 line 18, “... flight altitudes ( $\sim$ FL410, 12.5 km);. **Figure 3 shows the mean fuel consumption (in kg(fuel)/min<sup>-1</sup>) vs. mean flight altitude (in km) for individual flights for**

**the three routing options.** Because fuel consumption decreases due to as a result of aerodynamic drag reduction at high altitudes (Fichter et al., 2005; Schumann et al., 2011; Yamashita et al., 2016), the COC optimum trajectories select the high flight altitudes, as shown in Fig. 3. We acknowledge that limitations of BADA 3 affect the selection of the flight altitudes (the same applies to the fuel, the NO<sub>x</sub>, the H<sub>2</sub>O and the SOC options; see Fig. S3 in the Supplementary material). According to Nuic et al. (2010), BADA 3 has a tendency to underestimate aircraft fuel consumption at high altitudes and Mach numbers, as the compressibility effect and wave drag are not modeled. These effects will cause differences in the selection of the flight altitudes.”

Related to this, we added the paper to the References:

- On page 20 line 10, “Nuic, A., Poles, D., Mouillet, V.: BADA: An advanced aircraft performance model for present and future ATM systems, Int. J. Adapt. Control Signal Process., 24, 10, 850–866, <https://doi.org/10.1002/acs.1176>, 2010.”

As we add the new figure, we changed the original figure number: on page 10 line 21, “Figure 34 shows ...”; on page 10 line 25, “... it is apparent from Fig. 34 ...”; and on page 24 in the caption, “Figure 34.”

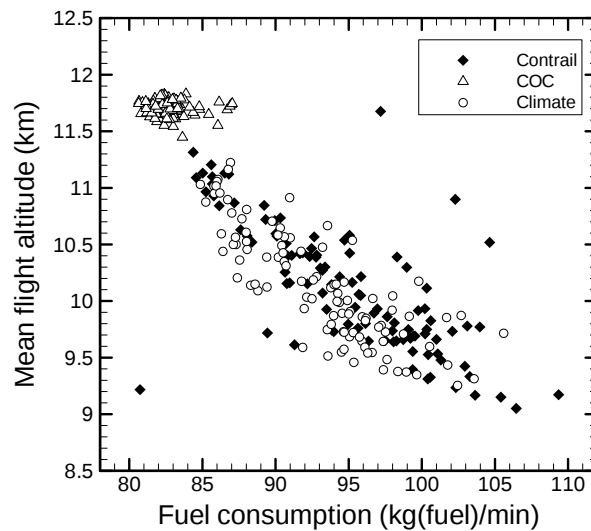


**Figure 3. Mean fuel consumption vs. mean flight altitude for 103 individual flights obtained by the contrail formation, the COC and the climate impact routing options.**

- 4) [Page 11, Lines 9 to 11] “The contrail option shows the minimum contrail distance and decreases ATR20<sub>total</sub>... This option allows aircraft to widely detour the potential contrail regions”. This sentence requires further clarification: given that the authors mentioned in Page 9 Line 26 that the “ATR20<sub>contrail</sub> can take positive and negative values, because of the day-time and night-time contrail effects”, it should be made clear in the discussion on if the algorithm: (i) actively forms cooling contrails during the day and avoids forming warming contrails during the night; or (ii) minimises the overall contrail length at all times.

Reply: Thank you very much. We added the new figure “Figure 5” and rewrote the text to make clear how the algorithm works on contrail avoidance: on page 11 line 11, “... is used in Eqs. (1) and (5); **see below for more discussion**”; and on page 11 line 24, “**Figure 5 shows the contrail distance (in  $\times 10^3$  km) vs. ATR20<sub>contrail</sub> (in  $\times 10^{-7}$  K) for individual flights for the contrail, the COC, and the climate options. We see that the contrail option decreases the contrail distance drastically and shows the positive values of ATR20<sub>contrail</sub> for almost all the flights. On the other hand, the climate option has the longer contrail distances than those of the contrail option (although the climate option achieves the second-shortest total contrail distance, as shown in Table 4) and shows the negative values of ATR20<sub>contrail</sub> for many flights. These results imply that the contrail option minimizes the overall contrail distance at all times, whereas the climate**

option actively forms cooling contrails during the day and avoids the formation of warming contrails during the day and night.”

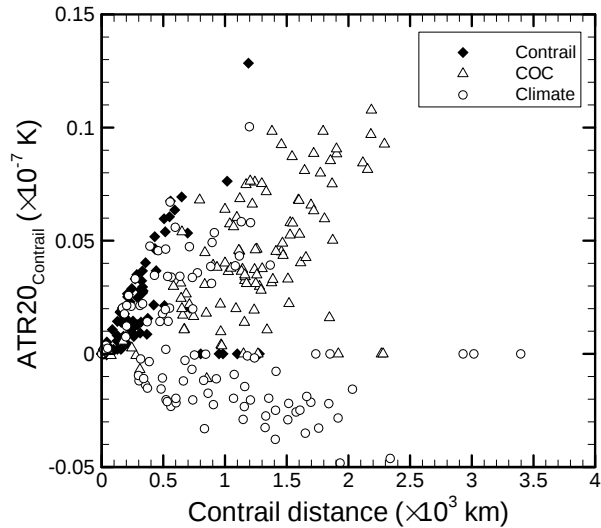


**Figure 5. Contrail distance vs. ATR20<sub>contrail</sub> for 103 individual flights obtained by the contrail formation, the COC and the climate impact routing options.**

- **Minor Comments:**

1) [Page 1, Line 22] Replace “non-volatile black carbon (BC or soot)” with “non-volatile particulate matter such as BC” for correctness in terminology [Ref.4]. This is because black carbon (BC) is a subset of non-volatile particulate matter (nvPM), while the term “soot” includes both nvPM (BC and metallic compounds) and organic compounds.

Reply: Thank you very much. We rewrote the word: on page 1 line 22, “... ~~nonvolatile black carbon (BC or soot)~~ **non-volatile particulate matter such as black carbon (BC)**....”

- 2) [Page 2, Line 7] The sentence, “The emitted CO<sub>2</sub> has a long residence time (a century)”, should be corrected. According to Joos et al.1, however, the emitted CO<sub>2</sub> can remain in the atmosphere after a millennium.

Reply: Thank you very much. In this sentence, we would like to note a long-lasting CO<sub>2</sub> impact in the atmosphere. Thus, we modified the sentence: on page 2 line 6, “~~The emitted CO<sub>2</sub> has a long residence time (a century) and becomes uniformly mixed in the whole atmosphere, the emitted CO<sub>2</sub> becomes uniformly mixed in the whole atmosphere and its perturbation remains for millennia.~~” This modification is related to our reply to the comment (9) of the referee #1.

- 3) [Page 3, Line 15] Remove “the” from this sentence “the today’s aircraft routing focuses on the minimum economic cost”.

Reply: We removed the word “the” from the sentence: on page 3 line 15, “... ~~the~~ today’s aircraft routing focuses on ~~the~~ minimum economic cost....”

- 4) [Page 8, Line 22] There appears to be inconsistencies in the acronyms:  $C_{time}$  and  $C_{fuel}$  was used in line 22. However,  $c_t$  and  $c_f$  are used in Eq. (6). This can confuse future readers.

Reply: Thank you very much. On page 8 line 22, we explain the definition of the cost index: Cost Index (CI) = time cost / fuel cost, where CI is a kind of dimensionless coefficient showing the ratio of time cost

[USDollar] to fuel cost [USDollar]; and  $C_{\text{time}}$  and  $C_{\text{fuel}}$  represent the “time cost” and the “fuel cost” of the definition. On the other hand,  $c_t$  and  $c_f$  used in Eq. (6) are the unit costs of time [USDollar/s] and fuel [USDollar/kg(fuel)], respectively, as listed in Table 1. Thus,  $C_{\text{time}}$  and  $C_{\text{fuel}}$  are different from  $c_t$  and  $c_f$ , respectively.

We agree that those parameters can confuse readers, and thus we rewrote the sentence: on page 8 line 22, “(CI =  $C_{\text{time}}$  time cost /  $C_{\text{fuel}}$  fuel cost, where C denotes a cost).” Related to this, we moved the phrase “where C denotes a cost” from the current position to the new position: on page 9 lines 13-14, “ $f = \text{COC} = \dots + C_{\text{engine}}$ , where C denotes a cost. A detailed....”

- 5) [Section 2.5.7] Please acknowledge the large uncertainties in the global temperature response, especially from contrails ( $\text{ATR20}_{\text{contrail}}$ ) due to uncertainties in the contrail efficacy [Ref.5,6].

Reply: We added the sentence to acknowledge the point: on page 9 line 26, “...  $\text{ATR20}_{\text{contrail},i}$  can take positive and negative values, because of the aCCF<sub>contrail</sub> consists of two formulas for the day-time and night-time contrail effects (see Eqs. (12) and (A5) in the Appendix). We acknowledge the large uncertainties in the global temperature response, especially from contrails ( $\text{ATR20}_{\text{contrail}}$ ) due to uncertainties in the efficacy of the contrail forcing (Hansen et al., 2005; Ponater et al., 2005). In addition, the aCCFs are derived....” The rewriting highlighted by blue texts comes from our reply to the comment (22) of the referee #1.

Related to this, we added the two papers to the References:

- On page 19 line 4, “Hansen, J., Sato, M., Ruedy, R., Nazarenko, L., Lacis, A., Schmidt, G.A., Russell, G., Aleinov, I., Bauer, M., Bauer, S., Bell, N., Cairns, B., Canuto, V., Chandler, M., Cheng, Y., Genio, A. Del., Faluvegi, G., Fleming, E., Friend, A., et al.: Efficacy of climate forcings, *Journal of Geophysical Research: Atmospheres*, 110, D18104, 1–45, <https://doi.org/10.1029/2005JD005776>, 2005.”
- On page 20 line 15, “Ponater, M., Marquart, S., Sausen, R., Schumann, U.: On contrail climate sensitivity, *Geophysical Research Letters*, 32, L10706, 1–5, <https://doi.org/10.1029/2005GL022580>, 2005.”

- 6) [Section 4: Discussion] The authors should highlight that these results (climate benefits) is likely an upper limit, because airspace congestion and air traffic management could minimise the flexibility for flights to perform these trajectory optimisations.

Reply: We agree with the referee comment. We rewrote the text: on page 11 line 24, “... on December 1, 2015, as shown in Table 3). Finally, we believe that the climate benefits described above are most likely an upper limit, because airspace congestion and air traffic management could reduce the flexibility for flights to perform these trajectory optimizations.” Similarly, we added the sentence to the conclusions to highlight the same point: on page 15 line 1, “... performance than the contrail option. We believe that these climate benefits are most likely an upper limit. The simulation results were....”

- 7) [Eq. (5) and Table 1] Consider using different notations for the mass fuel flow rate ( $f_{\text{ref}}$ ), as this is similar to the objective function ( $f$ ) and can lead to confusion.

Reply: We understood the referee comment, and we reconsidered to change the notation of  $f_{\text{ref}}$ . Nevertheless, we are hesitating to change it, because “ $f_{\text{ref}}$ ” has been already used from the previous version of AirTraf 1.0 (Sect. 2.3, Sect. 2.6 and Table 1 of Yamashita et al., 2016). For the sake of consistency, it could be better for readers to use the same notation. Nevertheless, if this change is essential for the revision of the manuscript, we will follow the suggestion by the referee #2 and change the notation, if the editor decides to do so.

Reference:

Yamashita, H., Grewe, V., Jöckel, P., Linke, F., Schaefer, M., and Sasaki, D.: Air traffic simulation in chemistry-climate model EMAC 2.41: AirTraf 1.0, *Geoscientific Model Development*, 9, 3363–3392, <https://doi.org/10.5194/gmd-9-3363-2016>, 2016.

- 8) [Appendix A, Eq. (A5)]  $aCCF_{contrail} = \dots$ , if  $Potcov \geq 0$ : should this be  $> 0$  instead? Similarly,  $aCCF_{contrail} = 0$ , if  $Potcov < 0$ : should this be  $\leq 0$  instead?

Reply: Thank you very much. We corrected the equations: on page 15 Appendix A, Eq. (A5),  $aCCF_{contrail} = \dots$ , if  $Potcov \geq 0$  .and. nighttime;  $aCCF_{contrail} = \dots$ , if  $Potcov \geq 0$  .and. daytime;  $aCCF_{contrail} = 0$ , if  $Potcov \leq 0$ .

### References provided by the referee #2

1. Joos F, Roth R, Fuglestvedt JS, Peters GP, Enting IG, von Bloh W, Brovkin V, Burke EJ, Eby M, Edwards NR, Friedrich T, Frölicher TL, Halloran PR, Holden PB, Jones C, Kleinen T, Mackenzie FT, Matsumoto K, Meinshausen M, et al. Carbon dioxide and climate impulse response functions for the computation of greenhouse gas metrics: a multi-model analysis. *Atmos Chem Phys*. 2013;13(5):2793-2825. doi:10.5194/acp-13-2793-2013.
2. Haywood JM, Allan RP, Bornemann J, Forster PM, Francis PN, Milton S, Rädel G, Rap A, Shine KP, Thorpe R. A case study of the radiative forcing of persistent contrails evolving into contrail-induced cirrus. *J Geophys Res Atmos*. 2009;114(D24201). doi:doi:10.1029/2009JD012650.
3. Nuic A, Poles D, Mouillet V. BADA: An advanced aircraft performance model for present and future ATM systems. *Int J Adapt Control Signal Process*. 2010;24(10):850-866. doi:10.1002/acs.1176.
4. Petzold A, Ogren JA, Fiebig M, Laj P, Li S-M, Baltensperger U, Holzer-Popp T, Kinne S, Pappalardo G, Sugimoto N. Recommendations for reporting “black carbon” measurements. *Atmos Chem Phys*. 2013;13(16):8365-8379.
5. Hansen J, Sato M, Ruedy R, Nazarenko L, Lacis A, Schmidt GA, Russell G, Aleinov I, Bauer M, Bauer S, Bell N, Cairns B, Canuto V, Chandler M, Cheng Y, Genio A Del, Faluvegi G, Fleming E, Friend A, et al. Efficacy of climate forcings. *J Geophys Res*. 2005;110(D18):D18104. doi:10.1029/2005JD005776.
6. Ponater M, Marquart S, Sausen R, Schumann U. On contrail climate sensitivity. *Geophys Res Lett*. 2005;32(10).

# Various Newly developed aircraft routing options for air traffic simulation in the chemistry-climate model EMAC 2.53: AirTraf 2.0

Hiroshi Yamashita<sup>1</sup>, Feijia Yin<sup>2</sup>, Volker Grewe<sup>1,2</sup>, Patrick Jöckel<sup>1</sup>, Sigrun Matthes<sup>1</sup>, Bastian Kern<sup>1</sup>, Katrin Dahlmann<sup>1</sup>, and Christine Frömming<sup>1</sup>

<sup>1</sup>Deutsches Zentrum für Luft- und Raumfahrt, Institut für Physik der Atmosphäre, Oberpfaffenhofen, Germany

<sup>2</sup>also at: Delft University of Technology, Aerospace Engineering, Delft, The Netherlands

**Correspondence:** H. Yamashita (hiroshi.yamashita@dlr.de)

**Abstract.** ~~Climate~~ Aviation contributes to climate change and the ~~climate~~ impact of aviation is expected to increase further. ~~Aircraft routings~~ Adaptions of aircraft routings in order to reduce the ~~climate impact~~ are an important ~~measure for climate impact~~ reductions. ~~To find an effective aircraft routing strategy for reducing the impact, the first version of the submodel AirTraf has been developed; this submodel can simulate global air traffic in the climate change mitigation measure.~~ The air traffic simulator AirTraf, as a submodel of the ECHAM/MESSy Atmospheric Chemistry (EMAC) model. ~~This paper describes the updated submodel AirTraf2.0. Seven new aircraft routing options are introduced, including contrail avoidance, minimum~~ enables the evaluation of such measures. For the first version of the submodel AirTraf, we concentrated on the general set-up of the model, including departure and arrival, performance and emissions, and technical aspects such as the parallelization of the aircraft trajectory calculation with only a limited set of optimization possibilities (time and distance). Here, in the second version of AirTraf, we focus on enlarging the objective functions by seven new options to enable assessing operational improvements in many more aspects including economic costs, ~~and minimum~~ contrail occurrence and climate impact. ~~Example~~ We verify that the AirTraf set-up, e.g. in terms of number and choice of design variables for the genetic algorithm, allows finding solutions even with highly structured fields such as contrail occurrence. This is shown by example simulations of the new routing options ~~are presented by using~~, including around 100 north-Atlantic flights of an Airbus A330 aircraft for a typical winter day. The results clearly show that ~~the family~~ AirTraf 2.0 can find the different families of optimum flight trajectories (three-dimensional) ~~varies according to the routing options. The comparison of the results for various routing options reveals characteristics of the routing with respect to air traffic performances~~ for specific routing options; those trajectories minimize the corresponding objective functions successfully. The minimum cost option ~~obtains a trade-off solution~~ lies between the minimum time and the minimum fuel ~~solutions~~ options. ~~Thus, aircraft operating costs are minimized by taking the best compromise between flight time and fuel use.~~ The aircraft routings for contrail avoidance and minimum climate impact reduce the potential climate impact, which is estimated by using algorithmic Climate Change Functions, whereas these two routings increase ~~flight~~ the aircraft operating costs. A trade-off between the aircraft operating costs and the climate impact is confirmed. The simulation results are compared with literature data and the consistency of the submodel AirTraf 2.0 is verified.

## 1 Introduction

Climate impact due to aviation emissions is an important issue. Nowadays the global aviation contributes only about 5 % to the anthropogenic climate impact (Skeie et al., 2009; Lee et al., 2009, 2010). ~~The aviation is not the largest contributor to climate impact at the moment (e.g., the road transport contributes 11 to the anthropogenic climate impact; Skeie et al., 2009)~~. However, 5 the aviation's contribution to climate impact is expected to increase further, because global air traffic strongly grows in terms of Revenue Passenger Kilometres (RPK) by 7.4 % in 2016 compared to 2015 (ICAO, 2017). The aviation climate impact consists of carbon dioxide (CO<sub>2</sub>) emissions and of non-CO<sub>2</sub> effects. The non-CO<sub>2</sub> effects comprise nitrogen oxides (NO<sub>x</sub>) leading to concentration changes of ozone and methane, water vapor (H<sub>2</sub>O), hydrocarbons (HC), carbon monoxide (CO), sulfur oxides (SO<sub>x</sub>), ~~nonvolatile~~ non-volatile particulate matter such as black carbon (BC or soot), persistent linear contrails, and contrail-10 induced cirrus clouds (Wuebbles et al., 2007; Lee et al., 2009; Brasseur et al., 2016). These effects change the radiative balance of the Earth's climate system and cause ~~a radiative impact (RI)~~. The RI radiative impact. The radiative impact potentially drives the climate system into a new state of equilibrium through temperature changes. Lee et al. (2009) stated that the CO<sub>2</sub> emission has the main impact and that the estimated RI radiative forcing (RF) of aviation CO<sub>2</sub> in 2005 was 28.0 mWm<sup>-2</sup> (15.2–40.8 mWm<sup>-2</sup>, 90 % likelihood range). The non-CO<sub>2</sub> emissions and the induced clouds also have a large effect on 15 RIsRFs; for example, the estimated RIsRFs in 2005 for total NO<sub>x</sub> and for persistent linear contrails were 12.6 mWm<sup>-2</sup> (3.8–15.7 mWm<sup>-2</sup>, 90 % likelihood range) and 11.8 mWm<sup>-2</sup> (5.4–25.6 mWm<sup>-2</sup>, 90 % likelihood range), respectively (Lee et al., 2009). Here, the difference between In particular, the radiative impact of contrails remains uncertain and recent studies report higher RF. Burkhardt and Kärcher (2011) estimated the contrail cirrus RF of 37.5 mWm<sup>-2</sup> for the year 2002; Schumann et al. (2015) reported the RF of 63 mWm<sup>-2</sup> for the year 2006; and Bock and Burkhardt (2016) estimated the RF of 20 56 mWm<sup>-2</sup> for the year 2006. As for time scales of their impacts is noted. The, the emitted CO<sub>2</sub> has a long residence time (a century) and becomes uniformly mixed in the whole atmosphere, i.e., its impact is proportional to fuel use and its perturbation remains for millennia. In contrast, the non-CO<sub>2</sub> effects occur on short time scales, e.g., the emitted NO<sub>x</sub> remains for a few 25 days to months; the contrails last several hours. Thus, the non-CO<sub>2</sub> effects depend strongly on the ambient (local) atmospheric conditions (Fichter et al., 2005; Mannstein et al., 2005; Gauss et al., 2006; Grewe and Stenke, 2008; Frömming et al., 2012; Brasseur et al., 2016; Lund et al., 2017). To investigate measures for reducing the aviation climate impact, the impact of both, CO<sub>2</sub> and non-CO<sub>2</sub> effects, must be considered; therefore, geographic location, altitude, the time of released non-CO<sub>2</sub> emissions and induced clouds, and corresponding local atmospheric conditions need to be considered.

In recent years, Grewe et al. (2017a, b) and Matthes et al. (2012, 2017) have proposed a climate-optimized routing as an important operational measure for reducing the aviation climate impact. This routing allows a significant reduction of the 30 climate impact by optimizing flight routes to avoid regions, where released emissions (including contrails) have a large climate impact. The climate-optimized routing is immediately applicable to present airline fleets. ~~Moreover, the routing can be used in addition to technological measures for reducing the aviation climate impact~~, whereas other, more technological measures (e.g., efficient engines, blended wing-body configurations, and laminar flow controls; Green, 2005) ~~require several years~~

before implementation. Moreover, the routing can be used in addition to the technological measures for reducing the aviation climate impact.

Benefits of the climate-optimized routing have been examined before (Gierens et al., 2008; Schumann et al., 2011; Sridhar et al., 2013; Søvde et al., 2014; Lührs et al., 2016); for example, Frömming et al. (2013) and Grewe et al. (2014b) developed Climate 5 Cost Functions (CCFs) for the climate-optimized routing. ~~The CCFs can identify climate sensitive regions with respect to They calculated global-average RFs resulting from local unit emissions (CO<sub>2</sub>, NO<sub>x</sub>, H<sub>2</sub>O and contrails) over the north-Atlantic for typical weather patterns by using the ECHAM/MESSy Atmospheric Chemistry (EMAC) model (Jöckel et al., 2010, 2016). Those RFs were used to calculate the global and temporal average near-surface temperature response over 20 years, which describe the climate impacts (i.e. future temperature changes) caused by those emissions on a per unit basis. The resulting data~~ 10 set is called the CCFs. The CCFs describe the climate impact which is induced by aviation's CO<sub>2</sub> and non-CO<sub>2</sub> effects (H<sub>2</sub>O, ozone, methane, ~~primary mode ozone~~ originating from methane changes, and contrails ~~) and estimate corresponding climate impacts. Here, ozone changes arizen from changes of methane are called primary mode ozone (Dahlmann et al., 2016).~~ including the spread into contrail-cirrus); and the CCFs of those effects except CO<sub>2</sub> are a function of geographic location, 15 altitude and time. Because of the long residence time of CO<sub>2</sub>, its impact is the same regardless of location, altitude and time of emission. The obtained CCFs can be used as a measure of the climate impact of aviation and form the basis for the climate-optimized routing. Grewe et al. (2014a) calculated the CCFs for a winter day and optimized one-day trans-Atlantic air traffic (391 eastbound and 394 westbound flights) using the CCFs in the ~~the~~ system for traffic assignment and analysis at macroscopic level (SAAM; Eurocontrol, 2012). They reported that the climate impact decreased by up to 25 % with a small increase in economic costs of less than 0.5 %. This revealed a great potential for the climate-optimized routing. On the other 20 hand, a trade-off between climate impact and economic cost existed, i.e., the climate-optimized and the cost-optimized routings were conflicting strategies. Grewe et al. (2017b) extended this study and investigated the feasibility of the climate-optimized routing for realistic conditions. Similar trans-Atlantic air traffic simulations (about 800 flights) were performed for five representative winter and three representative summer days, taking safety aspects into account. They found that a decrease in potential climate impact of 10 % was achieved by a cost increase of only 1 %.

25 ~~Lührs et al. (2016) performed a flight trajectory optimization for nine sample trans-Atlantic routes for a specific weather pattern in winter by the Trajectory Optimization Module (TOM). The trajectories were optimized for economic cost (expressed by the cash operating cost (COC; Liebeck et al., 1995; see Sect. 2.5.6), which is commonly used as a criterion for airline economies) and for climate impact (measured as average temperature response estimated by integrating the CCFs). The results showed that the climate-optimal route differed from the cost-optimal route. The climate-optimum trajectory (3D-optimized trajectory in lateral and vertical) decreased the climate impact by about 45 % over that of the economical route, whereas it increased COC by 2 %. Thus, the climate impact drastically decreased with a small increase of economic cost.~~

30 ~~In general, benefits of flying~~ The benefits of the climate-optimized ~~trajectories routing~~ were investigated by using different climate metrics. Ng et al. (2014) optimized flight trajectories for a total climate cost which was calculated by the absolute global temperature change potential (pulse AGTP values for three ~~different~~ time horizons; Shine et al., 2005) due to CO<sub>2</sub> emission and 35 contrails. A total of 960 trans-Atlantic flights (482 eastbound and 478 westbound flights) was analyzed for a specific summer

day. They reported that the climate-optimized routing reduced the total AGTP (for the medium-term climate goal, *i.e.*, the time horizon of 50 years) by 38 % with an additional flight time of 3.1 % and with extra fuel use of 3.1 % for the eastbound flights, whereas the routing reduced the total AGTP by 20 % with an additional flight time of 3.0 % and with extra fuel use of 3.7 % for the westbound flights. Generally, aircraft operating costs depend on time and on fuel. Thus, those results indicate 5 the aforementioned trade-off between climate impact and economic cost; this trade-off was also found for the short-term (25 years) and long-term (100 years) climate goals. Grewe et al. (2014a) compared the trade-off between economic costs and climate impact from the one-day trans-Atlantic air traffic simulations described above with respect to three climate metrics: the average temperature response with future increasing emissions (F-ATR20) and the absolute global warming potential with pulse emissions at a 20 year time horizon (P-AGWP20) for short-term climate impacts, and P-AGWP100 (time horizon of 100 10 years) for long-term climate impacts. The trade-offs obtained with the three metrics were very similar. Although many studies show the benefit of the climate-optimized routing, this routing is not used for the today's flight planning: the today's aircraft routing focuses on the minimum economic cost. However, if additional costs, such as environmental taxes, for aviation climate impact of CO<sub>2</sub> and non-CO<sub>2</sub> effects are included in the operating costs, a cost increase due to the climate-optimized routing is possibly compensated (Grewe et al., 2017b). This inclusion can change the current routing strategy, and incentivize airlines to 15 introduce a climate-optimized flight planning.

Here, we present an air traffic simulation model which serves as a basis for the following ultimate two aims: to investigate an eco-efficient aircraft routing strategy that reduces the climate impact of global air traffic over the next few decades, and to estimate its mitigation gain for different aircraft routing strategies. For these aims, the submodel AirTraf (version 1.0) has been developed as one of the submodels of the ECHAM/MESSy Atmospheric Chemistry (EMAC) model EMAC (Yamashita et al., 20 2015, 2016). AirTraf can simulate global air traffic in EMAC (online) for various aircraft routing strategies (options). Every flight trajectory is optimized for a selected routing option under daily changing local atmospheric conditions. AirTraf can take into account where and when aviation emissions are released or contrails form. The road map for our overall study has been shown elsewhere (Grewe et al., 2017b; Matthes et al., 2017).

This paper presents a technical description of AirTraf (version the new version of the submodel AirTraf 2.0). The simple aircraft routing options of great circle (minimum flight distance) and flight time (minimum time) were developed in the previous 25 version of AirTraf 1.0 (Yamashita et al., 2016). HereIn AirTraf 2.0, seven new aircraft routing options have been introduced: fuel use, NO<sub>x</sub> emission, H<sub>2</sub>O emission, contrail formation, simple operating cost (SOC), ~~CO~~ cash operating cost (COC), and climate impact estimated by the algorithmic Climate Change Functions (aCCFs; Van Manen, 2017; Yin et al., 2018a Yin et al., 2018b; Van Manen and Grewe, 2019; Yin et al. (manuscript in preparation, 20192020); the Climate Change Functions were previously 30 referred to as the Climate Cost Functions mentioned above). These options represent the objects to be minimized. Overall the nine options have been integrated in AirTraf 2.0, which enable air traffic simulations for the ultimate aims of our study (hereinafter the aircraft routing options are referred to simply as, e.g. the 'fuel option' 'fuel option'). Thus, the development described in this paper is an indispensable update. Moreover, this paper provides example applications of AirTraf 2.0. Some simulations of the nine routing options were carried out for trans-Atlantic routes for a typical winter day. Optimum flight 35 trajectories and characteristics of the routing options were analyzed.

Here, we ~~focus on the~~ mention the importance of the variety of the routing options. Various routing options have been made available in AirTraf 2.0, because not only the climate and the cost options, but also the other options are important subjects for air traffic routing studies. The time option is useful for delay recovery. ~~Delays~~ Because delays cause costs to airlines. ~~Thus~~, pilots are often forced to temporarily use the time option during a flight to maintain flight schedules, although the use of this option increases fuel costs (Cook et al., 2009). The NO<sub>x</sub> (Mulder and Ruijgrok, 2008) and contrail options (Fichter et al., 2005; Mannstein et al., 2005; Gierens et al., 2008; Sridhar et al., 2011; Schumann et al., 2011; Rosenow et al., 2017) have been examined as a routing strategy towards climate impact reduction. Moreover, conflicting scenarios (trade-offs) between different routing strategies have been studied; for example, ~~Irvine et al. (2014) assessed a~~ avoiding contrail formation generally increases fuel use and CO<sub>2</sub> emissions. Irvine et al. (2014) assessed the trade-off between ~~climate impact of contrails~~ and extra contrail avoidance and increased CO<sub>2</sub> emission ( $\sim$  ~~extra~~ increased fuel use) for a single flight. AirTraf 2.0 enables analyzing those subjects ~~-~~ all at once, because all the options are integrated. Normally, one or two specific routing options are available for a flight trajectory optimization in other models. Another aspect to be emphasized compared to other models is that AirTraf performs air traffic simulations not under International Standard Atmospheric (ISA) conditions, not under a fixed atmospheric condition for a specific day, but under comprehensive atmospheric conditions which are calculated by EMAC; that is, AirTraf can simulate air traffic for long-term periods in EMAC, which enables one to examine effects of aircraft routing strategies on climate impact on a long time scale. Last but not least, the aCCFs are new proxies for the climate-optimized routing. An important aim of the AirTraf development is to verify the aCCFs themselves and the routing strategy based on the aCCFs (i.e., the climate option) in multi-annual (long-term) simulations (Yin et al., 2018b).

This paper is organized as follows. Section 2 describes an overview of AirTraf 2.0. Particularly, key changes in the model components are stated. Section 3 presents the results and discussion for the example applications of AirTraf 2.0 using the nine routing options. Section 4 verifies the consistency of the results with literature data. Finally, Sect. 5 concludes this study.

## 2 Overview of AirTraf 2.0

### 2.1 Chemistry-climate model EMAC

The EMAC model is a numerical chemistry and climate simulation system that includes submodels describing tropospheric and middle atmosphere processes and their interaction with oceans, land, and influences coming from anthropogenic emissions (Jöckel et al., 2010, 2016). It uses the second version of the Modular Earth Submodel System (MESSy2) to link multi-institutional computer codes. The core atmospheric model is the 5th generation European Centre Hamburg general circulation model (ECHAM5; Roeckner et al., 2006). For the present study, we applied EMAC (ECHAM5 version 5.3.02 and MESSy version 2.53 updated from the version 2.41 for AirTraf 1.0) in the T42L31ECMWF resolution, i.e. with a spherical truncation of T42 (corresponding to a quadratic Gaussian grid of approximately 2.8° by 2.8° in latitude and longitude) with 31 vertical hybrid pressure levels up to 10 hPa (middle of the uppermost layer). The namelist setup for ECHAM5 simulations (referred to the E5 setup, no chemistry) was employed. Moreover, the submodel AirTraf was coupled to the submodel CONTRAIL (version 1.0; Frömming et al., 2014) for the contrail option, and to the submodel ACCF (version 1.0) for the climate option, using

the MESSy interfaces. Further information about MESSy, including the EMAC model system, is available from the MESSy Consortium Website (<http://www.messy-interface.org>).

## 2.2 Model components of submodel AirTraf

Figure 1 shows the flowchart of the submodel AirTraf 2.0. The present version is based on the model components of AirTraf 1.0. ~~Thus, and thus~~, this section outlines them ~~-(updates from AirTraf 1.0 are highlighted in Fig. 1)~~. First, air traffic data and AirTraf parameters are read in the main entry point `messy_initialize` (Fig. 1, dark blue). They consist of a one-day flight plan (including departure and arrival airport pairs, latitude and longitude of the airports, and departure time), Eurocontrol's Base of Aircraft Data (BADA Revision 3.9; Eurocontrol, 2011), ICAO engine performance data (ICAO, 2005), a load factor, jet fuel price, an aircraft routing option, etc. Any arbitrary number of flight plans is applicable and is reused for AirTraf simulations longer than two days. Table 1 lists the relevant data of an A330-301 aircraft and constant parameters used in AirTraf 2.0 ~~(the new parameters are listed in Table 1)~~. Second, all the entries are distributed in parallel by the message passing interface (MPI) standard (called for the main entry point `messy_init_memory`; Fig. 1, blue). Third, the air traffic simulation (called the AirTraf integration; Fig. 1, light blue) is called in the main entry point `messy_global_end`, considering local atmospheric conditions for every flight route. The AirTraf integration uses three modules: the aircraft routing module (Fig. 1, light green), the fuel-emissions-cost-climate calculation module (Fig. 1, light orange), and the flight trajectory optimization module (Fig. 1, dark green). The first module calculates flight trajectories corresponding to a selected routing option. The second module comprises a total energy model based on the BADA methodology (Eurocontrol, 2011; Schaefer, 2012) and the DLR fuel flow method (Deidewig et al., 1996). The third module consists of the Adaptive Range Multi-Objective Genetic Algorithm (ARMOGA version 1.2.0; Sasaki et al., 2002; Sasaki and Obayashi, 2004, 2005). Finally, simulation results are gathered from the MPI tasks. Optimum flight trajectories and global fields of flight properties (four-dimensional Gaussian grid; Fig. 1, rose red) are output. The same assumptions made in AirTraf 1.0 are applied in AirTraf 2.0, e.g., only the cruise flight phase is considered; trajectory conflicts and operating constraints (e.g., military air space) are neglected. Further details of the model components have been reported by Yamashita et al. (2016).

## 2.3 Calculation procedures of the AirTraf integration

AirTraf 2.0 follows the calculation procedures of AirTraf 1.0 described in detail in Sect. 2.4 of Yamashita et al. (2016). This section reviews the procedures of the AirTraf integration (Fig. 1, light blue) with emphasis on changes by introducing the new routing options.

A one-day flight plan includes departure time for every flight. A flight moves to the flying process (dashed box in Fig. 1, light blue) according to individual departure time in the time loop of EMAC. The flying process comprises four steps: flight trajectory calculation, fuel-emissions-cost-climate calculation, aircraft position calculation, and gathering global emissions (bold-black boxes in Fig. 1, light blue). The first step finds an optimum flight trajectory for a selected routing option by using the aircraft routing module (Fig. 1, light green) ~~, in which the seven new routing options are introduced in AirTraf 2.0~~. The flight trajectory optimization module (Fig. 1, dark green) executes the flight trajectory optimization under atmospheric

conditions at the departure day and time of the flight. Thus, the optimum flight trajectory varies day by day. Note that the three-dimensional wind components ( $u, v, w$ ) are considered in the flight trajectory optimization for all routing options. The resulting optimum flight trajectory consists of waypoints ( $i = 1, 2, \dots, n_{wp}$ ) and flight segments ( $i = 1, 2, \dots, n_{wp} - 1$ ), where  $i$  is the index arranged from the departure ( $i = 1$ ) to the arrival ( $i = n_{wp}$ ), and  $n_{wp}$  is the number of waypoints (see Fig. 3 of Yamashita et al., 2016). Table 2 lists flight properties calculated for the waypoints, the flight segments, and the whole trajectory. In AirTraf 2.0, 15 new properties are calculated, [as highlighted in Table 2](#).

The second step, which is linked to the fuel-emissions-cost-climate calculation module (Fig. 1, light orange), calculates the flight properties of fuel,  $NO_x$  emission, COC, etc. under the atmospheric conditions (Table 2, third group). This calculation is performed once at the departure time of the flight. [The methodologies of the fuel-emissions calculation module developed in AirTraf 1.0 are expanded in AirTraf 2.0](#). Details of the [fuel-emissions-cost-climate calculation module \(Fig. 1, light orange\)](#) [fuel-emissions calculation module](#) and its reliability have been reported in Sects. 2.5, 2.6, and 5 of Yamashita et al. (2016).

The third step moves the aircraft to a new position along the optimum flight trajectory corresponding to the time steps of EMAC, by referring to the estimated time when the aircraft passes through the waypoints (called the estimated time over ETO, Table 2).

At the fourth step, the individual flight properties corresponding to a flight path for one time step of EMAC are gathered into the aforementioned global fields:  $NO_x$  emission,  $H_2O$  emission, fuel use, flight distance, contrail distance ( $PCC_{dist}$ ), and average temperature responses for the time horizon of 20 years (ATR20s of ozone, methane, water vapor,  $CO_2$ , contrails, and total; see Sect. 2.5.7) are gathered along the flight segments (Table 2); [the global fields of  \$PCC\_{dist}\$  and ATR20s are newly calculated by AirTraf 2.0](#). If the aircraft reaches the last waypoint in the time loop of EMAC, the aircraft has landed (i.e., the flight quits) and the flying process ends for this flight.

## 2.4 Flight trajectory optimization

The flight trajectory optimization methodologies described by Yamashita et al. (2016) are also used for the new routing options and are outlined in this section. The flight trajectory optimization module (Fig. 1, dark green) executes the optimization. The module consists of ARMOGA (version 1.2.0; Sasaki et al., 2002; Sasaki and Obayashi, 2004, 2005), which is a stochastic optimization algorithm.

A solution  $\mathbf{x}$  (the term is synonymous with the flight trajectory) is a vector of  $n_{dv}$  design variables:  $\mathbf{x} = (x_1, x_2, \dots, x_{n_{dv}})^T$ , here  $n_{dv} = 11$ . With the design variable index  $j$  ( $j = 1, 2, \dots, n_{dv}$ ),  $x_j$  ( $j = 1, 2, \dots, 6$ ) indicate longitudes and latitudes, and  $x_j$  ( $j = 7, 8, \dots, 11$ ) indicate altitudes. The  $j^{\text{th}}$  design variable varies between lower and upper bounds  $[x_j^l, x_j^u]$ . The bounds of  $[x_j^l, x_j^u]$  ( $j = 1, 2, \dots, 6$ ) are automatically set for a given airport pair, whereas those of  $[x_j^l, x_j^u]$  ( $j = 7, 8, \dots, 11$ ) are set as  $[x_j^l, x_j^u] = [\text{FL290}, \text{FL410}]$  (flight levels; FL290 and FL410 denote 29 000 and 41 000 ft, respectively). Geographic locations of the airport pair are set according to the flight plan; altitudes of the airport pair are set to FL290. Given values of  $x_j$  ( $j = 1, 2, \dots, n_{dv}$ ), a three-dimensional flight trajectory is represented by a B-spline curve (third-order) between the airport pair (an illustration is given in Fig. 6 of Yamashita et al., 2016).

The initial population operator (Fig. 1, dark green) generates initial values of  $x_j$  ( $j = 1, 2, \dots, n_{dv}$ ) at random within the lower and upper bounds, and creates an initial population, which consists of “population,” which represents a random set of solutions (population approach; the population). The population size is set by  $n_p$ . An objective and ARMOGA starts its search with the solutions. An evaluation function  $f$  (called an objective function) is defined, depending on a selected routing option 5 (see Sect. 2.5), and a single-objective optimization problem can be written as follows:

$$\left. \begin{array}{l} \text{Minimize } f \\ \text{Subject to } x_j^l \leq x_j \leq x_j^u, \quad j = 1, 2, \dots, n_{dv} \end{array} \right\}, \quad (1)$$

where no constraint function is used. The ARMOGA solves the optimization problem by the following genetic operators: evaluation, selection, crossover, and mutation (Fig. 1, dark green; Holland, 1975; Goldberg, 1989). A value of  $f$  is calculated for each of the solutions by the evaluation operator. In this study, good solutions were identified in the population by the 10 Fonseca-Fleming Pareto ranking method (Fonseca et al., 1993); the stochastic universal sampling selection (Baker, 1985) was used for the selection operator to pick two solutions (parent solutions) from the population; the Blend crossover operator (BLX-alpha; Eshelman, 1993) was applied to the population parent solutions to create new solutions (child solutions) by picking two solutions (parent solutions) from the population; the revised polynomial mutation operator (Deb and Agrawal, 1999) was used to add a disturbance to the child solutions. When the evolution process is those processes are iterated for a number 15 of generations (the term “generation” represents one iteration of ARMOGA; this is set by  $n_g$ ), the population of solutions is improved by reducing  $f$ , and another superior population is created in subsequent generations. Finally, the ARMOGA finds the best solution (one optimum flight trajectory) with the minimum value of  $f$  through the whole generations; the flight properties of the solution are stored, as shown in Table 2. The flight trajectory optimization stated above is executed for every airport pair. Detailed descriptions of the optimization methodologies, appropriate ARMOGA parameter settings, and the accuracy of the 20 optimization module have been presented in Sect. 3.2 of Yamashita et al. (2016).

## 2.5 Formulations of objective functions for new aircraft routing options

Seven In AirTraf 2.0, seven new objective functions were developed for the new aircraft routing options. The following sub-sections describe formulations of the objective function  $f$  for those options. To calculate  $f$ , the fuel-emissions-cost-climate calculation module (Fig. 1, light orange) is used as necessary by the evaluation operator (Fig. 1, dark green) in the flight 25 trajectory optimization.

### 2.5.1 Fuel use

The objective function for the fuel option represents the sum of fuel use kg(fuel) of a flight:

$$f = \sum_{i=1}^{n_{wp}-1} \text{FUEL}_i, \quad (2)$$

where  $\text{FUEL}_i$  is the fuel use of the  $i^{\text{th}}$  flight segment (Table 2).

### 2.5.2 NO<sub>x</sub> emission

The objective function for the NO<sub>x</sub> option represents the sum of NO<sub>x</sub> emission g(NO<sub>x</sub>) of a flight:

$$f = \sum_{i=1}^{n_{wp}-1} NO_{x,i} = \sum_{i=1}^{n_{wp}-1} (FUEL_i EINO_{x,a,i}), \quad (3)$$

where NO<sub>x,i</sub> is the NO<sub>x</sub> emission of the *i*<sup>th</sup> flight segment; EINO<sub>x,a,i</sub> is the NO<sub>x</sub> emission index under actual flight conditions at the *i*<sup>th</sup> waypoint (Table 2) and is calculated using the ICAO engine performance data (ICAO, 2005; see Sect. 2.6 of Yamashita et al., 2016).

### 2.5.3 H<sub>2</sub>O emission

The objective function for the H<sub>2</sub>O option represents the sum of H<sub>2</sub>O emission g(H<sub>2</sub>O) of a flight:

$$f = \sum_{i=1}^{n_{wp}-1} H_2O_i = EIH_2O \sum_{i=1}^{n_{wp}-1} FUEL_i, \quad (4)$$

where H<sub>2</sub>O<sub>i</sub> is the H<sub>2</sub>O emission of the *i*<sup>th</sup> flight segment (Table 2); EI<sub>H<sub>2</sub>O</sub> is the emission index of H<sub>2</sub>O and was set as EI<sub>H<sub>2</sub>O</sub> = 1230 g(H<sub>2</sub>O)(kg(fuel))<sup>-1</sup> (Table 1). The H<sub>2</sub>O emission is proportional to the fuel use by assuming an ideal combustion of jet fuel. Thus, this option yields the same results as the fuel option in AirTraf 2.0. If an alternative fuel option is introduced, the H<sub>2</sub>O option probably differs from the fuel option, because the emission index may not be constant.

### 2.5.4 Contrail formation

Yin et al. (2018a) and Yin et al. (manuscript in preparation, 2019) developed the routing option for contrail avoidance. This option avoids regions where persistent contrail formation is expected. The objective function represents a total contrail distance to avoid contrail formations by using the submodel CONTRAIL (version 1.0; Frömming et al., 2014), which calculates the potential persistent contrail cirrus coverage Potcov (Ponater et al., 2002; Burkhardt et al., 2008; Burkhardt and Kärcher, 2009; Grewe et al., 2014b) within an EMAC grid box. The Potcov represents the fraction of the grid box, which can be maximally covered by contrails under the simulated atmospheric condition. The threshold for contrail formation is determined from a parameterization scheme based on the thermodynamic theory of contrails, i.e., the Schmidt-Appleman theory (Schmidt, 1941; Appleman, 1953; Schumann, 1996). In the CONTRAIL submodel, Potcov indicates the difference between the maximum possible coverage of both, contrails and cirrus, and the coverage of natural cirrus alone; values of Potcov along the waypoints are taken from the nearest grid box (Table 2). With that, we define a contrail distance (PCC<sub>dist</sub>) in km(contrail) as Potcov multiplied by the flight distance in km. The corresponding routing option minimizes the total contrail distance of a flight and thus the objective function is formulated as:

$$f = \sum_{i=1}^{n_{wp}-1} PCC_{dist,i} = 10^{-3} \sum_{i=1}^{n_{wp}-1} (POTCOV_i d_i), \quad (5)$$

where  $PCC_{dist,i}$  is the contrail distance of the  $i^{\text{th}}$  flight segment;  $Potcov_i$  is the potential persistent contrail cirrus coverage at the  $i^{\text{th}}$  waypoint; and  $d_i$  is the flight distance of the  $i^{\text{th}}$  flight segment (Table 2).  ~~$PCC_{dist,i}$  is calculated by using the potential contrail coverage Poteov (Ponater et al., 2002; Burkhardt et al., 2008; Burkhardt and Käreher, 2009; details of Poteov have been reported by Frömming et al., 2014). The Poteov represents fractional areas in which contrails can maximally occur under a given atmospheric condition. The Poteov is calculated by the submodel CONTRAIL (version 1.0; Frömming et al., 2014), using a parameterization scheme based on the thermodynamic theory of contrails, i.e., the Schmidt-Appleman theory (Schmidt, 1941; Appleman, 1953; Schumann, 1996)~~ Note that the objective function is formulated in the simple form to consider only the contrail distance. Thus, further physical processes such as contrail spreading, changes in contrail coverage area, contrail lifetime, and the contrail radiative forcing are not included.

### 10 2.5.5 Simple operating cost (SOC)

The cost index (CI) is set during a real flight to manage airline operation costs and is defined as the ratio of time cost to fuel cost ( ~~$CI = C_{\text{time}}/C_{\text{fuel}}$ , where  $C$  denotes a cost~~  $CI = \text{time cost}/\text{fuel cost}$ ). A low CI value causes an aircraft to minimize fuel use with a sacrifice of flight time, which enables a long-range flight. Conversely, a high CI value causes the aircraft to minimize flight time with an extra fuel use. Generally, the operating costs are a function of flight time and fuel. Thus, the minimum cost 15 solution lies in a trade-off between flight time and fuel (Cook et al., 2009; Marla et al., 2016). Here, the objective function simply represents the sum of the time and the fuel costs on the basis of the CI features:

$$f = SOC = c_t \sum_{i=1}^{n_{\text{wp}}-1} \frac{d_i}{V_{\text{ground},i}} + c_f \sum_{i=1}^{n_{\text{wp}}-1} \text{FUEL}_i, \quad (6)$$

where  $c_t$  and  $c_f$  are the unit costs of time and fuel, respectively (Table 1);  $V_{\text{ground},i}$  is the ground speed at the  $i^{\text{th}}$  waypoint (Table 2). Note that ~~the  $c_t$  includes the cost elements for flight crew, cabin crew, and maintenances for both, airframe and engines.~~

### 2.5.6 Cash operating cost (COC)

The COC is a comprehensive economic criterion for evaluating airline operation costs (Liebeck et al., 1995). The COC includes the cost elements for flight crew, cabin crew, landing fee, navigation fee, fuel, and maintenances for both, airframe and engines (no costs for depreciation, insurance, and interest are included). The COC calculation method for international 25 flights (Liebeck et al., 1995) was employed. Those cost elements were calculated on the basis of the price in 1993 and were scaled to 2015 by the average U.S. inflation rate of average consumer prices  $r_{\text{inf}}$  (Table 1; IMF, 2016). Only the fuel cost was directly calculated with the current jet fuel price JFP (Table 1; IATA, 2017). A block time and a block fuel originally used in the method were replaced by the total flight time FT and the fuel use of  $\sum_{i=1}^{n_{\text{wp}}-1} \text{FUEL}_i$  in AirTraf 2.0, respectively (Table 2). The objective function can be written as:

$$30 f = COC = C_{\text{flightcrew}} + C_{\text{cabincrew}} + C_{\text{landing}} + C_{\text{navigation}} + C_{\text{fuel}} + C_{\text{airframe}} + C_{\text{engine}}, \quad (7)$$

where  $C$  denotes a cost. A detailed description of the COC calculation method has been reported in Liebeck et al. (1995). Given the parameters and variables listed in Tables 1 and 2, Eq. (7) becomes a function of the flight time and the fuel.

### 2.5.7 Climate impact

The climate-optimized routing was carried out by using the aCCFs (Van Manen, 2017; Yin et al., 2018a Yin et al., 2018b; Van Manen and Grewe, 2019; Yin et al. (manuscript in preparation, 2019 2020)) calculated by the submodel ACCF. The aCCFs are approximation functions based on regression analyses for the simulated CCFs data set, which was obtained from detailed EMAC model simulations including radiative impacts (see Sect. 1); the CCFs data set for contrails was exceptionally obtained from contrail RF calculations based on the European Centre for Medium-Range Weather Forecasts (ECMWF) Re-Analysis Interim (ERA-Interim) data (Dee et al., 2011) and contrail trajectory data (Yin et al. (manuscript in preparation, 2020); the definition of the aCCFs is provided in the Appendix and examples are shown in Fig. S1 in the Supplementary material). The aCCFs represent a correlation of meteorological variables at the time of flight with anticipated climate impacts, i.e., ATR20s of ozone, methane, water vapour, CO<sub>2</sub>, and contrails are estimated on a per unit basis (the definition of the aCCFs are given in the Appendix and examples are shown in Fig. S1 in the Supplementary material). by

$$\text{ATR20}_{\text{O}_3,i} = \text{aCCF}_{\text{O}_3,i} \times \text{NO}_{x,i} \times 10^{-3}, \quad (8)$$

$$\text{ATR20}_{\text{CH}_4,i} = \text{aCCF}_{\text{CH}_4,i} \times \text{NO}_{x,i} \times 10^{-3}, \quad (9)$$

$$\text{ATR20}_{\text{H}_2\text{O},i} = \text{aCCF}_{\text{H}_2\text{O},i} \times \text{FUEL}_i, \quad (10)$$

$$\text{ATR20}_{\text{CO}_2,i} = \text{aCCF}_{\text{CO}_2} \times \text{FUEL}_i, \quad (11)$$

$$\text{ATR20}_{\text{contrail},i} = \text{aCCF}_{\text{contrail},i} \times \text{PCC}_{\text{dist},i}, \quad (12)$$

where the respective aCCF values of ozone, methane, water vapour, CO<sub>2</sub>, and contrails are given as flight properties at the  $i^{\text{th}}$  waypoint. These five ATR20s are calculated for flight segments (Table 2) and are combined into an objective function to represent an anticipated climate impact of a flight (in K):

$$\text{ATR20}_{\text{total},i} = \text{ATR20}_{\text{O}_3,i} + \text{ATR20}_{\text{CH}_4,i} + \text{ATR20}_{\text{H}_2\text{O},i} + \text{ATR20}_{\text{CO}_2,i} + \text{ATR20}_{\text{contrail},i}, \quad (13)$$

$$f = \sum_{i=1}^{n_{\text{wp}}-1} \text{ATR20}_{\text{total},i}, \quad (14)$$

where ATR20<sub>contrail,i</sub> can take positive and negative values, because of the aCCF<sub>contrail</sub> consists of two formulas for the day-time and night-time contrail effects. The (see Eq. (A5) in the Appendix). We acknowledge the large uncertainties in the global temperature response, especially from contrails (ATR20<sub>contrail</sub>) due to uncertainties in the efficacy of the contrail forcing (Hansen et al., 2005; Ponater et al., 2005). In addition, the aCCFs are derived based on the CCFs data of the north-Atlantic region and are applicable to the northern and high latitudes. Further details of the aCCFs have been reported in the literature mentioned above.

### 3 Example application: one-day simulation with new aircraft routing options

#### 3.1 Simulation setup

Nine one-day simulations were carried out for a demonstration of AirTraf 2.0. Table 3 lists the simulation setups. The same setups that we used for the consistency check for AirTraf 1.0 simulations (Yamashita et al., 2016) were employed; only the

5 simulation period was changed into a recent day, which showed a typical weather condition in winter with a strong jet stream (see Fig. S2 in the Supplementary material). The flight altitude for the great circle option was set to FL350; the altitude for the other options was calculated in the trajectory optimization within [FL290, FL410], as mentioned in Sect. 2.4. The trans-Atlantic flight plan (103 flights) of an Airbus A330 aircraft was provided by Grewe et al. (2014a) and REACT4C (2014). The setups for the optimization parameters were determined by the benchmark tests (Yamashita et al., 2016).

#### 10 3.2 Optimized flight trajectories and global fields

To ~~verify demonstrate~~ the simulation output, the obtained optimized trajectories and global fields for the contrail, the COC, and the climate options are shown. Figure 2 shows the optimized trajectories for those options (optimized trajectories for other options are shown in Supplement Fig. S3).

Obviously, the optimum trajectories vary with the routing options. Figures 2c and 2d show that the COC optimum trajectories of the eastbound flights leap up over the North Atlantic Ocean, whereas ~~these~~

15 ~~trajectories are shifted northward for the trajectories of~~ the westbound flights ~~are shifted northward~~. As the jet stream is located at around 50°W and 40°N (see Fig. S2 in the Supplementary material), the eastbound trajectories are optimized to benefit from tailwinds of the jet stream and the westbound trajectories avoid headwinds of the jet by detouring northward. In addition, most of those trajectories are located at high flight altitudes (~FL410, 12.5 km), ~~because fuel consumption decreases due to~~. ~~Figure 3 shows the mean fuel consumption (in kg(fuel)min<sup>-1</sup>) vs. mean flight altitude (in km) for individual flights for the three~~  
20 ~~routing options. Because fuel consumption decreases as a result of aerodynamic drag reduction at high altitudes~~ (Fichter et al., 2005; Schumann et al., 2011; Yamashita et al., 2016), ~~the COC optimum trajectories select the high flight altitudes, as shown~~  
25 ~~in Fig. 3. We acknowledge that limitations of BADA 3 affect the selection of the flight altitudes (the same applies to the fuel, the NO<sub>x</sub>, the H<sub>2</sub>O and the SOC options; see Fig. S3 in the Supplementary material). According to Nuic et al. (2010), BADA 3 has a tendency to underestimate aircraft fuel consumption at high altitudes and Mach numbers, as the compressibility effect and wave drag are not modeled. These effects will cause differences in the selection of the flight altitudes.~~ In contrast, the contrail and the climate options show complex shaped trajectories with various flight altitude changes (see Figs. 2a, 2b, 2e, and 2f).

~~Figure 3 shows the~~ The global fields of fuel use, contrail distance, and climate impact indicated by ATR20<sub>total</sub> for the three options. ~~We see are shown in Fig. 4, where distributions represent sum of all the flights during the day. We see from Figs.~~

30 ~~4b, 4e and 4h that the contrail option certainly decreases the contrail distance; the COC option shows the formation, which is mostly located over northwest Europe and over the east coast of the U.S. Comparison of Figs. 4a, 4d and 4g shows that the COC option produces a narrower fuel distribution than that of the contrail and climate options; and. In addition, Figs. 4c, 4f and 4i show that the climate option shows the net climate impact reduction (the local negative values, i.e. cooling effects, are~~

~~mainly caused by contrails~~) decreases the positive values of  $ATR20_{total}$  (warming effects) over northwest Europe and over the east coast of the U.S., and produces regionally negative values (cooling effects) near Iceland and over eastern Canada, which result in the net climate impact reduction. A comprehensive analysis of the optimized trajectories for the calculated fields is beyond the scope of this paper. However, it is apparent from Fig. 3–4 that the optimized trajectories successfully decrease the 5 respective objects (target measures) ~~to which should~~ be minimized (this point is discussed quantitatively in Sect. 3.3).

### 3.3 Characteristics of aircraft routing options

To examine the characteristics of the routing options, Table 4 lists a summary of ~~typical~~ ~~nine~~ performance measures of the one-day air traffic (total 103 flights) for specific routing options (bar charts are given in Supplement Fig. S4). Relative changes (in %) to the COC option are also listed in Table 4, considering this option as a reference (the COC option is assumed to be the 10 current aircraft routing strategy). Table 4 shows that individual options successfully minimize their own object (target measure; see measures marked with an asterisk in Table 4). These results confirm ~~the correctness of the that the~~ new routing options ~~in AirTraf~~ work correctly in AirTraf 2.0, since we solve a single-objective minimization problem defined by Eq. (1) for each routing option.

The individual routing options are now discussed in turn. We see from Table 4 that the great circle option has the minimum 15 flight distance ~~of  $660.3 \times 10^3$  km~~, whereas this option increases ~~the~~ other measures. The time option shows the minimum flight time ~~with a~~ ~~of 739.4 h with a large~~ penalty on fuel use,  $NO_x$  emission,  $H_2O$  emission, SOC, COC, and  $ATR20_{total}$  (further discussion in Sect. 4). The fuel option shows the minimum fuel use of 3758.5 ton. Of the nine routing options, the fuel (and also the  $H_2O$ ), the  $NO_x$ , the SOC, and the COC options obtain similar values on all the measures (see also Supplement Fig. S4). Of the nine routing options, these options show decreased fuel use,  $NO_x$  and  $H_2O$  emissions, SOC, and COC, whereas 20 contrail distance and  $ATR20_{total}$  increase. The difference among these options is considered significant for airline operations and thus is discussed in more detail in Sect. 4. The contrail option shows the minimum contrail distance ~~and decreases of  $26.3 \times 10^3$  km and the second-lowest  $ATR20_{total}$  of  $3.45 \times 10^{-7}$  K~~, whereas the other measures ~~considerably increase~~ increase considerably. This option allows aircraft to widely detour the potential contrail regions (because no constraint function is used in Eqs. (1) and (5); see below for more discussion). Thus, the flight distance, the flight time and the fuel use ~~drastically increase~~ 25 increase drastically, which results in the increase of  $NO_x$  and  $H_2O$  emissions, SOC, and COC. The In particular, the contrail option shows the highest ~~SOC and COC of COC of 5.99~~ Mil.USD of the nine routing options. Comparing the contrail option with the COC option indicates that the contrail distance decreases with an additional fuel use of  $8.3 \text{ kg(fuel)}(\text{km(contrail)})^{-1}$  (i.e., the additional COC of  $6.20 \text{ USD}(\text{km(contrail)})^{-1}$ ). The SOC and the COC options are comparable. The two options show similar values for all the measures and have the same minimum SOC ~~and COC~~. This is because the objective function of 30 the two options is a function of flight time and fuel ~~of 3.96~~ Mil.USD and COC of 5.35 Mil.USD. In fact, the obtained optimum trajectories for ~~the SOC and the COC those~~ options are approximately the same (see Figs. 2c, 2d and Supplement Figs. S3k and S3l). This is because the objective function of the two options is a function of flight time and fuel, as defined in Eqs. (6) and (7). An interesting aspect of their performance measures is that both options do not correspond to the minimum flight time and fuel use (see further discussion in Sect. 4). The climate option achieves the minimum  $ATR20_{total}$  ~~and decreases~~

the contrail distance, whereas this option increases all other measures, particularly SOC and COC increase sharply of  $1.96 \times 10^{-7}$  K and shows the second-shortest contrail distance of  $92.6 \times 10^3$  km, whereas the other measures increase, particularly this option shows the second-highest COC of 5.87 Mil.USD. The present results indicate that the contrail and the climate options considerably reduce the climate impact indicated by  $ATR20_{total}$ ; however, these options increase COC. The cost-benefit performance (i.e., the COC increment per  $ATR20_{total}$  reduction) for the contrail and the climate options are 0.24 and 0.13 Mil.USD( $10^{-7}$  K) $^{-1}$ , respectively. Thus, the climate option seems to be a more cost-effective option. Note that this performance is a narrow result obtained using AirTraf 2.0 under the specific conditions (e.g., the simulations were carried out with the 103 north-Atlantic flights on December 1, 2015, as shown in Table 3). Figure 5 shows the contrail distance (in  $10^3$  km) vs.  $ATR20_{contrail}$  (in  $10^{-7}$  K) for individual flights for the contrail, the COC, and the climate options. We see that the contrail option decreases the contrail distance drastically and shows the positive values of  $ATR20_{contrail}$  for almost all the flights. On the other hand, the climate option has the longer contrail distances than those of the contrail option (although the climate option achieves the second-shortest total contrail distance, as shown in Table 4) and shows the negative values of  $ATR20_{contrail}$  for many flights. These results imply that the contrail option minimizes the overall contrail distance at all times, whereas the climate option actively forms cooling contrails during the day and avoids the formation of warming contrails during the day and night. Finally, we believe that the climate benefits described above are most likely an upper limit, because airspace congestion and air traffic management could reduce the flexibility for flights to perform these trajectory optimizations.

#### 4 Discussion: verification of the one-day AirTraf simulation results

This paper presents the extended version of the submodel AirTraf, which offers additional aircraft routing options for defining overall target functions for aircraft the flight trajectory optimization. To confirm the consistency of AirTraf simulations, the relative changes in the performance measures among the routing options (listed in Table 4 in parentheses) are compared with previous studies. The quantitative values of the changes in the performance measures vary, depending on different methodologies, atmospheric conditions, simulation periods, flight plans, aircraft/engine types, cost/climate impact metrics, etc. Thus, a direct comparison in magnitude of our results with published studies is difficult; the sign of the relative changes in the measures is compared. Note that the great circle and the time options have been verified before (Yamashita et al., 2016). In addition, the  $H_2O$  option yields the same results as the fuel option (see Sect. 2.5.3 and Table 4); the SOC option is comparable to the COC option (see Sect. 3.3 and Table 4). Thus, we omit any discussion of the  $H_2O$  and the SOC options here.

First, the time, the fuel, and the COC options are analyzed. As defined in Sect. 2.5.6, COC is a combined function of flight time and fuel. To minimize COC, one may attempt to reduce both factors simultaneously; however, a trade-off between the flight time and the fuel generally exists. Table 4 shows that the time penalty of flying minimum fuel trajectories is 2.4 percentage points (%pt), whereas the fuel penalty of flying minimum time trajectories is 20.3 %pt. A similar trade-off was reported by two published studies. Celis et al. (2014) addressed a single-objective flight trajectory optimization on total flight time and fuel use, respectively, under International Standard Atmospheric (ISA) ISA conditions. A typical single-aisle aircraft (150 passengers) with twin turbofan engines was assumed; the aircraft speed and the flight altitude in eight flight segments

were optimized for a given flight trajectory (a quasi-full flight profile optimization). Compared to the minimum time trajectory, the fuel optimum trajectory decreased the fuel use by 31.7 %pt with increasing flight time by 14.0 %pt. Rosenow and Fricke (2016) compared performances for the minimum time and the minimum fuel trajectories for a flight from Frankfurt (Main) to Dubai for a Boeing B777 freighter on February 2, 2016, at 12 a.m. The comparison showed that the fuel optimum trajectory 5 decreased fuel use by 8.0 % with increasing time by 3.7 %. These studies imply that the minimum COC solution lies between the minimum time and the minimum fuel solutions. In fact, Table 4 shows that the COC option has more flight time than that of the time option, and that the COC option consumes more fuel than that of the fuel option. The COC option yields the values of compromise (i.e. not minimum) of flight time and fuel. Nonetheless, this option achieves the minimum COC. The submodel AirTraf 2.0 can consistently differentiate those three solutions.

10 To support the discussion above, the fuel and the COC options are compared in detail. Erzberger and Lee (1980) compared the minimum fuel and the minimum direct operating cost (DOC) trajectories for a short-haul route for a Boeing 727-100 aircraft on the basis of optimum control theory (Bryson and Ho, 1969) under U.S. Standard Atmospheric conditions. They showed that flying “minimum fuel” reduced fuel use by 6.9 %, whereas the time and the DOC penalties of the trajectory were 23 and 6 %, respectively (constrained thrust case). Our results in Table 4 show that the fuel option reduces fuel use by 0.1 %, whereas the 15 time and the COC penalties of the option are 0.1 and 0.03 %, compared to those measures of the COC option. The signs of these relative changes obtained from our results agree with those shown by Erzberger and Lee (1980). In addition, the time and the COC options are compared in a perspective of airline operating economics. Although the time option increases fuel use,  $\text{NO}_x$  emission,  $\text{H}_2\text{O}$  emission, SOC, COC, and ATR20<sub>total</sub> (fuel use and COC increase by 20.2 and by 6.1 %, respectively), the option decreases flight time by 2.3 %, compared to that of the COC option. In other words, the time option reduces flight 20 time with the extra cost of 19 034.74 USDh<sup>-1</sup> (= 269.66 EURmin<sup>-1</sup>; converted by 1 USD = 0.85 EUR on September 18, 2018 (European Central Bank, 2018)). In a context of delay recovery, this extra cost is the same order of magnitude to flight delay costs. If the flight delay costs exceed the extra cost due to the time option, operators would determine to fly faster by using the time option to recover the delay. Cook et al. (2004, 2009) reported that the flight delay costs, which are associated with delayed passengers, additional fuel use, flight crew, cabin crew, and marginal maintenance costs, reached several hundred 25 Euros per minute. The extra cost calculated from our results agrees well with this report.

Compared to the COC option, the  $\text{NO}_x$  option decreases the  $\text{NO}_x$  emission by 0.5 %, leading to a COC increase of 0.2 %. Mulder and Ruijgrok (2008) analyzed effects of varying cruise conditions on  $\text{NO}_x$  emission and on DOC from the cruise  $\text{NO}_x$  simulation model (Bremmers, 1999) by assuming a cruise range of 5800 km with a Boeing 747-400 aircraft under ISA conditions. They clearly concluded that a reduction of  $\text{NO}_x$  emission caused a cost increase. Our results agree well with this 30 conclusion. Moreover, the  $\text{NO}_x$  option differs from the fuel option, because the amount of  $\text{NO}_x$  emission depends not only on fuel use, but also on the  $\text{NO}_x$  emission index, as defined in Eq. (3). The emission index depends strongly on the ambient atmospheric conditions at every waypoint (see Sect. 2.6 of Yamashita et al., 2016). Table 4 shows that the  $\text{NO}_x$  option decreases the  $\text{NO}_x$  emission by 0.3 %pt, whereas this option increases flight time by 0.2 %pt and fuel use by 0.2 %pt, compared to those measures of the fuel option. Celis et al. (2014) addressed a single-objective flight trajectory optimization on total fuel use and 35 on  $\text{NO}_x$  emission, respectively, with the same simulation setup described above. Compared to the minimum fuel trajectory, the

minimum  $\text{NO}_x$  trajectory decreased  $\text{NO}_x$  emission by 10.4 %pt, whereas the trajectory increased time by 1.0 %pt and fuel use by 3.9 %pt. The signs of the relative changes obtained from our results are in good agreement with those shown by Celis et al. (2014).

The contrail option drastically decreases contrail distance by 79.8 % and  $\text{ATR20}_{\text{total}}$  by 43.4 %, whereas this option increases fuel use by 23.0 % and COC by 12.0 %, compared to those measures of the COC option. The contrail option is effective in order to reduce the climate impact, as pointed out by previous studies introduced in Sect. 1. Here, those relative changes in the measures are compared with two published studies. Rosenow et al. (2017) performed a one-day European's air traffic optimization on July 25, 2016. The total number of 13 584 flights over Europe (containing 16 aircraft types) was employed; their three dimensional flight profiles were optimized for airline costs (termed as the cost performance indicators CPI) and environmental impacts (termed as the ecological performance indicators EPI). They revealed that an additional contrail avoidance intent decreased contrail costs by 31.5 % (contrail formations were converted into a monetary value) and EPI by 5.2 %, whereas the intent increased fuel use by 0.05 % and CPI by 0.5 % over those of the minimum cost strategy. The signs of the relative changes obtained from our simulations are consistent with those shown by Rosenow et al. (2017). Furthermore, Sridhar et al. (2013) applied a contrail reducing strategy to aircraft flying between 12 airport pairs (287 flights) in the United States on April 12, 2010. The three-dimensional contrail reducing strategy showed a trade-off between contrail formation time (time spent in traveling through contrail formation regions) and fuel consumption. Representative points on the trade-off curve showed that the contrail formation time decreased by 4415 and by 5301 min with an additional fuel use of 20 000 and of 131 000 kg(fuel), respectively, over those of a wind-optimal strategy (this strategy is regarded as an economically optimal strategy; see Sect. 2.4 of Yamashita et al., 2016). This study clearly indicated the fuel increase by avoiding contrail formations. Our results agree well with the finding of Sridhar et al. (2013).

Table 4 clearly shows a trade-off between economic cost and climate impact (see also Supplement Fig. S4). Compared to the COC option, the climate option decreases  $\text{ATR20}_{\text{total}}$  by 67.9 % with an additional COC of 9.8 %. A similar trade-off certainly exists between the minimum COC and the minimum climate impact trajectories for each airport pair. The trade-off obtained from our results agrees with that indicated by many studies (see Sect. 1). Moreover, Niklaß et al. (2017) performed an aircraft trajectory optimization for nine north-Atlantic flight routes varying weighting factors on average temperature response over 100 years ( $\text{ATR100}$ ) and on COC under ISA conditions. They showed a clear trade-off between the cost and the climate impact. The minimum climate impact trajectories, on average, reduced  $\text{ATR100}$  by 28.4 % with an additional COC of 7.1 %, compared to those measures of the minimum COC trajectories. Our results agree with those shown by Niklaß et al. (2017).

As discussed above, the many previous studies ~~verify corroborate~~ the consistency of the AirTraf simulations. ~~Before concluding the discussion, two superior aspects of the AirTraf submodel are emphasized, compared to the simulation models used in the previous studies. First, AirTraf enables an intercomparison for various aircraft routing options all at once, because all the options are integrated. Normally, one or two specific routing options are available for a flight trajectory optimization in other models. Second, AirTraf performs air traffic simulations not under ISA conditions, not under a fixed atmospheric condition for a specific day, but under comprehensive atmospheric conditions which are calculated by the chemistry-climate model~~

~~EMAC. AirTraf can simulate air traffic for long-term period in EMAC, which enables one to examine effects of aircraft routing strategies on climate impact on a long time scale.~~

## 5 Conclusions

We introduced updates to the air traffic simulation model AirTraf in the chemistry-climate model EMAC. The submodel AirTraf 2.0 was developed according to the MESSy standard and was described in detail in this paper. This submodel introduces seven new aircraft routing options for air traffic simulations: the fuel use, the  $\text{NO}_x$  emission, the  $\text{H}_2\text{O}$  emission, the contrail formation, the simple operating cost, the cash operating cost, and the climate impact options. Our flight trajectory optimization methodology consists of genetic algorithms; the methodology was similarly used and was validated beforehand (Yamashita et al., 2016). The particular strength of AirTraf is to enable a flight trajectory optimization for a global flight movement set in the atmosphere which is comprehensively described by EMAC. The novel routing option, i.e., the climate impact option, has been integrated in AirTraf 2.0. This option uses meteorological variables in terms of (spatially and temporally varying) aviation climate impact estimated by the aCCFs, and optimizes flight trajectories by minimizing their anticipated climate impact. As the aCCFs are new proxies for the climate-optimized routing, AirTraf takes a role in verifying the aCCFs themselves and the climate impact option based on the aCCFs in multi-annual (long-term) simulations.

To ~~verify demonstrate~~ the submodel AirTraf 2.0, example simulations were carried out with 103 north-Atlantic flights of an Airbus A330 aircraft for a typical winter day. ~~The~~ AirTraf 2.0 simulates the one-day air traffic successfully for ~~each routing option~~, ~~the newly developed routing option concerning different optimization objectives, e.g., contrail avoidance, cash operating cost, and climate impact (represented by average temperature response over 20 years), and finds the different families of optimum flight trajectories, which minimize the corresponding objective functions.~~ The characteristics of ~~the routing options~~ ~~were analyzed on the basis of the nine performance measures. Aircraft was~~ ~~these routing options include that aircraft is~~ flown as the minimum economic cost with both, the SOC and the COC options. These options are comparably effective for economic cost indices. ~~The~~ AirTraf 2.0 differentiates the minimum time, the minimum fuel, and the minimum COC ~~solutions; that is, the COC option obtains a trade-off solution options. The COC option lies~~ between the minimum time and the minimum fuel ~~solutions~~ options, and thus minimizes COC by taking the best compromise between the flight time and the fuel use into account. The  $\text{NO}_x$  option minimizes  $\text{NO}_x$  emission; this option differs from the fuel and the COC options. The contrail and the climate options decrease ~~the~~ climate impact (indicated by  $\text{ATR20}_{\text{total}}$ ), which causes extra operating costs. A trade-off between the cost and the climate impact ~~certainly~~ exists. Compared to the COC option, the climate and the contrail options decrease  $\text{ATR20}_{\text{total}}$  by 67.9 and by 43.4 % with an increase of COC by 9.8 and by 12.0 %, respectively. Thus, the climate option seems to be more effective on the cost-benefit performance than the contrail option. ~~We believe that these climate benefits are most likely an upper limit.~~ The simulation results were compared with literature data. The relative changes in the performance measures among the various routing options agree well in sign with those shown by many previous studies. This comparison has limitations because of different methodologies, different atmospheric conditions, etc. Nonetheless, the many literature data offer evidence to indicate the consistency of the AirTraf simulations.

The integration of AirTraf into EMAC allows one to optimize flight trajectories and to study flight trajectories-aircraft routings under historical, present-day and future conditions of the climate system. We acknowledge that the simulation results depend on the atmospheric conditions of the target day. Thus, it is important to examine whether the findings, e.g., the trade-off between the cost and the climate impact, are common under any atmospheric conditions. Recently, Yamashita et al. (2020) examined 5 this for representative weather types over the North Atlantic by using EMAC with AirTraf 2.0. Furthermore, the integrated aircraft routing options could be extended to conflicting scenarios. Recently, Yin et al. (2018a) investigated a trade-off between flight time and contrail formation for trans-Atlantic flights, by combining the time and the contrail options. Another option could easily be created by adding a corresponding objective function. The AirTraf development presented in this paper leads to a further detailed understanding of characteristics of various aircraft routing strategies.

## 10 Appendix A: The algorithmic Climate Change Functions

The aCCFs are calculated by the submodel ACCF (version 1.0). The derivation and validation of the aCCFs of ozone, methane, water vapour have been published by Van Manen (2017), Yin et al. (2018b), and Van Manen and Grewé (2019); the aCCF of contrails is described by Yin et al. (2018a) and Yin et al. (manuscript in preparation, 2019). The aCCFs for ozone, methane, water vapour, CO<sub>2</sub> and contrails are formulated as follows:

$$15 \quad aCCF_{O_3} = \begin{cases} -5.20 \times 10^{-11} + 2.30 \times 10^{-13}T + 4.85 \times 10^{-16}\Phi - 2.04 \times 10^{-18}TF, & \text{if } aCCF_{O_3} > 0, \\ 0, & \text{if } aCCF_{O_3} \leq 0, \end{cases} \quad (A1)$$

$$aCCF_{CH_4} = \begin{cases} -9.83 \times 10^{-13} + 1.99 \times 10^{-18}\Phi - 6.32 \times 10^{-16}F_{in} + 6.12 \times 10^{-21}\Phi F_{in}, & \text{if } aCCF_{CH_4} \leq 0, \\ 0, & \text{if } aCCF_{CH_4} > 0, \end{cases} \quad (A2)$$

$$aCCF_{H_2O} = 4.05 \times 10^{-16} + 1.48 \times 10^{-16}|PV|, \quad (A3)$$

20

$$aCCF_{CO_2} = 6.35 \times 10^{-15}, \quad (A4)$$

$$aCCF_{contrail} = \begin{cases} 1.0 \times 10^{-10}(0.0073 \times (10^{0.0107T} - 1.03)) \times 0.114, & \text{if Potcov} > 0 \text{ and nighttime,} \\ 1.0 \times 10^{-10}(-1.7 - 0.0088OLR) \times 0.114, & \text{if Potcov} > 0 \text{ and daytime,} \\ 0, & \text{if Potcov} \leq 0, \end{cases} \quad (A5)$$

where  $T$  is the atmospheric temperature in K,  $\Phi$  is the geopotential in m<sup>2</sup>s<sup>-2</sup>,  $F_{in}$  is the incoming solar radiation at the top of atmosphere in Wm<sup>-2</sup>,  $PV$  is the potential vorticity in PVU (1 PVU = 10<sup>-6</sup>Km<sup>2</sup>kg<sup>-1</sup>s<sup>-1</sup>), and OLR is the outgoing long-wave radiation in Wm<sup>-2</sup>. Given values of these meteorological variables, Eqs. (A1) and (A2) yield  $aCCF_{O_3}$  and  $aCCF_{CH_4}$  in K(kg(NO<sub>2</sub>))<sup>-1</sup>; Eqs. (A3) and (A4) yield  $aCCF_{H_2O}$  and  $aCCF_{CO_2}$  in K(kg(fuel))<sup>-1</sup>; and Eq. (A5) yields  $aCCF_{contrail}$

in  $K(km(\text{contrail}))^{-1}$ . The  $aCCF_{CO_2}$  is the sole constant value (Dahlmann, 2018). The  $aCCF_{CO_2}$  is calculated by using the non-linear climate-chemistry response model AirClim (Grewe and Stenke, 2008; Dahlmann, 2012; Dahlmann et al., 2016), assuming a 1 Tg fuel use in 2010 with the annual growth rate according to the future global aircraft scenario Fa1 (Penner et al., 1999). The  $aCCF_{CO_2}$  is the averaged temperature response of  $CO_2$  for the period 2010–2029 (in K per kilogram of fuel) 5 calculated by AirClim. The  $aCCF_{\text{contrail}}$  for the night-time contrails takes positive values; if the temperature is less than 201 K,  $aCCF_{\text{contrail}}$  for the night-time contrails is set to zero. The  $aCCF_{\text{contrail}}$  for the day-time contrails can take positive and negative values, depending on the OLR (the threshold is  $-193.18 \text{ Wm}^{-2}$ ). As for the time boundaries of day and night, the local time and solar zenith angle are calculated for locations where contrails could form ( $Potcov > 0$ ). For locations in darkness, the time of sunrise is then calculated. If the time between the local time and sunrise is greater than six hours, the 10  $aCCF_{\text{contrail}}$  for the night-time contrails is applied. If the contrail forms in daylight, or in darkness but with less than six hours before sunrise, the  $aCCF_{\text{contrail}}$  for the day-time contrails is applied. These calculations are performed online in EMAC by the submodel ACCF. In AirTraf 2.0, those five  $aCCF$ s are calculated as flight properties for waypoints and then the corresponding ATR20s are calculated for flight segments (see Table 2).

*Code and data availability.* AirTraf is implemented as a submodel of the Modular Earth Submodel System (MESSy). MESSy is continuously further developed and applied by a consortium of institutions. The usage of MESSy and access to the source code is licenced to all 15 affiliates of institutions which are members of the MESSy Consortium. Institutions can become a member of the MESSy Consortium by signing the MESSy Memorandum of Understanding. More information can be found on the MESSy Consortium Website (<http://www.messy-interface.org>). The submodel AirTraf 2.0 presented here has been developed on the basis of MESSy version 2.53 and is available since the official release of MESSy version 2.54. The status information for AirTraf including the license conditions is available on the website. The 20 data from the simulations will be provided by the authors on request.

*Author contributions.* HY, FY and VG designed the submodel AirTraf 2.0. HY, FY, PJ, SM, and BK implemented the coupling of AirTraf 2.0 with the Modular Earth Submodel System (MESSy). FY, VG, SM, KD, and CF developed the algorithmic Climate Change Functions (aCCFs). FY and VG designed the submodel ACCF. HY performed the simulations and analyzed the results presented in this paper.

*Competing interests.* The authors declare that they have no conflict of interest.

25 *Acknowledgements.* This study was supported by the project ATM4E (Air Traffic Management for Environment; <https://www.atm4e.eu/>) funded from the SESAR Joint Undertaking under grant agreement No. 699395 under European Union's Horizon 2020 research and innovation program. This study was also supported by the DLR project WeCare (Utilizing Weather Information for Climate Efficient and Eco Efficient Future Aviation) and Eco2Fly. The flight plan was provided by the European Union FP7 Project REACT4C (Reducing Emissions

from Aviation by Changing Trajectories for the Benefit of Climate; <https://www.react4c.eu/>). We gratefully acknowledge the computational resources for the simulations, which were provided by the Deutsches Klimarechenzentrum (DKRZ). We wish to acknowledge the valuable contributions of the Department of Meteorology at the University of Reading, especially Emma Irvine, for her development of the aCCF<sub>contrail</sub>. We also wish to acknowledge our colleagues, especially Robert Sausen, for his support of the projects. We wish to thank

5 Malte Niklaß for providing comparison data on the trajectory optimization. We wish to thank Duy Sinh Cai for his invaluable help on the model development. We would like to thank Anton Stephan for providing an internal review. We would like to express our gratitude to anonymous reviewers for their helpful comments and discussion.

## References

Aircraft Commerce: Owner's & operator's guide: A330-200/-300, 57, 9, Nimrod Publications Ltd., 2008.

Anthony, P.: The fuel factor, *ICAO Journal*, 64, 1, 12, 2009.

Appleman, H.: The formation of exhaust condensation trails by jet aircraft, *Bulletin of the American Meteorological Society*, 34, 14–20, 5 <https://doi.org/10.1175/1520-0477-34.1.14>, 1953.

Baker, J. E.: Adaptive selection methods for genetic algorithms, *First International Conference on Genetic Algorithms and their Applications*, 101–111, <https://doi.org/10.4324/9781315799674>, 1985.

Bock, L. and Burkhardt, U.: Reassessing properties and radiative forcing of contrail cirrus using a climate model, *Journal of Geophysical Research: Atmospheres*, 121, 9717–9736, <https://doi.org/10.1002/2016JD025112>, 2016.

Brasseur, G. P., Gupta, M., Anderson, B. E., Balasubramanian, S., Barrett, S., Duda, D., Fleming, G., Forster, P. M., Fuglestvedt, J., Gettelman, A., et al.: Impact of aviation on climate: FAA's aviation climate change research initiative (ACCR) Phase II, *Bulletin of the American Meteorological Society*, 97, 561–583, <https://doi.org/10.1175/BAMS-D-13-00089.1>, 2016.

Bremmers, D.: The low NO<sub>x</sub> flight, Master thesis, Delft University of Technology, The Netherlands, 1999.

Bryson, A. E. J. and Ho, Y.-C.: *Applied optimal control*, Blaisdell, Waltham, Mass., Chap. 2., 1969.

Burkhardt, U. and Kärcher, B.: Process-based simulation of contrail cirrus in a global climate model, *Journal of Geophysical Research: Atmospheres*, 114, D16201, 1–13, <https://doi.org/10.1029/2008JD011491>, 2009.

Burkhardt, U. and Kärcher, B.: Global radiative forcing from contrail cirrus, *Nature climate change*, 1, 54–58, <https://doi.org/10.1038/nclimate1068>, 2011.

Burkhardt, U., Kärcher, B., Ponater, M., Gierens, K., and Gettelman, A.: Contrail cirrus supporting areas in model and observations, *Geophysical Research Letters*, 35, L16808, 1–5, <https://doi.org/10.1029/2008GL034056>, 2008.

Celis, C., Sethi, V., Zammit-Mangion, D., Singh, R., and Pilidis, P.: Theoretical optimal trajectories for reducing the environmental impact of commercial aircraft operations, *Journal of Aerospace Technology and Management*, 6, 29–42, <http://dx.doi.org/10.5028/jatm.v6i1.288>, 2014.

Cook, A., Tanner, G., Williams, V., and Meise, G.: Dynamic cost indexing – Managing airline delay costs, *Journal of air transport management*, 15, 26–35, <https://doi.org/10.1016/j.jairtraman.2008.07.001>, 2009.

Cook, A. J., Tanner, G., and Anderson, S.: Evaluating the true cost to airlines of one minute of airborne or ground delay, Final report by the University of Westminster for Performance Review Comission (Eurocontrol), Edition 4, 1–134, 2004.

Dahlmann, K.: Eine Methode zur effizienten Bewertung von Maßnahmen zur Klimaoptimierung des Luftverkehrs, Ph.D. thesis, Ludwig-Maximilians-Universität, Germany, ISSN 1434-8454, urn:nbn:de:bvb:19-141992, 2012.

Dahlmann, K.: Private communication, 2018.

Dahlmann, K., Grawe, V., Frömming, C., and Burkhardt, U.: Can we reliably assess climate mitigation options for air traffic scenarios despite large uncertainties in atmospheric processes?, *Transportation Research Part D: Transport and Environment*, 46, 40–55, <https://doi.org/10.1016/j.trd.2016.03.006>, 2016.

Deb, K. and Agrawal, S.: A niched-penalty approach for constraint handling in genetic algorithms, in: *Artificial neural nets and genetic algorithms*, Springer, 235–243, [https://doi.org/10.1007/978-3-7091-6384-9\\_40](https://doi.org/10.1007/978-3-7091-6384-9_40), 1999.

Dee, D. P., Uppala, S. M., Simmons, A., Berrisford, P., Poli, P., Kobayashi, S., Andrae, U., Balmaseda, M., Balsamo, G., Bauer, d. P., et al.: The ERA-Interim reanalysis: Configuration and performance of the data assimilation system, *Quarterly Journal of the royal meteorological society*, 137, 553–597, <https://doi.org/10.1002/qj.828>, 2011.

Deidewig, F., Döpelheuer, A., and Lecht, M.: Methods to assess aircraft engine emissions in flight, 20th Congress of the International Council 5 of the Aeronautical Sciences, ICAS-96-4.1.2, 131–141, 1996.

EASA: Type Certificate Data Sheet for General Electric CF6-80E1 series engines, No. IM.E.007, 2, 1–8, 2011.

EASA: Type Certificate Data Sheet for Airbus A330, No. EASA.A.A004, 34, 1–39, 2013.

Erzberger, H. and Lee, H.: Constrained optimum trajectories with specified range, *Journal of Guidance, Control, and Dynamics*, 3, 78–85, <https://doi.org/10.2514/3.55950>, 1980.

10 Eshelman, L. J.: Real-coded genetic algorithms and interval-schemata, *Foundations of Genetic Algorithms*, 2, 187–202, <https://doi.org/10.1016/B978-0-08-094832-4.50018-0>, 1993.

Eurocontrol: User Manual for the Base of Aircraft Data (BADA) Revision 3.10, EEC Technical/Scientific Report No.12/04/10-45, 1–89, 2011.

Eurocontrol: SAAM Reference Manual 4.2.0 Beta, Version 21-12-2012, 434, 2012.

15 European Central Bank: Euro foreign exchange reference rates, <https://www.ecb.europa.eu/home/html/index.en.html>, 2018.

Fichter, C., Marquart, S., Sausen, R., and Lee, D. S.: The impact of cruise altitude on contrails and related radiative forcing, *Meteorologische Zeitschrift*, 14, 563–572, <https://doi.org/10.1127/0941-2948/2005/0048>, 2005.

Fonseca, C. M., Fleming, P. J., et al.: Genetic algorithms for multiobjective optimization: formulation, discussion, and generalization, *ICGA*, 93, 416–423, 1993.

20 Frömming, C., Ponater, M., Dahlmann, K., Grewe, V., Lee, D., and Sausen, R.: Aviation-induced radiative forcing and surface temperature change in dependency of the emission altitude, *Journal of Geophysical Research: Atmospheres*, 117, D19104, 1–15, <https://doi.org/10.1029/2012JD018204>, 2012.

Frömming, C., Grewe, V., Jöckel, P., Brinkop, S., Dietmüller, S., Garny, H., Ponater, M., Tsati, E., and Matthes, S.: Climate cost functions as basis for climate optimized flight trajectories, Tenth USA/Europe Air Traffic Management Research and Development Seminar 25 2013, Chicago, Illinois USA, 239, 1–9, [http://www.atmseminar.org/seminarContent/seminar10/papers/239-Frömming\\_0126130830-Final-Paper-4-15-13.pdf](http://www.atmseminar.org/seminarContent/seminar10/papers/239-Frömming_0126130830-Final-Paper-4-15-13.pdf), 2013.

Frömming, C., Grewe, V., Brinkop, S., and Jöckel, P.: Documentation of the EMAC submodels AIRTRAC 1.0 and CONTRAIL 1.0, supplementary material of Grewe et al., 2014b, *Geoscientific Model Development*, 7, 175–201, <https://doi.org/10.5194/gmd-7-175-2014>, 2014.

30 Gauss, M., Isaksen, I., Lee, D., and Søvde, O.: Impact of aircraft NO<sub>x</sub> emissions on the atmosphere – tradeoffs to reduce the impact, *Atmospheric Chemistry and Physics*, 6, 1529–1548, <https://doi.org/10.5194/acp-6-1529-2006>, 2006.

Gierens, K., Lim, L., and Eleftheratos, K.: A review of various strategies for contrail avoidance, *The Open Atmospheric Science Journal*, 2, 1–7, doi:10.2174/1874282300802010001, 2008.

Goldberg, D. E.: *Genetic algorithms in search, optimization and machine learning*, Addison-Wesley, Reading, MA, 1989.

35 Green, J. E.: Future aircraft – greener by design?, *Meteorologische Zeitschrift*, 14, 583–590, <https://doi.org/10.1127/0941-2948/2005/0052>, 2005.

Grewe, V. and Stenke, A.: AirClim: an efficient tool for climate evaluation of aircraft technology, *Atmospheric Chemistry and Physics*, 8, 4621–4639, <https://doi.org/10.5194/acp-8-4621-2008>, 2008.

Grewe, V., Champougny, T., Matthes, S., Frömming, C., Brinkop, S., Søvde, O. A., Irvine, E. A., and Halscheidt, L.: Reduction of the air traffic's contribution to climate change: A REACT4C case study, *Atmospheric Environment*, 94, 616–625, <https://doi.org/10.1016/j.atmosenv.2014.05.059>, 2014a.

Grewe, V., Frömming, C., Matthes, S., Brinkop, S., Ponater, M., Dietmüller, S., Jöckel, P., Garny, H., Tsati, E., Dahlmann, K., et al.: Aircraft 5 routing with minimal climate impact: the REACT4C climate cost function modelling approach (V1.0), *Geoscientific Model Development*, 7, 175–201, <https://doi.org/10.5194/gmd-7-175-2014>, 2014b.

Grewe, V., Dahlmann, K., Flink, J., Frömming, C., Ghosh, R., Gierens, K., Heller, R., Hendricks, J., Jöckel, P., Kaufmann, S., et al.: Mitigating the climate impact from aviation: achievements and results of the DLR WeCare project, *Aerospace*, 4(3), 34, 1–50, <https://doi.org/10.3390/aerospace4030034>, 2017a.

10 Grewe, V., Matthes, S., Frömming, C., Brinkop, S., Jöckel, P., Gierens, K., Champougny, T., Fuglestvedt, J., Haslerud, A., Irvine, E., et al.: Feasibility of climate-optimized air traffic routing for trans-Atlantic flights, *Environmental Research Letters*, 12, 034003, 1–9, <https://doi.org/10.1088/1748-9326/aa5ba0>, 2017b.

Hansen, J., Sato, M., Ruedy, R., Nazarenko, L., Lacis, A., Schmidt, G., Russell, G., Aleinov, I., Bauer, M., Bauer, S., et al.: Efficacy of 15 climate forcings, *Journal of Geophysical Research: Atmospheres*, 110, 1–45, <https://doi.org/10.1029/2005JD005776>, 2005.

15 Holand, J. H.: *Adaptation in natural and artificial systems*, Ann Arbor, MI: The University of Michigan Press, 1975.

IATA: Fuel price analysis: jet fuel price for March 3, 2017, <https://www.iata.org/publications/economics/fuel-monitor/Pages/index.aspx>, 2017.

ICAO: ICAO Engine Exhaust Emissions Data, Doc 9646-AN/943 (Issue 18 is used for this study), 2005.

ICAO: State of global air transport and ICAO forecasts for effective planning, ICAO Air Services 20 Negotiation Event, 1–36, <https://www.icao.int/Meetings/ICAN2017/Documents/ICAO%20Workshop%20-State%20of%20Industry%20and%20ICAO%20Forecasts.pdf>, 2017.

IMF: World Economic Outlook Database October, <https://www.imf.org/external/pubs/ft/weo/2016/02/weodata/index.aspx>, 2016.

Irvine, E., Hoskins, B., and Shine, K.: A simple framework for assessing the trade-off between the climate impact of aviation carbon dioxide 25 emissions and contrails for a single flight, *Environmental Research Letters*, 9, 064021, 1–6, doi:10.1088/1748-9326/9/6/064021, 2014.

Jöckel, P., Kerkweg, A., Pozzer, A., Sander, R., Tost, H., Riede, H., Baumgaertner, A., Gromov, S., and Kern, B.: Development cycle 2 of 30 the modular earth submodel system (MESSy2), *Geoscientific Model Development*, 3, 717–752, <https://doi.org/10.5194/gmd-3-717-2010>, 2010.

Jöckel, P., Tost, H., Pozzer, A., Kunze, M., Kirner, O., Brenninkmeijer, C. A., Brinkop, S., Cai, D., Dyroff, C., Eckstein, J., et al.: Earth 35 system chemistry integrated modelling (ESCI Mo) with the modular Earth submodel system (MESSy, version 2.51), *Geoscientific Model Development*, 9, 1153–1200, <https://doi.org/10.5194/gmd-9-1153-2016>, 2016.

Lee, D., Pitari, G., Grewe, V., Gierens, K., Penner, J., Petzold, A., Prather, M., Schumann, U., Bais, A., Berntsen, T., et al.: Transport impacts on atmosphere and climate: Aviation, *Atmospheric Environment*, 44, 4678–4734, <https://doi.org/10.1016/j.atmosenv.2009.06.005>, 2010.

Lee, D. S., Fahey, D. W., Forster, P. M., Newton, P. J., Wit, R. C., Lim, L. L., Owen, B., and Sausen, R.: Aviation and global climate change 40 in the 21st century, *Atmospheric Environment*, 43, 3520–3537, <https://doi.org/10.1016/j.atmosenv.2009.04.024>, 2009.

45 Liebeck, R. H., Andrastek, D. A., Chau, J., Girvin, R., Lyon, R., Rawdon, B. K., Scott, P. W., and Wright, R. A.: Advanced subsonic airplane design and economic studies, NASA CR-195443, 1–31, <https://ntrs.nasa.gov/search.jsp?R=19950017884>, 1995.

Lührs, B., Niklaß, M., Frömming, C., Grewe, V., and Gollnick, V.: Cost-benefit assessment of 2d and 3d climate and weather optimized trajectories, 16th AIAA Aviation Technology, Integration, and Operations Conference, AIAA 2016-3758, 1–14, <https://doi.org/10.2514/6.2016-3758>, 2016.

Lund, M. T., Aamaas, B., Berntsen, T. K., Bock, L., Burkhardt, U., Fuglestvedt, J. S., and Shine, K. P.: Emission metrics for quantifying 5 regional climate impacts of aviation, *Earth System Dynamics*, 8, 547–563, <https://doi.org/10.5194/esd-8-547-2017>, 2017.

Mannstein, H., Spichtinger, P., and Gierens, K.: A note on how to avoid contrail cirrus, *Transportation Research Part D: Transport and Environment*, 10, 421–426, <https://doi.org/10.1016/j.trd.2005.04.012>, 2005.

Marla, L., Vaaben, B., and Barnhart, C.: Integrated disruption management and flight planning to trade off delays and fuel burn, *Transportation Science*, 51, 88–111, <https://doi.org/10.1287/trsc.2015.0609>, 2016.

10 Matthes, S., Schumann, U., Grewe, V., Frömming, C., Dahlmann, K., Koch, A., and Mannstein, H.: Climate optimized air transport, in: *Atmospheric physics*, Springer, 727–746, 2012.

Matthes, S., Grewe, V., Dahlmann, K., Frömming, C., Irvine, E., Lim, L., Linke, F., Lührs, B., Owen, B., Shine, K., et al.: A concept 15 for multi-criteria environmental assessment of aircraft trajectories, *Aerospace*, 4(3), 42, 1–25, <https://doi.org/10.3390/aerospace4030042>, 2017.

15 Michael A., B.: Cost index estimation, 1–23, <https://www.iata.org/whatwedo/workgroups/Documents/ACC-2015-GVA/0845-0915-cost-index.pdf>, 2015.

Mulder, T. J. and Ruijgrok, G.: On the reduction of  $\text{NO}_x$ -emission levels by performing low  $\text{NO}_x$  flights, 26th Congress of the International Council of the Aeronautical Sciences Including the Eighth AIAA Aviation Technology, Integration, and Operations Conference, ICAS2008-4.7 ST2, 14–19, [http://icas.org/ICAS\\_ARCHIVE/ICAS2008/PAPERS/532.PDF](http://icas.org/ICAS_ARCHIVE/ICAS2008/PAPERS/532.PDF), 2008.

20 Ng, H. K., Sridhar, B., Chen, N. Y., and Li, J.: Three-dimensional trajectory design for reducing climate impact of trans-atlantic flights, 14th AIAA Aviation Technology, Integration, and Operations Conference, AIAA 2014-2289, 1–12, <https://doi.org/10.2514/6.2014-2289>, 2014.

Niklaß, M., Gollnick, V., Lührs, B., Dahlmann, K., Frömming, C., Grewe, V., and van Manen, J.: Cost-benefit assessment of climate-restricted 25 airspaces as an interim climate mitigation option, *Journal of Air Transportation*, 25, 27–38, <https://doi.org/10.2514/1.D0045>, 2017.

Nuic, A., Poles, D., and Mouillet, V.: BADA: An advanced aircraft performance model for present and future ATM systems, *International 25 journal of adaptive control and signal processing*, 24, 850–866, <https://doi.org/10.1002/acs.1176>, 2010.

Penner, J., Lister, D., Griggs, D., Dokken, D., and McFarland, M.: Aviation and the global atmosphere – A special report of IPCC working groups I and III, Intergovernmental Panel on Climate Change, 1–23, Cambridge University Press, <https://www.ipcc.ch/report/aviation-and-the-global-atmosphere-2/>, 1999.

Ponater, M., Marquart, S., and Sausen, R.: Contrails in a comprehensive global climate model: Parameterization and radiative forcing results, 30 Journal of Geophysical Research: Atmospheres, 107, D13, 4164, 1–18, <https://doi.org/10.1029/2001JD000429>, 2002.

Ponater, M., Marquart, S., Sausen, R., and Schumann, U.: On contrail climate sensitivity, *Geophysical Research Letters*, 32, 1–5, <https://doi.org/10.1029/2005GL022580>, 2005.

REACT4C: EU FP7 Project: Reducing Emissions from Aviation by Changing Trajectories for the benefit of Climate, <http://www.react4c.eu>, 2014.

35 Roeckner, E., Brokopf, R., Esch, M., Giorgetta, M., Hagemann, S., Kornblueh, L., Manzini, E., Schlese, U., and Schulzweida, U.: Sensitivity of simulated climate to horizontal and vertical resolution in the ECHAM5 atmosphere model, *Journal of Climate*, 19, 3771–3791, <https://doi.org/10.1175/JCLI3824.1>, 2006.

Rosenow, J. and Fricke, H.: Flight performance modeling to optimize trajectories, Deutscher Luft- und Raumfahrtkongress 2016, 420127, 1–8, <https://www.dglr.de/publikationen/2016/420127.pdf>, 2016.

Rosenow, J., Förster, S., Lindner, M., and Fricke, H.: Impact of multi-criteria optimized trajectories on European air traffic density, efficiency and the environment, Twelfth USA/Europe Air Traffic Management Research and Development Seminar 2017, Seattle, Washington USA, 5 113, 1–8, [http://atmseminar.org/seminarContent/seminar12/papers/12th\\_ATM\\_RD\\_Seminar\\_paper\\_113.pdf](http://atmseminar.org/seminarContent/seminar12/papers/12th_ATM_RD_Seminar_paper_113.pdf), 2017.

Sasaki, D. and Obayashi, S.: Development of efficient multi-objective evolutionary algorithms: ARMOGAs (adaptive range multi-objective genetic algorithms), 16, 11–18, Institute of Fluid Science, Tohoku University, 2004.

Sasaki, D. and Obayashi, S.: Efficient search for trade-offs by adaptive range multi-objective genetic algorithms, *Journal of Aerospace Computing, Information, and Communication*, 2, 44–64, <https://doi.org/10.2514/1.12909>, 2005.

10 Sasaki, D., Obayashi, S., and Nakahashi, K.: Navier-Stokes optimization of supersonic wings with four objectives using evolutionary algorithm, *Journal of Aircraft*, 39, 621–629, <https://doi.org/10.2514/2.2974>, 2002.

Schaefer, M.: Development of forecast model for global air traffic emissions, Ph.D. thesis, Ruhr University Bochum, Germany, 2012.

Schmidt, E.: Die Entstehung von Eisnebel aus den Auspuffgasen von Flugmotoren, in *Schriften der Deutschen Akademie für Luftfahrtforschung*: lecture on March 15, 1940, term 1940/41, 44, 1–15, edited by R. Oldenbourg, 1941.

15 Schumann, U.: On conditions for contrail formation from aircraft exhausts, *Meteorologische Zeitschrift*, 5, 4–23, doi:10.1127/metz/5/1996/4, 1996.

Schumann, U., Graf, K., and Mannstein, H.: Potential to reduce the climate impact of aviation by flight level changes, 3rd AIAA Atmospheric and Space Environments Conference, AIAA 2011-3376, 1–22, <https://doi.org/10.2514/6.2011-3376>, 2011.

Schumann, U., Penner, J. E., Chen, Y., Zhou, C., and Graf, K.: Dehydration effects from contrails in a coupled contrail-climate model, 20 Atmospheric Chemistry and Physics, 15, 11 179–11 199, <https://doi.org/10.5194/acp-15-11179-2015>, 2015.

Shine, K. P., Fuglestvedt, J. S., Hailemariam, K., and Stuber, N.: Alternatives to the global warming potential for comparing climate impacts of emissions of greenhouse gases, *Climatic Change*, 68, 281–302, <https://doi.org/10.1007/s10584-005-1146-9>, 2005.

Skeie, R. B., Fuglestvedt, J., Berntsen, T., Lund, M. T., Myhre, G., and Rypdal, K.: Global temperature change from the transport sectors: Historical development and future scenarios, *Atmospheric Environment*, 43, 6260–6270, <https://doi.org/10.1016/j.atmosenv.2009.05.025>, 25 2009.

Søvde, O. A., Matthes, S., Skowron, A., Iachetti, D., Lim, L., Owen, B., Hodnebrog, Ø., Di Genova, G., Pitari, G., Lee, D. S., et al.: Aircraft emission mitigation by changing route altitude: A multi-model estimate of aircraft NO<sub>x</sub> emission impact on O<sub>3</sub> photochemistry, *Atmospheric Environment*, 95, 468–479, <https://doi.org/10.1016/j.atmosenv.2014.06.049>, 2014.

Sridhar, B., Ng, H., and Chen, N.: Aircraft trajectory optimization and contrails avoidance in the presence of winds, *Journal of Guidance, 30 Control, and Dynamics*, 34, 1577–1584, <https://doi.org/10.2514/1.53378>, 2011.

Sridhar, B., Chen, N. Y., and Ng, H. K.: Energy efficient contrail mitigation strategies for reducing the environmental impact of aviation, Tenth USA/Europe Air Traffic Management Research and Development Seminar 2013, Chicago, Illinois USA, 212, 1–10, [http://www.atmseminar.org/seminarContent/seminar10/papers/212-Sridhar\\_0125130119-Final-Paper-4-9-13.pdf](http://www.atmseminar.org/seminarContent/seminar10/papers/212-Sridhar_0125130119-Final-Paper-4-9-13.pdf), 2013.

Van Manen, J.: Aviation H<sub>2</sub>O and NO<sub>x</sub> climate cost functions based on local weather, Master thesis, Delft University of Technology, The 35 Netherlands, <http://resolver.tudelft.nl/uuid:597ed925-9e3b-4300-a2c2-84c8cc97b5b7>, 2017.

Van Manen, J. and Grewe, V.: Algorithmic climate change functions for the use in eco-efficient flight planning, *Transportation Research Part D: Transport and Environment*, 67, 388–405, <https://doi.org/10.1016/j.trd.2018.12.016>, 2019.

Wuebbles, D., Gupta, M., and Ko, M.: Evaluating the impacts of aviation on climate change, *Eos, Transactions American Geophysical Union*, 88, 157–160, <https://doi.org/10.1029/2007EO140001>, 2007.

Yamashita, H., Grewe, V., Jöckel, P., Linke, F., Schaefer, M., and Sasaki, D.: Towards climate optimized flight trajectories in a climate model: AirTraf, Eleventh USA/Europe Air Traffic Management Research and Development Seminar 2015, Lisbon, Portugal, 433, 1–10, 5 [http://www.atmseminar.org/seminarContent/seminar11/papers/433-yamashita\\_0126151229-Final-Paper-5-6-15.pdf](http://www.atmseminar.org/seminarContent/seminar11/papers/433-yamashita_0126151229-Final-Paper-5-6-15.pdf), 2015.

Yamashita, H., Grewe, V., Jöckel, P., Linke, F., Schaefer, M., and Sasaki, D.: Air traffic simulation in chemistry-climate model EMAC 2.41: AirTraf 1.0, *Geoscientific Model Development*, 9, 3363–3392, <https://doi.org/10.5194/gmd-9-3363-2016>, 2016.

Yamashita, H., Yin, F., Grewe, V., Jöckel, P., Matthes, S., Kern, B., Dahlmann, K., and Frömming, C.: Comparison of various aircraft routing strategies using the air traffic simulation model AirTraf 2.0, 3rd ECATS Conference, Gothenburg, Sweden, Book of Abstracts, 1, 180–183, 10 ISBN 978-1-910029-58-9, 2020.

Yin, F., Grewe, V., Frömming, C., and Yamashita, H.: Impact on flight trajectory characteristics when avoiding the formation of persistent contrails for transatlantic flights, *Transportation Research Part D: Transport and Environment*, 65, 466–484, <https://doi.org/10.1016/j.trd.2018.09.017>, 2018a.

Yin, F., Grewe, V., van Manen, J., Matthes, S., Yamashita, H., Linke, F., and Lührs, B.: Verification of the ozone algorithmic climate change 15 functions for predicting the short-term NO<sub>x</sub> effects from aviation en-route, *International Conference on Research in Air Transportation 2018*, Barcelona, Spain, 57, 1–8, [http://icrat.org/ICRAT/seminarContent/2018/papers/ICRAT\\_2018\\_paper\\_57.pdf](http://icrat.org/ICRAT/seminarContent/2018/papers/ICRAT_2018_paper_57.pdf), 2018b.

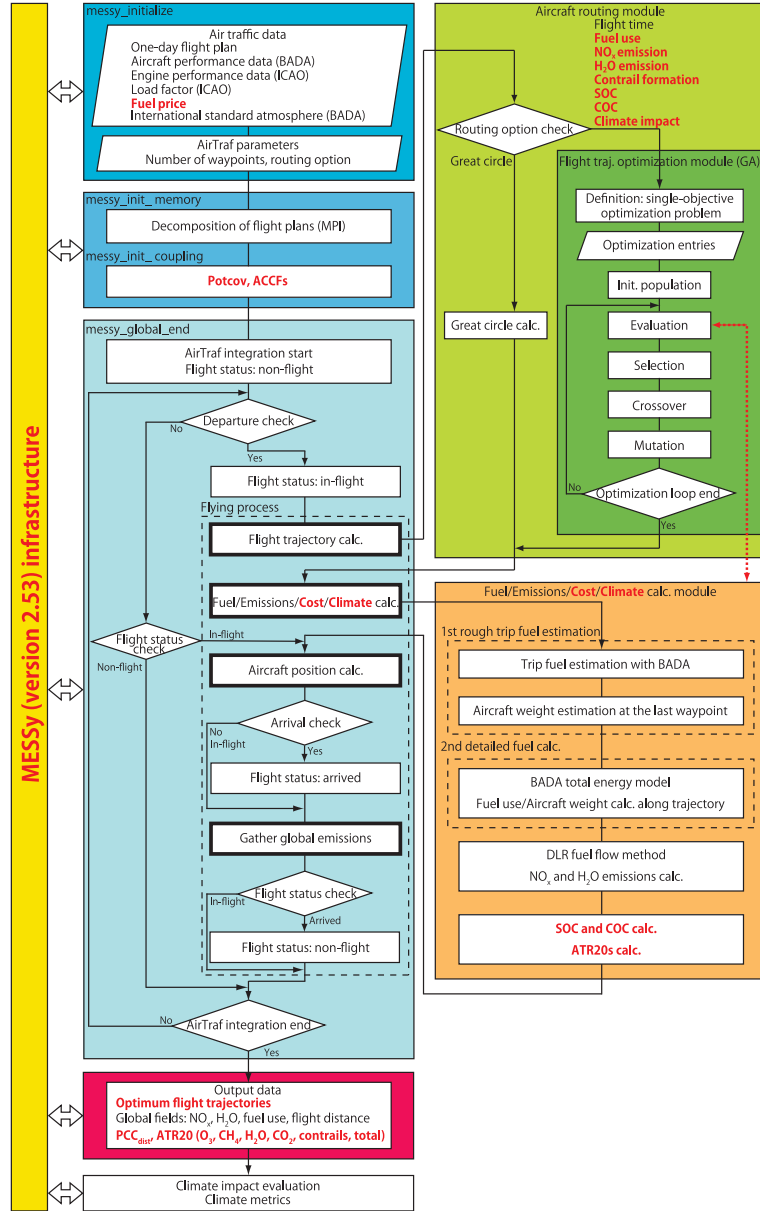


**Figure 1.** Updated flowchart of the MESSy submodel AirTraf 2.0 (updates from AirTraf 1.0 are highlighted by red texts and arrows). MESSy as part of EMAC provides interfaces (yellow) to couple various submodels for data exchange, run control and data input/output. AirTraf 2.0 is coupled to the submodel CONTRAIL (version 1.0; Frömming et al., 2014) and the submodel ACCF (version 1.0). Air traffic data and AirTraf parameters are imported in the initialization phase (**messy\_initialize**, dark blue). AirTraf includes the flying process in **messy\_global\_end** (dashed box, light blue), which comprises four main computation procedures (bold-black boxes). AirTraf uses three modules: the aircraft routing module (light green), the fuel-emissions-cost-climate calculation module (light orange), and the flight trajectory optimization module (dark green). Resulting optimum flight trajectories and global fields of flight properties are output (rose red).

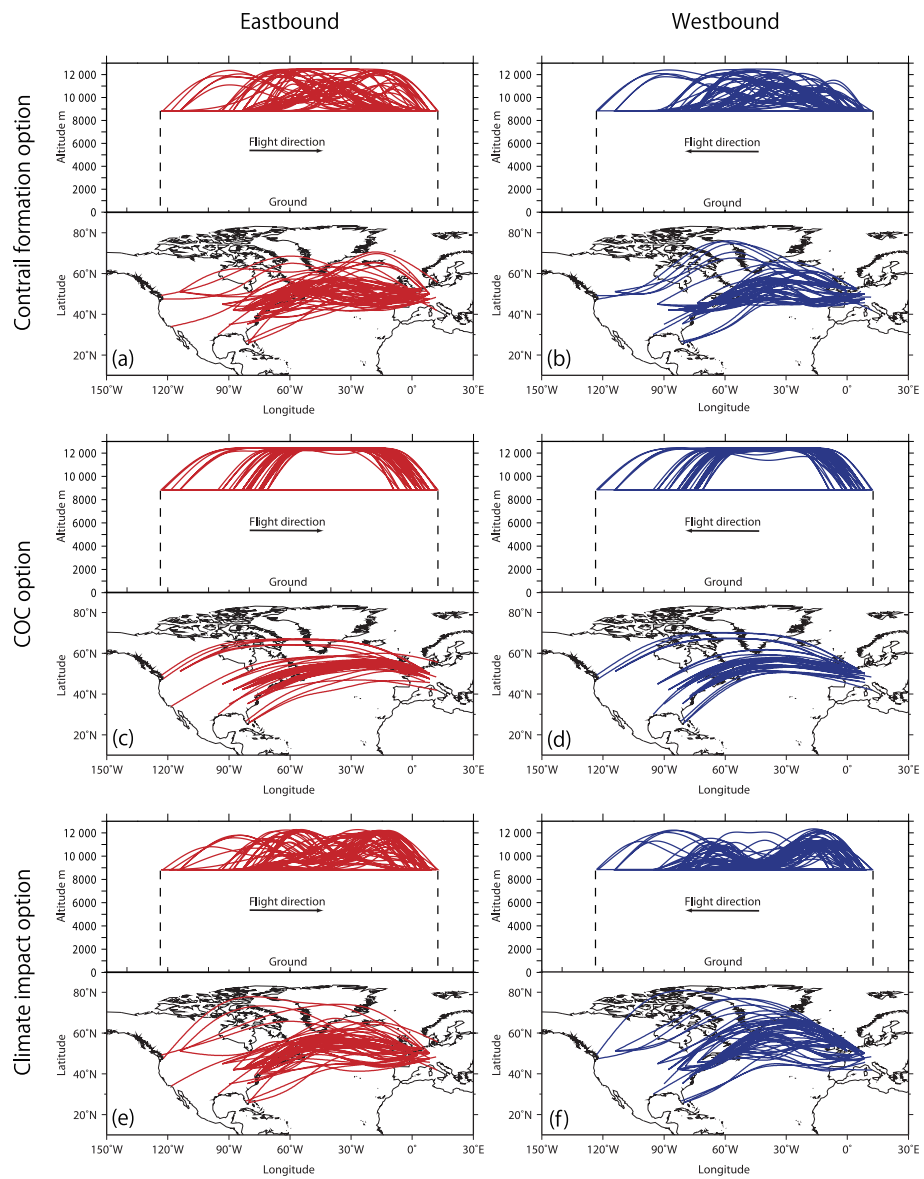


**Figure 2.** Optimized flight trajectories from a one-day AirTraf simulation (52 eastbound and 51 westbound flights) for the contrail formation (a, b), the COC (c, d), and the climate impact routing options (e, f). For each figure, the trajectories are shown in the vertical cross-section (top) and projected on the ground (bottom).

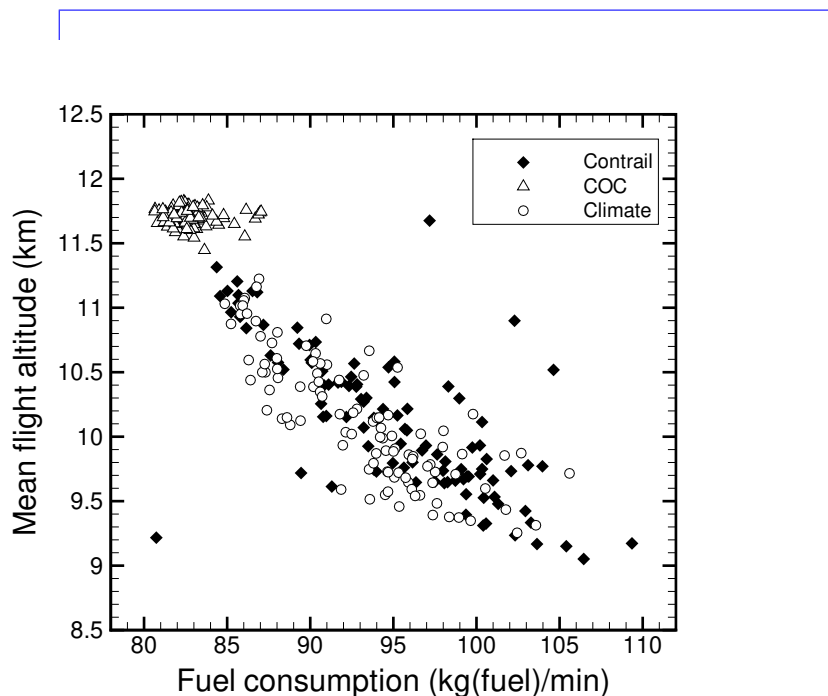


**Figure 3.** Vertically integrated distribution of Mean fuel use, contrail distance, and climate impact indicated by ATR20<sub>total</sub> for one-day (from December 1, 2015 00:00:00 to December 2, 2015 00:00:00 UTC) consumption vs. Top: mean flight altitude for 103 individual flights obtained by the contrail formation option. Middle: the COC option. Bottom: and the climate impact option routing options. These distributions were obtained with the optimized flight trajectories shown in Fig. 2 (sum of 103 flights).

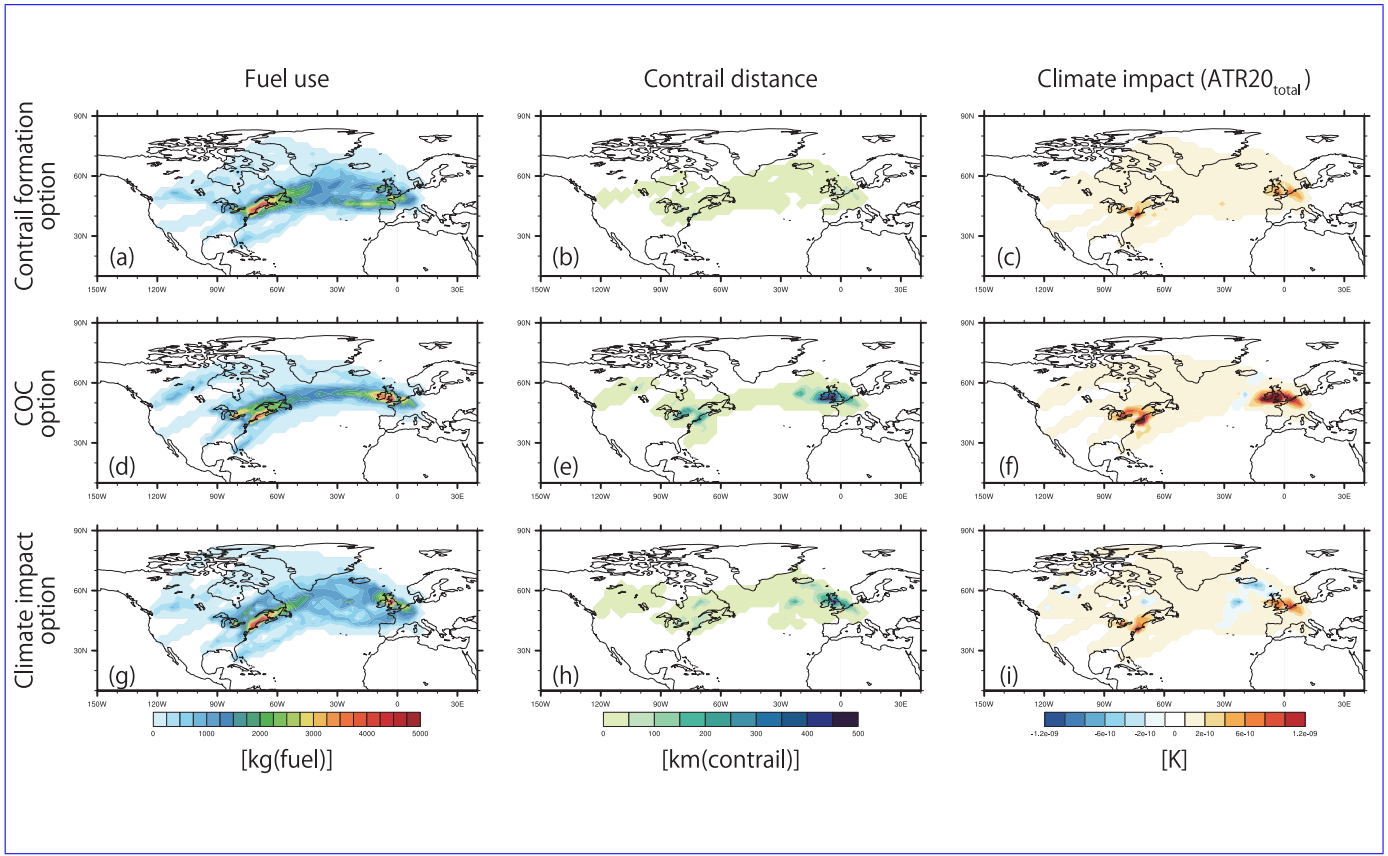


**Figure 4.** Vertically integrated distribution of fuel use, contrail distance, and climate impact indicated by ATR20<sub>total</sub> during the day (from December 1, 2015 00:00:00 to December 2, 2015 00:00:00 UTC). Top: contrail formation option. Middle: COC option. Bottom: climate impact option. These distributions were obtained with the optimized flight trajectories shown in Fig. 2 (sum of 103 flights).

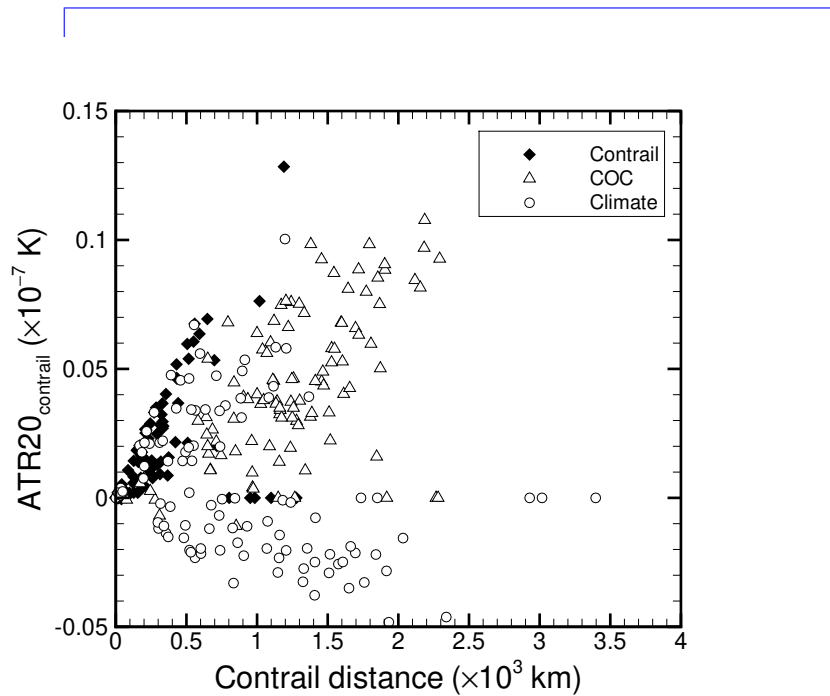


**Figure 5.** Contrail distance vs.  $ATR20_{\text{contrail}}$  for 103 individual flights obtained by the contrail formation, the COC and the climate impact routing options.

**Table 1.** Relevant data of an Airbus A330-301 aircraft and constant parameters applied for AirTraf 2.0. The column “New in V2.0” denotes parameters newly introduced in AirTraf 2.0.

Parameter	Value	Unit	New in V2.0	Description
AFW	103 070	kg	x	Airframe weight estimated by AFW = MEW – $N_{\text{eng}}$ EDW
$c_t$	0.75	(USDollar)s <sup>-1</sup>	x	Unit time costs <sup>a</sup>
$c_f$	0.51	(USDollar)kg <sup>-1</sup>	x	Unit fuel costs <sup>a</sup>
$C_{D0}$	0.019805	–		Parasitic drag coef. (cruise) <sup>b</sup>
$C_{D2}$	0.031875	–		Induced drag coef. (cruise) <sup>b</sup>
$C_{f1}$	0.61503	kg min <sup>-1</sup> kN <sup>-1</sup>		First thrust specific fuel consumption (TSFC) coef. (jet engines) <sup>b</sup>
$C_{f2}$	919.03	kt		Second TSFC coef. <sup>b</sup>
$C_{\text{fcr}}$	0.93655	–		Cruise fuel flow correction coef. <sup>b</sup>
EDW	5091.62	kg	x	Engine dry weight. CF6-80E1A2 engine <sup>c</sup>
EINO <sub>x,ref</sub>	4.88; 12.66; 22.01; 28.72	g(NO <sub>x</sub> )(kg(fuel)) <sup>-1</sup>		Reference NO <sub>x</sub> emission index at take off, climb out, approach and idle conditions (sea level). CF6-80E1A2 (2GE051) <sup>d</sup>
EIH <sub>2</sub> O	1230	g(H <sub>2</sub> O)(kg(fuel)) <sup>-1</sup>		H <sub>2</sub> O emission index <sup>e</sup>
$f_{\text{ref}}$	0.228; 0.724; 2.245; 2.767	kg(fuel)s <sup>-1</sup>		Reference fuel flow at take off, climb out, approach and idle conditions (sea level). CF6-80E1A2 (2GE051) <sup>d</sup>
$g$	9.8	ms <sup>-2</sup>		Gravity acceleration
JFD	0.804	kg l <sup>-1</sup>	x	Jet fuel density at 15°C (Jet A-1)
JFP	0.41	(USDollar)l <sup>-1</sup>	x	Jet fuel price <sup>f</sup>
$M$	0.82	–		Cruise Mach number <sup>b</sup>
MEW	113 253	kg	x	Baseline manufacturers empty weight. MEW = 0.9053OEW <sup>g</sup>
MPL	47 900	kg		Maximum payload <sup>b</sup>
MTOGW	212 000	kg	x	Maximum take-off weight <sup>h</sup>
$N_{\text{seat}}$	295	–	x	Number of seats (3-class) <sup>i</sup>
$N_{\text{eng}}$	2	–	x	Number of engines <sup>h</sup>
OEW	125 100	kg		Operational empty weight <sup>b</sup>
OLF	0.62	–		ICAO overall (passenger/freight/mail) weight load factor in 2008 <sup>j</sup>
$P_0$	101 325	Pa		Reference pressure (sea level)
$r_{\text{inf}}$	2.28	%	x	Ave. U.S. inflation rate (1994-2014) <sup>k</sup>
$R$	287.05	JK <sup>-1</sup> kg <sup>-1</sup>		Gas constant for dry air
$S$	361.6	m <sup>2</sup>		Reference wing surface area <sup>b</sup>
SLST	268.7	kN	x	Thrust per engine (maximum continuous). CF6-80E1A2 <sup>h</sup>
SPD	86 400	sday <sup>-1</sup>		Time (Julian date) $\times$ SPD = Time (s)
$T_0$	288.15	K		Reference temperature (sea level)
$Y_{\text{pre}}$	2015	year	x	Present year for COC calculation
$Y_{\text{ref}}$	1993	year	x	Reference year for COC calculation
$\gamma$	1.4	–		Adiabatic gas constant

<sup>a</sup> Michael A. (2015);<sup>b</sup> Eurocontrol (2011);<sup>c</sup> EASA (2011);<sup>d</sup> ICAO (2005);<sup>e</sup> Penner et al. (1999);<sup>f</sup> IATA (2017);<sup>g</sup> MEW was estimated, because the exact value was unavailable; <sup>h</sup> EASA (2013);<sup>i</sup> Aircraft Commerce (2008);<sup>j</sup> Anthony (2009);<sup>k</sup> IMF (2016)

**Table 2.** Properties assigned to a resulting flight trajectory. The properties of the three groups (divided by rows) are obtained from the nearest grid **point~~box~~** of EMAC at departure time of the flight, the flight trajectory calculation (Fig. 1), and the fuel-emissions-cost-climate calculation (Fig. 1; some properties are calculated in flight trajectory optimizations depending on a selected routing option), respectively. The attribute type indicates where the values of properties are allocated. “ $\mathbf{W}$ ” and “ $\mathbf{S}$ ” stand for waypoints ( $i = 1, 2, \dots, n_{\text{wp}}$ ), flight segments ( $i = 1, 2, \dots, n_{\text{wp}} - 1$ ), and a whole flight trajectory in column 3, respectively. The column “New in V2.0” denotes properties newly introduced in AirTraf 2.0.

Property	Unit	Attribute type	New in V2.0	Description
$\text{aCCF}_{\text{O}_3}$	$\text{K}(\text{kg}(\text{NO}_2))^{-1}$	W	x	Algorithmic Climate Change Function of ozone <sup>a,b</sup> . See Eq. (A1)
$\text{aCCF}_{\text{CH}_4}$	$\text{K}(\text{kg}(\text{NO}_2))^{-1}$	W	x	Algorithmic Climate Change Function of methane <sup>a,b</sup> . See Eq. (A2)
$\text{aCCF}_{\text{H}_2\text{O}}$	$\text{K}(\text{kg}(\text{fuel}))^{-1}$	W	x	Algorithmic Climate Change Function of water vapor <sup>a,b</sup> . See Eq. (A3)
$\text{aCCF}_{\text{CO}_2}$	$\text{K}(\text{kg}(\text{fuel}))^{-1}$	W	x	Algorithmic Climate Change Function of $\text{CO}_2$ <sup>c</sup> . See Eq. (A4)
$\text{aCCF}_{\text{contrail}}$	$\text{K}(\text{km}(\text{contrail}))^{-1}$	W	x	Algorithmic Climate Change Function of contrails <sup>d</sup> . See Eq. (A5)
Potcov	fraction	W	x	Potential persistent contrail cirrus coverage <sup>e</sup>
$P$	Pa	W		Pressure
$T$	K	W		Temperature
$\rho$	$\text{kg m}^{-3}$	W		Air density
$u, v, w$	$\text{ms}^{-1}$	W		Three dimensional wind components
$a$	$\text{ms}^{-1}$	W		Speed of sound
$\text{ATR20}_{\text{O}_3}$	K	S	x	Anticipated climate impact of ozone. See Eq. (8)
$\text{ATR20}_{\text{CH}_4}$	K	S	x	Anticipated climate impact of methane. See Eq. (9)
$\text{ATR20}_{\text{H}_2\text{O}}$	K	S	x	Anticipated climate impact of water vapor. See Eq. (10)
$\text{ATR20}_{\text{CO}_2}$	K	S	x	Anticipated climate impact of $\text{CO}_2$ . See Eq. (11)
$\text{ATR20}_{\text{contrail}}$	K	S	x	Anticipated climate impact of contrails. See Eq. (12)
$\text{ATR20}_{\text{total}}$	K	S	x	Anticipated climate impact (total). See Eq. (13)
$d$	m	S		Flight distance
ETO	Julian date	W		Estimated time over
FT	s	T		Flight time. $\text{FT} = (\text{ETO}_{n_{\text{wp}}} - \text{ETO}_1) \times \text{SPD}$
$h$	m	W		Flight altitude
$\bar{h}$	m	T		Mean flight altitude. $\bar{h} = 1/n_{\text{wp}} \sum_{i=1}^{n_{\text{wp}}} h_i$ with waypoint number $n_{\text{wp}}$ .
$\text{PCC}_{\text{dist}}$	$\text{km}(\text{contrail})$	S	x	Contrail distance <sup>f</sup>
$V_{\text{TAS}}$	$\text{ms}^{-1}$	W		True air speed
$V_{\text{ground}}$	$\text{ms}^{-1}$	W		Ground speed
$\lambda$	deg	W		Longitude
$\phi$	deg	W		Latitude
COC	USDollar	T	x	Cash operating cost <sup>g</sup>
$\text{EINO}_{x,a}$	$\text{g}(\text{NO}_x)(\text{kg}(\text{fuel}))^{-1}$	W		$\text{NO}_x$ emission index
$F_{\text{cr}}$	$\text{kg}(\text{fuel})\text{s}^{-1}$	W		Fuel flow of an aircraft (cruise)
FUEL	kg	S		Fuel use
$\text{H}_2\text{O}$	$\text{g}(\text{H}_2\text{O})$	S		$\text{H}_2\text{O}$ emission
$m$	kg	W		Aircraft weight
$\text{NO}_x$	$\text{g}(\text{NO}_x)$	S		$\text{NO}_x$ emission
SOC	USDollar	T	x	Simple operating cost

<sup>a</sup> Van Manen (2017); <sup>b</sup> Van Manen and Grewe (2019); <sup>c</sup> Dahlmann (2018); <sup>d</sup> Yin et al. (manuscript in preparation, 2020); <sup>e</sup> Frömming et al. (2014); <sup>f</sup> Yin et al. (2018a); <sup>g</sup> Liebeck et al. (1995)

**Table 3.** Setup for AirTraf one-day simulations. The ~~setup~~-setups of the two groups (divided by rows) are used for AirTraf/EMAC and for ARMOGA (Sasaki et al., 2002; Sasaki and Obayashi, 2004, 2005), respectively.  $\alpha$  is an user-specified crossover parameter;  $r_m$  is a mutation rate; and  $\eta_m$  is a parameter controlling the shape of a probability distribution. Details of these parameters are described in Yamashita et al. (2016).

Parameter	Description
ECHAM5 resolution	T42L31ECMWF ( $2.8^\circ$ by $2.8^\circ$ )
Simulation period	December 1, 2015 00:00:00 – December 2, 2015 00:00:00 UTC
Time step of EMAC	12 min
Flight plan	103 trans-Atlantic flights (eastbound 52/westbound 51) <sup>a</sup>
Aircraft type	A330-301
Engine type	CF6-80E1A2, 2GE051 (with 1862M39 combustor)
Flight altitude changes	[FL290, FL410] (fixed at FL350 for the great circle option)
Mach number	0.82
Number of waypoints, $n_{wp}$	101
Design variable, $n_{dv}$	11 (6 locations and 5 altitudes)
Population size, $n_p$	100
Number of generations, $n_g$	100
Selection	Stochastic universal sampling
Crossover	Blend crossover BLX-0.2 ( $\alpha = 0.2$ )
Mutation	Revised polynomial mutation ( $r_m = 0.1$ ; $\eta_m = 5.0$ )

<sup>a</sup> Grawe et al. (2014a) and REACT4C (2014)

**Table 4.** The nine performance measures obtained from the one-day AirTraf simulations with different aircraft routing options (the values indicate the sum of 103 flights). The minimum values of each performance measure are marked with an asterisk; changes (in %) relative to the COC option are given in parentheses. Bar charts of the same data are given in Fig. S4 in the Supplementary material.

Routing option	Flight distance $10^3\text{km}$	Flight time h	Fuel use ton	$\text{NO}_x$ emission ton	$\text{H}_2\text{O}$ emission ton	Contrail distance $10^3\text{km}$	SOC Mil.USD	COC Mil.USD	$\text{ATR20}_{\text{total}}$ $10^{-7}\text{K}$
Great circle	660.3* (-0.4)	757.4 (+0.1)	3979.1 (+5.8)	44.6 (+5.5)	4894.2 (+5.8)	154.9 (+19.1)	4.072 (+2.9)	5.463 (+2.1)	6.85 (+12.5)
Flight time	663.2 (+0.02)	739.4* (-2.3)	4521.9 (+20.2)	57.8 (+36.8)	5562.0 (+20.2)	127.7 (-1.9)	4.299 (+8.6)	5.673 (+6.1)	10.44 (+71.5)
Fuel use	663.3 (+0.03)	757.3 (+0.1)	3758.5* (-0.1)	42.2 (-0.2)	4623.0 (-0.1)	128.5 (-1.2)	3.960 (+0.03)	5.351 (+0.03)	5.85 (-3.9)
$\text{NO}_x$ emission	664.5 (+0.2)	758.8 (+0.3)	3766.8 (+0.1)	42.1* (-0.5)	4633.1 (+0.1)	131.8 (+1.3)	3.968 (+0.2)	5.360 (+0.2)	5.83 (-4.2)
$\text{H}_2\text{O}$ emission	663.3 (+0.03)	757.3 (+0.1)	3758.5 (-0.1)	42.2 (-0.2)	4623.0* (-0.1)	128.5 (-1.2)	3.960 (+0.03)	5.351 (+0.03)	5.85 (-3.9)
Contrail formation	717.4 (+8.2)	812.3 (+7.4)	4625.5 (+23.0)	57.0 (+34.9)	5689.3 (+23.0)	26.3* (-79.8)	4.549 (+14.9)	5.990 (+12.0)	3.45 (-43.4)
SOC	663.2 (+0.02)	756.6 (+0.03)	3760.4 (-0.02)	42.2 (-0.1)	4625.3 (-0.02)	130.2 (+0.1)	3.959* (0.0)	5.349 (0.0)	6.02 (-1.1)
COC	663.1	756.4	3761.1	42.3	4626.2	130.1	3.959	5.349*	6.09
Climate impact	703.2 (+6.0)	801.4 (+5.9)	4474.0 (+19.0)	52.3 (+23.8)	5503.1 (+19.0)	92.6 (-28.8)	4.443 (+12.2)	5.874 (+9.8)	1.96* (-67.9)

## Supplementary Materials

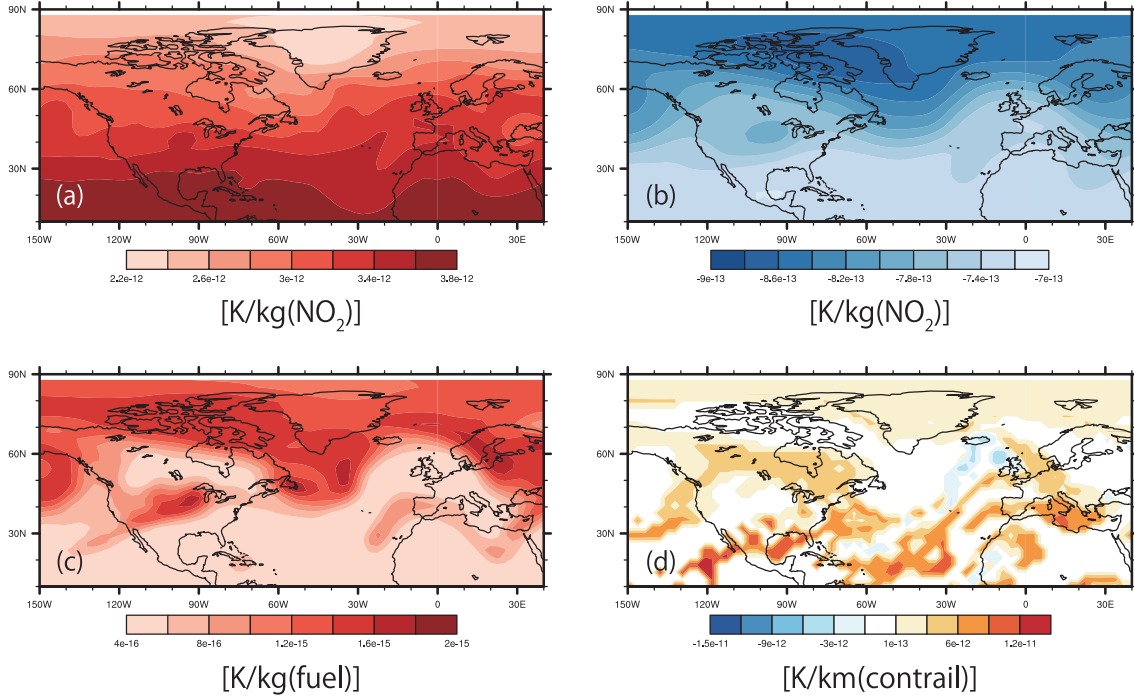


**Figure S1.** Example of the submodel ACCF calculations. The instantaneous distributions of aCCFs at FL350 (~240 hPa, 10.7 km) on December 1, 2015 at 12:00:00 UTC: (a) aCCF<sub>O<sub>3</sub></sub>, (b) aCCF<sub>CH<sub>4</sub></sub>, (c) aCCF<sub>H<sub>2</sub>O</sub>, and (d) aCCF<sub>contrail</sub>. aCCF<sub>CO<sub>2</sub></sub> is given in Eq. (A4) in the Appendix.

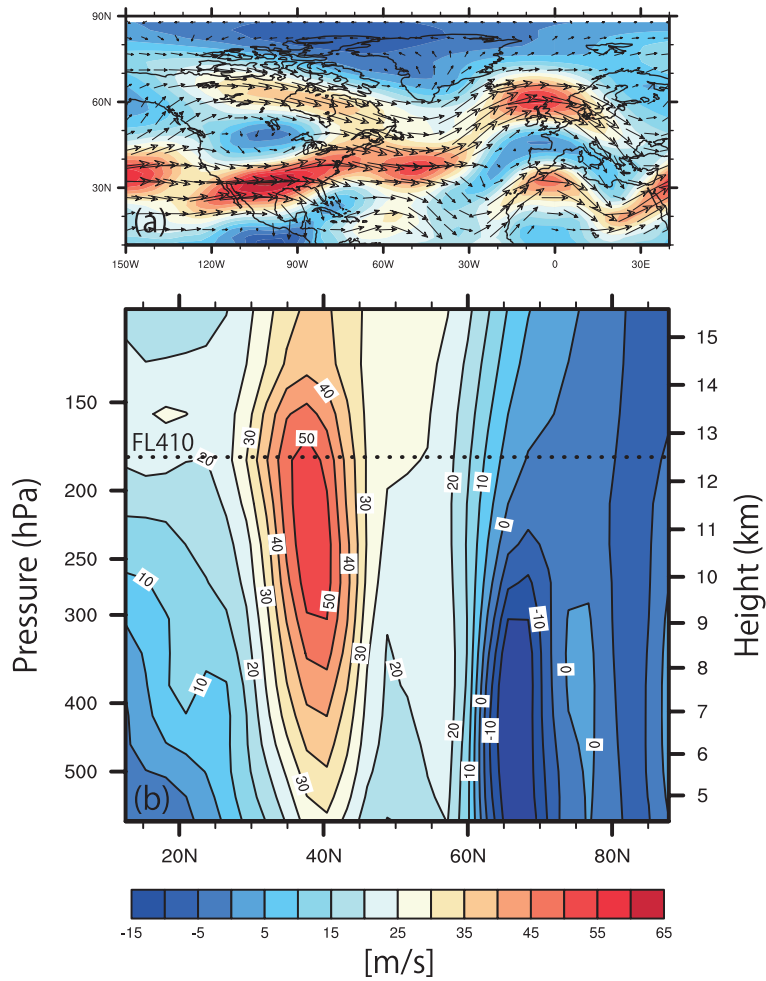


**Figure S2.** Averaged wind fields on December 1, 2015: (a) the contours show the  $u$  component of wind at FL410 ( $\sim 180$  hPa, 12.5 km) and arrows show the wind vector  $(u, v)$ ; (b) similarly, the  $u$  component of wind on the cross section at  $45^\circ\text{W}$ . The dotted line indicates FL410, corresponding to the altitude of (a).

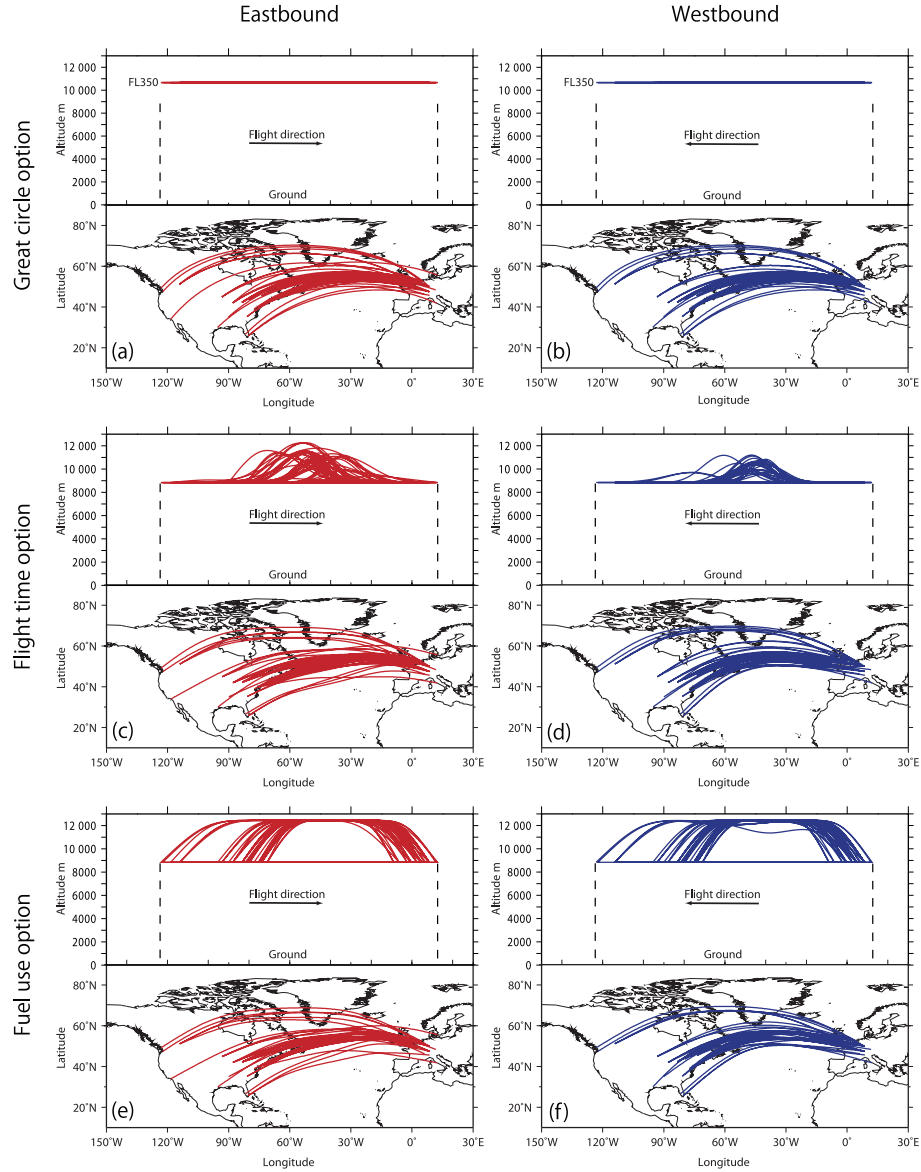


**Figure S3.** Optimized flight trajectories from a one-day AirTraf simulation (52 eastbound and 51 westbound flights) for the following aircraft routing options: the great circle (at FL350; a, b), the flight time (c, d), the fuel use (e, f), the  $\text{NO}_x$  emission (g, h), the  $\text{H}_2\text{O}$  emission (i, j), and the SOC (k, l) options. For each figure, the trajectories are shown in the vertical cross-section (top) and projected on the ground (bottom). In brief, the time option shows similar optimum trajectories as those of the COC option (see Figs. 2c and 2d) with respect to geographic locations, whereas most of the flights choose different flight altitudes. This option aims to benefit from tailwinds and to avoid headwinds only for time minimization. On the other hand, the fuel, the  $\text{NO}_x$ , the  $\text{H}_2\text{O}$  and the SOC options show similar optimum trajectories as those of the COC option (see Figs. 2c and 2d) with respect to geographic locations and in the vertical direction, because their objective functions depend on time and on fuel. The difference among these routing options is discussed in the text.

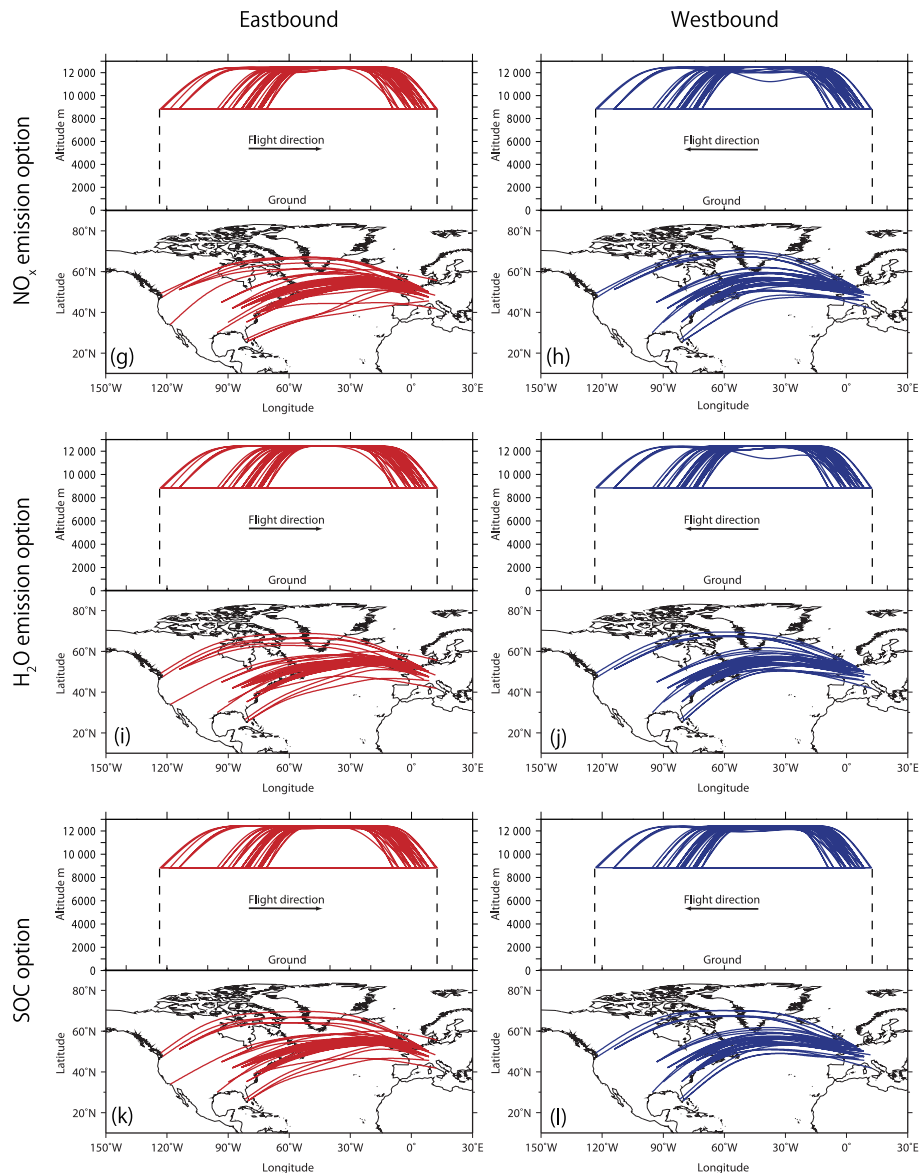


**Figure S3.** (continued.)

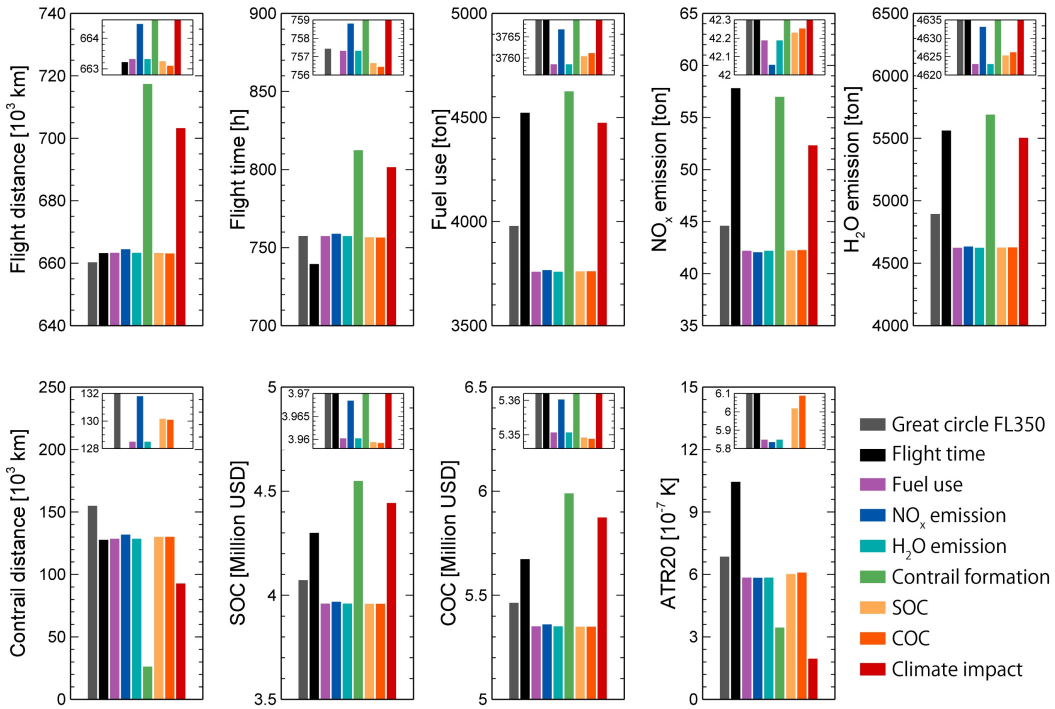


**Figure S4.** Bar charts of the nine performance measures obtained from one-day AirTraf simulations with different aircraft routing options (the bars indicate the sum of 103 flights), including the enlarged drawings around the values of the COC option. The summary data are listed in Table 4 in the text.